

THESIS FOR THE DEGREE OF LICENTIATE OF ENGINEERING

Stainless Steel Corrugated Web Girders for Composite Road Bridges

Concept Evaluation and Flange Buckling
Resistance

FATIMA HLAL

Department of Architecture and Civil Engineering
Division of structural engineering
CHALMERS UNIVERSITY OF TECHNOLOGY
Gothenburg, Sweden 2023

Stainless Steel Corrugated Web Girders for Composite Road Bridges Concept Evaluation and Flange Buckling Resistance

Fatima Hlal

© Fatima Hlal, 2023.

Thesis for the Degree of Licentiate Engineering

Technical Report No ACE 2023:9

Department of Architecture and Civil Engineering
Division of Structural Engineering, Lightweight Structures
Chalmers University of Technology SE-412 96
Gothenburg, Sweden
Telephone + 46 (0)736 290 443

Cover:

The figure illustrates a composite road bridge with stainless steel corrugated web girders, which is the focus of evaluation in this research

Printed by Chalmers Digitaltryck
Gothenburg, Sweden 2023

تَعَلَّمْ فَلَيْسَ الْمَرْءُ يُوَلَدُ عَالِمًا وَلَيْسَ أَخُو عِلْمٍ كَمَنْ هُوَ جَاهِلٌ

“Learn, for no one is born a scholar, and the knowledgeable person is never the same as the ignorant.”

Al-Imam Al-Shafi'i

Abstract

Achieving a sustainable bridge design requires careful consideration of economic viability and environmental impact over the entire lifespan of the structure. While stainless steel is recognized for its excellent life cycle performance, its high cost prevents it from being used to a larger extent in bridges. In this thesis work, a new solution is investigated to mitigate this issue. The new solution comprises the use of corrugated webs in stainless steel girders which is expected to result in reduced material consumption and cost. The work in this thesis focuses on two problem areas in this field. First, a study is performed to examine the competitiveness of the new concept in relation to conventional designs of steel-concrete composite road bridges. The second part of the work focuses on the problem of flange buckling in girders with corrugated webs. Previous research has shown that the design models developed for flange buckling resistance, including the one in EN 1993-1-5, frequently result in unsafe design. Furthermore, these models were developed for carbon steel and have not been updated for stainless steel.

To explore the economic and environmental benefits of the new concept, two studies have been conducted. Firstly, three design solutions are examined on a case study bridge with three continuous spans. These design solutions include carbon steel flat web, stainless steel flat web, and stainless steel corrugated web girder bridges. A genetic algorithm is used to optimize each design solution in terms of weight. The three optimal solutions are then assessed in terms of investment costs, life cycle costs (LCC), and environmental life cycle impact. Secondly, two of the considered design solutions, namely carbon steel flat web and stainless-steel corrugated web girders, are employed to conduct multiple parametric studies using a simply supported reference bridge. For both design solutions, the effects of optimization targets on weight, investment cost, life cycle cost, and environmental life cycle impact are initially investigated. Following that, the focus is put on the life cycle cost (LCC) as an optimization target, and the impact of various design input parameters is investigated. These parameters include span length, girder depth, average daily traffic (ADT) with the associated number of heavy vehicles per slow lane (N_{obs}), and time intervals and expenses for maintenance activities. Furthermore, a sensitivity analysis is conducted to study the influence of the inflation rate and discount rate. The results indicate that the new concept offers considerable potential saving in weight, life cycle costs, and life cycle impacts for both simply supported and continuous bridges. The saving is more apparent with deeper girders, higher ADT, and more intense

maintenance activities. Saving is also larger when inflation is high and discount rate is low.

After studying the potential of corrugated web girders to reduce costs and environmental impacts in the case of employing stainless steel, a study of the flange buckling behaviour in duplex stainless-steel girders is conducted in this work. A parametric finite element model is developed and validated with tests conducted on beams made of carbon steel. The material is then changed to EN1.4162, and linear buckling analysis (LBA) and geometrically and materially nonlinear analysis with imperfections (GMNIA) are carried out on 410 girders with typical bridge girder dimensions. The results are compared to previously developed models for carbon steel, and a new buckling curve and flange local buckling design procedure for duplex stainless-steel girders with corrugated webs are proposed. The study shows that the new proposed design model generates more accurate estimates of flange buckling resistance than previous proposed models.

Keywords

Optimization, Genetic algorithm, Investment cost, LCC, LCA, Composite bridges, Road bridges, Corrugated web, Duplex stainless steel, Flange buckling resistance.

FATIMA HLAL

Institutionen för Arkitektur och samhällsbyggnadsteknik

Avdelningen för konstruktionsteknik

Chalmers tekniska högskola

Sammanfattning

För att uppnå en mer hållbar brodesign krävs noggrant övervägande av olika val ur ekonomisk och miljöpåverkansperspektiv så väl under produktion som under hela brons livslängd. Även om rostfritt stål är känt för sin utmärkta livscykelprestanda, utgör detta stål höga kostnad oftast ett hinder att materialet användas i broar i större utsträckning. En ny lösning undersöks i detta arbete för att adressera detta problem. Den nya lösningen innebär att använda korrugerade liv i rostfria stålbalkar vilket förväntas resultera i minskad materialåtgång och därmed kostnad. Arbetet i denna avhandling fokuserar på två frågeställningar inom detta område. Först genomförs en studie för att undersöka det nya konceptets konkurrenskraft i förhållande till konventionella lösningar för samverkansbroar. Den andra delen av arbetet fokuserar på problemet med flänsbuckling i balkar med korrugerade liv. Tidigare studier har visat att designmodeller som tidigare föreslagits – inklusive den som används i EN 1993-1-5 – ofta ger osäker design. Dessutom har dessa modeller utvecklats för kolstål och har inte uppdaterats för rostfritt stål.

För att undersöka det nya konceptets ekonomiska och miljömässiga prestanda utförs två studier. I den första studien undersöks tre lösningar för design av en fallstudiebro med tre kontinuerliga spann. Dessa designlösningar inkluderar plant liv av kolstål, plant liv av rostfritt stål och korrugerade liv balkar i rostfritt stål. En genetisk algoritm används för att optimera varje designlösning med avseende på vikt. De tre optimala lösningarna utvärderas sedan ur olika perspektiv: investeringskostnader, livscykelkostnader (LCC) och miljömässig livscykelpåverkan. I den andra studien används två av de tidigare studerade designlösningarna, nämligen balkar med plana liv av kolstål och korrugerade liv av rostfritt stål, för att utföra flera parametriska studier. En fritt-upplagd bro används i denna studie som referensbro. För båda designlösningarna undersöks initialt effekterna av optimeringsmål, dvs vikt, investeringskostnad, livscykelkostnad eller miljömässig livscykelpåverkan. Baserat på resultaten, används livscykelkostnaden (LCC) som ett optimeringsmål i resten av studien,

och inverkan av olika designparametrar undersöks. Dessa parametrar inkluderar spannlängd, balkhöjd, årsmedeldygnstrafik (ÅDT) med tillhörande antal tunga fordon per långsamt körfält (N_{obs}), samt tidsintervall och kostnader för underhållsaktiviteter. Vidare görs en känslighetsanalys för att studera inverkan av inflation och kalkylränta. Resultaten indikerar att det nya konceptet erbjuder betydande potentiella besparingar i vikt, livscykelkostnader och livscykelpåverkan för både fritt upplagda och kontinuerliga broar. Dessa besparingar är mer tydliga när balkar med större höjd tillåts och lika så med högre ÅDT och mer intensiva underhållsaktiviteter. Livscykelkostnaderna för det nya konceptet är också mer gynnsamma när inflationen är hög och kalkylränta låg.

Del 2 av arbetet som beskrivs i denna avhandling avser problemet med flänsbuckling i balkar med korrugerat liv i duplexbalkar av rostfritt stål. En parametrisk finita elementmodell utvecklas och valideras med tester utförda på kolstål. Materialet ändras sedan till EN1.4162, och linjär bucklingsanalys (LBA) och geometrisk och materialmässigt olinjär analys med imperfektion (GMNIA) utförs på 410 balkar med typiska brobalksdimensioner. Resultaten jämförs med tidigare utvecklade modeller för kolstål, och en ny bucklingskurva och fläns-lokal bucklingsdesignprocedur för duplexbalkar av rostfritt stål med korrugerade liv framtas. Studien visar att den nya föreslagna designmodellen genererar mer exakta uppskattningar av flänsens bucklingsmotstånd än tidigare föreslagna modeller.

Nyckelord

Optimering, Genetisk algoritm, Investeringskostnad, LCC, LCA, Samverkansbroar, Vägbroar, Korrugerad bro balk, Duplex rostfritt stål, Flänsbucklingsmotstånd.

List of publications

- Hlal, F., Amani, M., Nilsson, P., Hollberg, A., Al-Emrani, M., (2023) Life Cycle Cost and Life Cycle Assessment of Composite Bridge with Flat and Corrugated Webs. Accepted to be published in Eurosteel 2023 conference.
- Hlal, F., Amani, M., Al-Emrani, M., (2023) Stainless Steel Corrugated Web Girders for Composite Road Bridges: Optimization and Parametric Studies. Submitted to Engineering Structures journal.
- Hlal, F., Al-Emrani, M., (2023) Flange Buckling in Stainless-Steel Corrugated Webs I-Girders under Pure Bending: Numerical Study. Journal of Constructional Steel Research 208 (2023) 108031.
<https://doi.org/10.1016/j.jcsr.2023.108031>

Additional contributions from the author

- Hlal, F., Mli, Z., Achour, A., Al-Emrani, M., (2022) Numerical Study of Flange Buckling Behaviour of Stainless-Steel Corrugated Webs I-Girders. Sixth Stainless Steel Experts Seminar.
- Hlal, F., Al-Emrani, M., Amani, M., (2022) Preliminary Study on Plate Girders with Corrugated Webs. Report ACE 2022:3.
- Al-Emrani, M., Amani, M., Björnstedt, P., Borg, P., Forsgren, E., Hedegård, J., Hällmark, R., Hlal, F., Janiak, P., Lundstjälk, A., Nilsson, P., Persson, L., Trydell, K., Zachrisson, J., Zamiri, F., (2022) SUNLIGHT – Sustainable, maintenance-free and lighter beams for stronger Swedish infrastructure

Preface

The thesis research was conducted at Chalmers University of Technology, department of Architecture and Civil Engineering, division of Structural Engineering, from September 2021 to August 2023. It was carried out as a part of the "Sustainable and Maintenance-Free Bridges" project, which received funding from the Swedish Transport Administration [Project No. TRV 2020/117504].

My deepest gratitude goes to my supervisor, Professor Mohammad Al-Emrani. I'm very grateful for your continuous support, patience, encouragement, and belief in me. Thank you for your dedication and commitment to my academic and personal development throughout the first half of my PhD journey and looking forward to what is ahead.

I would extend my gratitude to my co-supervisors, Dr Mozhdeh Amani, and Dr Peter Nilsson. I am grateful to both of you for all your interesting discussions and valuable feedback throughout this work. I'd also like to thank Docent Alexander Hollberg for his assistance with the LCC and LCA sections of the work. And of course, my examiner Holger Wallbaum for his support.

I would also like to express my appreciation to all my colleagues at Chalmers' Structural Engineering Division and WSP's Bridge Department for fostering a friendly and collaborative environment. I would also like to thank Dorotea, Fabio, Andreas, Vera, and all my PhD mates who have made this academic journey more inspiring and enjoyable.

Finally, I would express my gratitude to my parents for believing in me and to my little family, Saad, Omar, and Sirina. Saad, thank you for your consistent support, encouragement, and invaluable assistance with my scripting tasks. And to my little ones, thank you for growing older and making my life easier. Your presence and love make all the challenges worth it.

Fatima Hlal, Gothenburg, 2023

Contents

Abstract.....	I
Sammanfattning.....	III
List of publications.....	V
Additional contributions from the author	V
Preface.....	VII
1 Introduction.....	1
1.1 Background.....	1
1.2 Aim and objective	6
1.3 Methodology.....	7
1.4 Limitations	8
1.5 Outlines	9
2 The state-of-the-art	11
2.1 Optimization algorithms for structural engineering problems 11	
2.2 Genetic algorithm.....	12
2.3 Life cycle assessment (LCA)	15
2.4 Life cycle cost analysis (LCCA).....	16
2.5 Stainless steel for bridge construction	17
2.6 Duplex stainless steel.....	24
2.7 Corrugated web beams.....	27
3 Design optimization of composite road bridges	37
3.1 Developed optimization routine.....	37
3.2 Case study: Bridge over Dalälven	51
3.3 Parametric studies	56
3.4 Optimal corrugation parameters.....	70
4 Flange buckling resistance	73

4.1	Flange buckling problem description and approach.....	73
4.2	Parametric study and design model development.....	79
4.3	Evaluation of the developed design model and previous design models	82
5	Conclusions and future work	85
5.1	Conclusions on the benefits of using stainless steel corrugated web girders in road bridges (Paper I and II).....	85
5.2	Conclusions on flange buckling resistance (Paper III) .	87
5.3	Future work.....	88
	References	91
	Appendix	102
1	LCC data	102
2	LCA data	103
	Appended Papers	107
	Life Cycle Cost and Life Cycle Assessment of Composite Bridge with Flat and Corrugated Webs.....	I
	Stainless Steel Corrugated Web Girders for Composite Road Bridges: Optimization and Parametric Studies.....	III
	Flange Buckling in Stainless-Steel Corrugated Webs I-Girders under Pure Bending: Numerical Study.....	V

Chapter 1

1 Introduction

1.1 Background

Sustainable development is frequently discussed in today's business and public sector strategies. The 2030 Agenda for Sustainable Development and its 17 Sustainable Development Goals (SDGs) were created by the United Nations in 2015 [1]. The European Union (EU) also emphasizes its transition to a sustainable society, as stated in the Communication "Next Steps for a Sustainable European Future" [2]. Mitigating the negative environmental impacts of buildings and constructions is one of the biggest challenges the EU faces in reaching its goal to slow global warming. In the EU, the construction and building industry is responsible for about 40% of all final energy consumption, 35% of greenhouse gas emissions, and more than 50% of all material extractions [3]. Additionally, a third of the waste produced annually in the EU comes from the construction industry [4].

Given the potential effects that the bridge industry may have on the economy and environment, the bridge industry has demonstrated a rising interest in sustainable development [5]. Composite (steel-concrete) bridges belong to a well-known bridge concept and are usually designed with flat-web steel girders connected to a concrete deck using shear studs. The shear studs allow a composite action and enable the best possible utilization of the two materials [6]. The steel girders are typically made of conventional carbon steel, which is prone to corrosion. This necessitates additional costs for corrosion protection coating in production and frequent maintenance over the bridge service life in the form of inspection, repainting, and replacement of this coating. In addition to the costs of these activities, the impact on the environment and the disruption of traffic during the maintenance work are also considerable [7].

To mitigate the problems associated with maintenance activities for bridges, stainless steel can be an interesting solution [8, 9]. Corrosion resistance is often the main justification for using stainless

steel [9]. One type of stainless steel that is mostly selected in bridge construction is duplex stainless steel. This is because of the combination of high strength and corrosion resistance these types of stainless steel poses [8]. Duplex stainless steel consists of both austenite and ferrite. Ferrite increases strength, whereas austenite is perfect for structural uses due to its ductility, toughness, and superior corrosion resistance [10]. Moreover, duplex stainless steel has a higher strength-to-weight ratio compared to conventional carbon steel S355. Additionally, stainless steel has an aesthetically pleasing appearance, as shown in Figure 1 with two examples of stainless-steel bridges.



(a) Helix bridge, photo:
Andrea Goh [11]



(b) Folke Bernadotte bridge,
photo courtesy of Stål and
Rörmontage [11]

Figure 1 Examples of stainless-steel bridges

Several studies have previously demonstrated the potential saving in life-cycle cost (LCC) that can be achieved by using stainless steel. For instance, in a case study of a continuous road bridge, Karabulut et al. [12] demonstrated that stainless steel can lower life cycle costs, particularly when the design life span is longer than 75 years. Similar results were supported by Zilli et al. [13], Gedge [14], Säll et al. [15], Siklander et al. [16], and Wahlsten et al. [7], all of which highlight the LCC benefits of using stainless steel. However, despite the evident long-term benefits and excellent structural properties of stainless steel, it is not yet widely adopted in bridge construction due to the higher investment costs compared to conventional carbon steel. The higher price of stainless steel, nearly three times that of carbon steel S355 per kilogram, accounts for this difference [7]. Hechler et al. [17] argued that, due to the high investment cost, stainless steel bridges are unlikely to gain market share unless bridge owners considers the maintenance expenses when assessing the bridge cost.

Typically, in a steel or composite bridge, flat plates are used to build the webs and flanges of steel girders (ref. Figure 2a). A higher web is expected to have higher shear and bending resistance. However, to assure stability for deeper girders, the web must either be made thicker (to reduce its slenderness), or stiffeners must be

added. This will, of course, increase material usage and production costs, and add more fatigue-prone details that might govern the design of the bridge. Corrugated web (Figure 2b) can provide the required shear capacity with significantly thinner plates and without the need for extra transversal stiffeners, resulting in a significant material saving [7, 18].

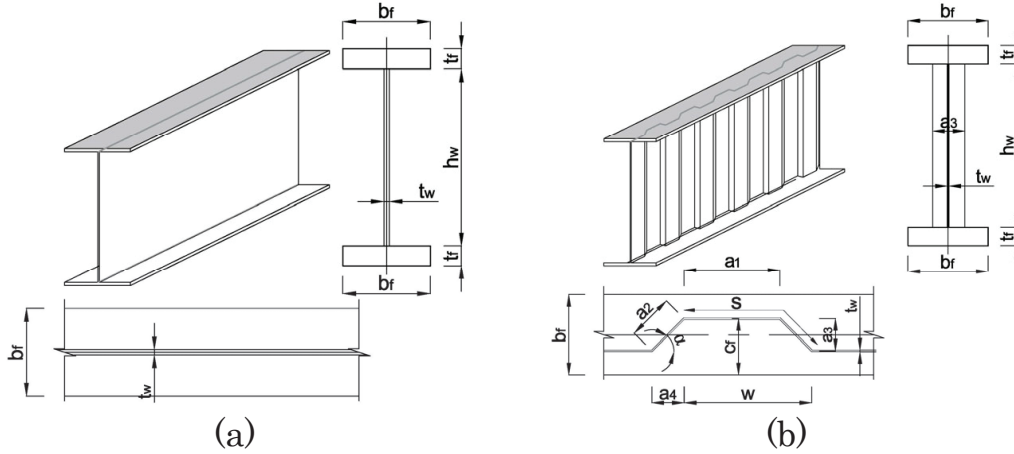


Figure 2 Composite bridge girder: (a) with flat web (b) with corrugated web

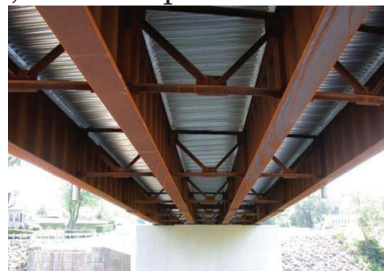
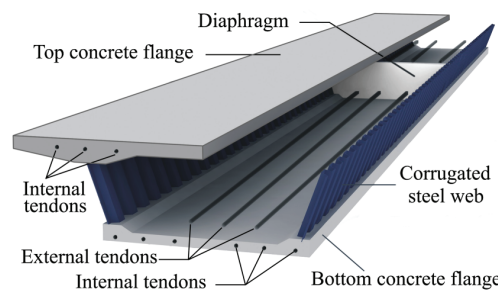
The use of corrugated steel web as a substitute for web stiffeners in steel-girder bridges was first investigated in Japan in 1965. This study created the groundwork for the use of corrugated webs in bridge construction [19]. During the 1980s, France built the first composite bridge with corrugated steel webs and upper and lower concrete slabs. This concept was chosen to overcome the problems generated by concrete slab creep, which caused the prestressing force to expand into the steel plates, resulting in severe losses when flat web girders were used. As a result, this technology was used to design and build several bridges with this concept in France [19]. Figure 3a shows an example of a box-girder bridge (Pont en poutre-caisson [20]) which was built with corrugated webs in France. Expanding on the composite technology pioneered by France, Japan embarked on the development of corrugated-web precast box-girder bridges in the 1990s and by 2015 had over 140 corrugated-web bridges [19]. Regarding girder bridges, to the knowledge of the author, the only bridge built with corrugated web was in 2005 in Bradford County, Pennsylvania, which was chosen as the site for a demonstration bridge made of High-Performance Steel (HPS) with a corrugated web design, see Figure 3b. The bridge, developed by the Pennsylvania Department of Transportation (PennDOT), has two spans and two lanes. The steel girders of the bridge have trapezoidal-shaped corrugated webs. The bridge was built using HPS 70W, which included the web, flanges, and splice plates. This unique bridge served as a showcase for the benefits and potential of HPS technology [21].

The use of corrugated webs in this bridge sought to decrease material usage and maximise the benefits of HPS technology.

Similarly, incorporating corrugated webs in stainless steel bridge girders can offer a competitive design solution that helps in reducing the gap in material cost between stainless steel and carbon steel girders. This design solution allows for a decrease in material usage and may thereby compensate for the higher material cost of stainless steel. Wahlsten et al. [7] conducted a preliminary study on this concept as part of the SIFRA project at Chalmers University of Technology. The study revealed significant potential cost savings in terms of both material and life cycle costs, although the initial investment cost was still considerably higher, ranging from approximately 20% to 37%. However, this study, along with the previously mentioned studies [12] [7, 13, 14], focused on specific case studies where the comparison between stainless steel and carbon steel involved merely changing the material while keeping other design parameters, such as the number of cross beams and cross-sectional changes, the same. However, due to the substantial difference in material prices between [20] Carbon steel and stainless steel, a direct transfer of design parameters from one material to another may not yield a fair comparison. Consequently, there is a need for more detailed studies that compare *optimal* designs of different concepts to accurately assess the potential benefits of this new design concept and explore its design space. In such studies, the various design situations and parameters that are expected to have an influence on the outcome of design need to be studied before one can stipulate general conclusions on the potential of this concept.



(a) Box-girder bridge, Pont en poutre-caisson, France [20]



(b) Girder bridge, Demonstration bridge in Bradford County, PA, USA [21]

Figure 3 Bridges with corrugated webs

Moreover, to enable a safe design for stainless steel corrugated web beams, it is imperative to establish a complete design procedure that enables safe utilization of these elements. This requires the inclusion of several design aspects, such as moment capacity, which incorporates considerations for buckling reduction when flanges are in cross-section class 4, as well as lateral torsional buckling, shear capacity, patch loading resistance, and fatigue resistance.

Currently, Annex D in EN1993-1-5 provides design rules for corrugated web beams but these rules are derived for carbon steel and have not been updated for stainless steel. They are also currently limited to the calculation of the bending moment and shear resistance of such girders. Various studies on the behaviour and strength of beams with corrugated webs have been performed at Chalmers University of Technology over the last 10 years. The first study on stainless steel corrugated web beams was done on the shear capacity of these beams. An experimental study was conducted as a part of the SUNLIGHT project, and according to the findings, using stainless steel material for beams with intermediate slenderness can result in considerably higher shear strength [22]. Furthermore, according to the literature study conducted by Hlal et al. [23], the EN1993-1-5 design model for shear capacity in the current generation of Eurocode [24] and patch loading resistance proposal in a draft for the coming generation [25] can be safely applied for stainless steel corrugated web beams [26-28] (however, with a high degree of conservatism). Moreover, according to the study done by Save et al. [29], the characteristic fatigue category for corrugated web to flange detail falls into fatigue category 120 MPa which surpasses the corresponding category for flat web girders (detail category 80 MPa for welded vertical stiffeners).

However, it has been proven that the EN1993-1-5 (Annex D) flange buckling resistance design model can generate unsafe resistances even for carbon steel girders and both the elastic buckling coefficient (k_σ) and buckling reduction factor (ρ) need to be revised [30] [23]. Johnson and Cafolla [31] conducted a thorough investigation that included both experimental and numerical approaches to determine which flange outstand should be used in the EN1993-1-5 expression for relative slenderness. They concluded that if the enclosing effect parameter (R), Figure 13, is less than 0.14, the average flange outstands ($b_f/2$) is an appropriate parameter for calculating the relative slenderness ratio of corrugated web girders. If the enclosing effect parameter (R) is larger than 0.14, the large flange outstand (C_f), Figure 2b, should be considered in the calculation. Another model is proposed by DASt-Richtlinie 015 [32] considering an upper limit for the elastic buckling coefficient of 0.6, which is similar to the limit established in the EN1993-1-5 model. Furthermore, Koichi and

Masahiro [33] performed experimental and numerical studies, leading them to suggest a design relationship with an upper limit for k_σ of 1.28. However, all of these models were developed primarily for carbon steel and have been shown to poorly represent flange buckling resistance in beams with corrugated webs [30] [23], [34]. In response to these concerns, Jáger et al. [30] suggested a new design model developed also for carbon steel. This model proposes new formulas for the elastic buckling coefficient (k_σ) with an upper limit of 1.3, as well as the buckling reduction factor (ρ) [30]. The authors also presented an equivalent imperfections amplitude for the flange buckling problem and set a limit for cross-section class 4. However, the application of this model expressions to stainless steel remains unknown, highlighting the need for further investigation. If necessary, a new model for stainless steel that incorporates the elastic buckling coefficient (k_σ), buckling reduction factor (ρ), equivalent imperfections amplitude, and limit for cross section class 4, should be established.

1.2 Aim and objective

The overall aim of this thesis is to contribute to the development of sustainable infrastructure by making the benefits offered by stainless steel more attainable in the construction of road bridges. This is achieved through the introduction of a new concept that incorporates stainless steel corrugated web girders for composite road bridges. This concept is expected to provide a design solution that is more efficient in terms of life cycle costs, reasonably priced in terms of investment costs, and with low environmental impact.

To achieve this aim, the first step is to thoroughly assess the advantages offered by the new concept in terms of reduced investment cost and enhanced life-cycle cost and life-cycle performance. This needs to be done considering a wider design space (i.e., considering different design parameters) to have an overview of when, where, and to what extent it is beneficial to construct using this design concept. Therefore, the first objective of this thesis is to evaluate the new concept in comparison to the commonly employed design concept which employs flat web carbon steel S355 girders in composite road bridges.

The second step is to establish a basis to design stainless steel corrugated web beams. According to the literature study conducted by Hlal et al. [23], the Eurocode design models for shear buckling, patch loading, lateral torsional buckling, as well as the fatigue resistance of the connection between the corrugated web and the flanges can be safely applied to stainless steel. However, the flange buckling resistance design model given in EN1993-1-5 does not consistently offer conservative estimates for the problem of flange buckling.

Among the different design aspects, this emerges as the most essential concern. As a result, the second objective of this thesis is to investigate the flange buckling behaviour in stainless steel corrugated web beams. This study aims to assess the applicability of existing models such as the model proposed by DAST Richtlinie 015 [32], the model proposed by Jäger et al. [30], as well as the EN1993-1-5 model, to stainless steel corrugated web beams. If necessary, the research aims at proposing a new design model to solve this issue.

Within the scope of this thesis, two research questions are addressed:

- How does the new concept perform in relation to the conventional concept in terms of investment cost, life cycle cost, and life cycle impact?
- How do the current design models, originally developed for addressing flange buckling in carbon steel, perform when applied to stainless steel? If these models are not applicable, what alternative model can be proposed for stainless steel flanges? What is the limit for cross-section class 4 in stainless steel flanges? Additionally, what is the reasonable imperfection amplitude that can account for initial imperfections?

1.3 Methodology

With reference to the first objective of comparing the new design concept for composite road bridges with the traditional concept, a design tool is developed to perform a complete design of the bridge. The tool is connected to GA optimization to ensure that the compared designs are optimum. Functions for calculating life cycle cost (LCC), life cycle impact, and investment cost are developed. These functions are used either to evaluate the optimized solutions or as objective functions in the optimization. The tool is then used to investigate a specific case study of a continuous bridge located in Avesta municipality in Sweden. Following the case-study assessment, a parametric evaluation, including several design parameters that are anticipated to influence the performance of the new concept, is conducted. Parameters investigated include the cost and the time intervals for painting activities, average daily traffic (ADT), together with the indicated number of heavy vehicles per slow lane (N_{obs}), girder height restrictions, and span length. Furthermore, the sensitivity of the findings to the inflation and discount rates is assessed.

With reference to the 2nd objective of investigating the flange buckling behavior in stainless steel corrugated web girders, the approach adopted is to use numerical analysis. A parametric finite element model is developed and validated using tests made on carbon steel beams. Sensitivity analysis to the initial imperfections is then

conducted to establish an adequate initial imperfection amplitude. After that, material and geometrically nonlinear analysis is performed on 410 girders. The space of geometrical parameters studied is selected to represent bridge girders. Regression analysis is used to derive expressions for the buckling factor and a buckling curve that can be used in the design of plate girders with corrugated webs with reference to flange buckling.

1.4 Limitations

The limitations related to the first part of the work regarding the design space of the new design concept are listed here:

- The study focuses on steel-concrete composite road bridges, in which the bridge deck is made of concrete and the twin girders are made of steel. The developed optimization routine focuses exclusively on the bridge superstructure (the main girders cross sections along with the cross bracings). Moreover, some geometrical parameters are not subjected to optimization such as the center-to-center distance between the two main girders and the concrete deck design (the concrete deck is designed and included in LCC/LCA calculations but is not optimized).
- A comparison of only two different steel types, S355 carbon steel and EN 1.4162 stainless steel, is performed. However, the developed tool has been designed to accommodate for the inclusion of additional steel grades, allowing for greater flexibility and adaptability for future studies.
- The structural analysis is linearly elastic, and the resistances are confined to the yielding capacity without considering any strain hardening in the material's behaviour.
- Material prices and environmental impacts are provided by one producer of stainless steel and another of carbon steel in Sweden. Steel prices have been fluctuating over time and the results presented in this thesis in terms of cost and environmental impact may differ dependent on the input.
- The established production cost model is based on the current market prices (the year 2022) of two manufacturers located in Sweden.
- Since the environmental data for material production is highly location-dependent and the case study bridges are located in Sweden, the environmental product declarations (EPDs) for the studied steel materials (S355 and EN1.4162) per kg acquired from two Swedish factories are used instead of the global average data. However, to assist in the collection of all the other material and process-related data, the commercial database Ecoinvent is used. All data sources are presented in the appendix.

- The calculated environmental impact only considers the climate change impact category, evaluating the contribution of the bridge life cycle to Global Warming Potential over a 100-year time horizon (GWP 100a).

In relation to the second part regarding the flange buckling problem, the following limitations apply:

- One grade of stainless steel (EN 1.4162) is investigated.
- The proposed design model is based on the range of geometrical parameters studied.
- The flange buckling behaviour is studied under a pure moment, i.e., the additional stress that can arise from shear flow has not been considered.

1.5 Outlines

The content of the current licentiate thesis work is organized and presented in five chapters as follows:

Chapter 1 gives background on the work and describes the objective of the research, the method, and its limitations.

Chapter 2 introduces the theoretical framework of the thesis and reviews the state-of-the-art optimization algorithms used for structural engineering problems, life cycle assessment (LCA) and life cycle cost analysis (LCCA), stainless steel in bridge construction, and finally a summary of available studies on various design aspects of corrugated web beams.

Chapter 3 presents the developed optimization routine, the developed life cycle cost and life cycle environmental impact calculation models, and the findings of the study on the possible advantages of incorporating stainless steel and corrugated web into composite road bridge girders. This chapter extracts results from papers I and II.

Chapter 4 presents the main findings on the applicability of the EN1993-1-5, DASt Richtlinie 015, and Jáger et al. design models for the flange buckling resistance of carbon steel for stainless steel material, along with the newly developed design procedure for flange buckling resistance in stainless-steel corrugated web girders. In this chapter, extracted results from Paper III are discussed.

Chapter 5 summarizes the main conclusions and findings of this work, along with suggestions for further research.

Chapter 2

2 The state-of-the-art

2.1 Optimization algorithms for structural engineering problems

Many structural engineering problems, such as parameter identification, optimal design, and topology optimization, involve the use of optimization algorithms. These problems are referred to as “black box problems” in optimization which refers to the challenge of finding the optimal solution for a problem when the objective function is not explicitly known or is difficult to evaluate. In other words, the function that maps the input variables to the output variables is unknown, and only its inputs and outputs are accessible. An example of that is trying to find the set of design parameters that gives the minimum life cycle cost or weight for the specific inputs. In this case, optimization algorithms use various strategies to explore the input space and find a solution that minimizes or maximizes the objective function. These strategies include stochastic methods such as evolutionary algorithms (GA), which mimic the genetic and natural selection processes inspired by Darwin’s Theory of Evolution. Employing evolutionary processes including mutation, crossover, and selection, a population of viable solutions is generated over numerous generations. Each solution is assessed for fitness using a fitness function, and the procedure is repeated until a feasible option is identified. Another stochastic method is particle swarm optimization (PSO). The algorithm uses a population of candidate solutions called particles to explore the input space, where each particle iteratively updates its position and speed that defines its fitness until the termination criteria are met. Both the social and cognitive components affect the velocity update in PSO. The cognitive component focuses on the particle’s individual learning and personal best position which encourages research into the particle’s optimal performance. The social component represents the collective behaviour of the swarm when the global optimal position found by each particle is taken into consideration. It makes it possible to learn from successful particles and directs search activity to potentially

promising regions of the search space. There are also gradient-based methods, such as gradient descent (GD), that iteratively update the input variables based on the direction of the gradient of the objective function.

2.2 Genetic algorithm

Genetic algorithms (GA), in particular, have proven to be an effective framework for black-box problems and are general enough to be applied to the majority of problems in engineering practice [35, 36]. Several optimization studies on various types of civil engineering structures and materials have been conducted [36]. Over the last few decades, the bridge industry has been interested in structural optimization, which focuses on the material, design variables, or structural configuration to optimize the design in terms of environmental impact and cost [36]. Hassan [37] employed FEM, B-spline curves, and a genetic algorithm to reduce the cost of cables in cable stay bridges. Park et al. [38] evaluated the cost of an arch bridge using the Korean design standard. A conventional steel (365 MPa yield strength) arch bridge was designed, as was a combination of conventional steel and HSS (690 MPa yield strength). By assigning HSS steel to the most stressed elements, a genetic algorithm was employed to optimize the design of the key steel members (arch rib, main girders, and cross beams) in terms of cost. Skoglund et al. [39] employed genetic algorithm optimization to determine the optimal design solution for composite steel and concrete bridges, with the aim of identifying the potential advantages of employing high-strength steel over conventional steel. Furthermore, Chalouhi [36] adopted a genetic algorithm in conjunction with an automated design to find the optimal design solution for three types of bridges (RC road beam bridges, RC overhang bridge slabs for road bridges, and composite road bridge decks) and compared them to existing structures to demonstrate potential saving in terms of embedded environmental impact and cost for optimal and conventional design solutions.

Genetic algorithm optimization and other meta-heuristic algorithms combine randomized and local search. The local search part of the method is used to improve the reliability of the solution, while randomization helps prevent getting stuck at a local minimum or maximum [40]. The flowchart of the genetic algorithm adopted from Bozorg [41] is illustrated in Figure 4, and a full explanation of the genetic algorithm, the natural processes that inspired the algorithm, and the general steps of a standard GA are described in Bozorg's book [41].

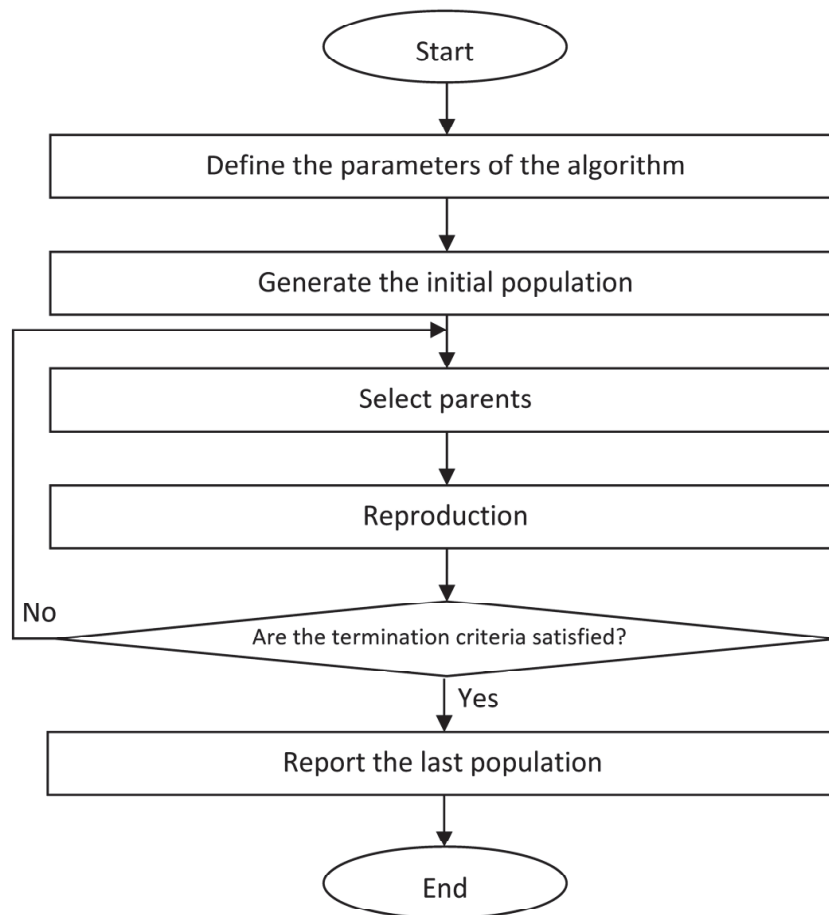


Figure 4 Flowchart of the genetic algorithm [41]

2.2.1 Mapping the genetic algorithm to natural selection

The GA is based on Darwin's theory of the survival of the fittest in species in danger from predators and environmental risks [41]. Members who are the fittest have a higher chance of surviving than others. They are more likely to adapt to changing environments, and their children may acquire and learn their qualities, generating even more fit future generations. Furthermore, genetic mutations occur at random in members of species, and some of these variations may boost the probability of the long-term survival of fit individuals as well as their evolutionary descendants. Each individual created by the GA (called a chromosome) represents a potential solution to the optimization problem at hand. Each chromosome contains genes that reflect decision variables. Individuals' fitness values determine their ability to survive. Each generation has a combination of a parent population (surviving people (chromosomes) from the previous generation) and their offspring. Genetic operators such as crossover and mutation produce offspring or children, which represent new solutions. Parents are picked in such a way that their likelihood of

selection is proportional to their fitness scores. The greater the fitness value, the greater the chances of survival and reproduction [41].

According to Bozorg [41], standard GA starts with a population of randomly generated potential solutions (individuals). The fitness of the individuals is calculated, and some of them are chosen as parents based on their fitness levels. By applying the crossover operator to the parent population and subsequently the mutation operator to their offspring, a new population (or generation) of possible solutions (the children's population) is created. Iterations in which the original generation (an old individual) is replaced by a new generation (children) are repeated until the stopping requirements are met. The number of children belonging to the three categories (elite children, mutation children, and crossover children) is defined by the user. Elite and crossover children represent the local component of the search, while mutation children represent the global component obtained through randomization.

2.2.2 Genetic algorithm python library “geneticalgorithm”

“geneticalgorithm” is a python library distributed on [“https://pypi.org/”](https://pypi.org/) for implementing standard and elitist genetic algorithms (GA). The algorithm was developed by Solgi [42], and it provides an easy implementation of genetic algorithm (GA) in python. It can be installed for free using the package manager “pip”.

For design optimization of structural elements, it is necessary to limit the utilization ratios to values lower than one. Solgi [42] suggests addressing a penalty function that is larger than the maximum value of the objective function for such optimization problems with constraints if this value is known or can be estimated. As a result, if a trial solution, despite having a small objective function, is outside of the feasible zone, the penalized objective function (fitness function) is poorer than any possible solution. However, in cases where the optimum is precisely on the edge of the viable zone (or extremely close to the constraints), which is common in some types of problems, a highly rigid and significant penalty may prevent the algorithm from approaching the optimal region. In this case, a proper penalty function is needed [42]. More information about the definition of the penalty function can be found in Bozorg’s book [41]. Bozorg [41] and Solgi [42] also provide definitions for the genetic algorithm parameters, which are listed below:

- Initial population size, which determines how many trial solutions there will be in each iteration. The population may be seen as a $M \times N$ matrix, where M is the total number of

solutions for each variable and N is the total number of design variables (genes) that will be optimized.

- Parents portion: the percentage of the population that is made up of individuals from the preceding generation.
- Mutation probability: determines the probability that a random value will be substituted for each gene in each solution. The default setting set by Solgi is 0.1, or 10%.
- Elite ratio: identifies the elite percentage of the population. One percent, or 0.01, is the default setting set by Solgi. For instance, if the population is 100 and the `elit_ratio` is 0.01, there is only one elite in the population. If this parameter is set to zero, “geneticalgorithm” will utilize a standard genetic algorithm rather than an elitist GA.
- Crossover probability: controls the probability that an existing solution will pass on its genome to subsequent trial solutions; the default value set by Solgi is 0.5 (or 50%).
- Crossover type: there are three options to choose from one-point, two-point, and uniform crossover functions. The difference between these types is explained in Bozorg et al.’s book [41]. Uniform crossover is the default set by Solgi.
- The maximum number of iterations without improvement: The genetic algorithm stops and reports the best-identified solution before the maximum number of iterations is reached if the objective function is not improved throughout the number of subsequent iterations defined by this parameter. None is the default value [42].

2.3 Life cycle assessment (LCA)

LCA, according to the international standard ISO 14040 [43], is a method to assess the environmental impacts of a product's life cycle, from material extraction to manufacture, use, and disposal. The analysis is an iterative process divided into four phases: goal and scope definition, inventory analysis, impact assessment, and interpretation.

In the first phase of LCA (the goal and scope definition), the aim, purpose, and target audience of the research must be thoroughly discussed to determine the goal and scope of the assessment.

In the second phase (the life cycle inventory analysis), data is collected and flowcharts through, from, and into the product system are modelled.

In the third phase (the life cycle impact assessment (LCIA) phase), a trial is conducted to predict the number of emissions and resource consumption that would result in an environmental impact related to a category indicator such as global warming and abiotic depletion.

The interpretation phase, according to ISO 14040 [43], is when results from the impact assessment and life cycle inventory phases are in line with the aim and scope specification. Based on the constraints identified during the LCA analysis, the results should offer some recommendations and conclusions.

The European Standard EN 15978:2011 [44] provides a systematic approach for evaluating a building's environmental performance based on Life Cycle Assessment (LCA) and other quantitative environmental data. All phases of the building life cycle are covered by the assessment approach, which is based on information from Environmental Product Declarations (EPD), their "information modules" (EN 15804 [45]), and other data that is essential and relevant for conducting the evaluation. All building-related construction materials, methods, and services that are utilized during a building's lifetime are covered by the evaluation. The life cycle stages of a building following European Standard EN 15978:2011, as shown in Table 1, may be utilized as a general framework for a bridge's life cycle assessment to establish the system boundary.

Table 1 System boundary for building construction (adapted from EN 15978:2011) [44]

Product stage		Construction stage	Use stage					End of Life stage				Benefits and loads beyond the system boundaries		
A1: Raw material supply	A2: Transport	A3: Manufacturing	A4: Transport	A5: Construction/ installation	B1: Use	B2: Maintenance	B3: Repair	B4: Replacement	B5: Refurbishment	C1: Deconstruction - demolition	C2: Transport	C3: Waste processing	C4: Disposal	D: Reuse, recovery, and recycling potential
					B6 Operational energy use									
					B7 Operation water use									

2.4 Life cycle cost analysis (LCCA)

The life cycle cost analysis (LCCA) is a method for properly evaluating the life cycle cost over a given assessment time [46]. Many bridge

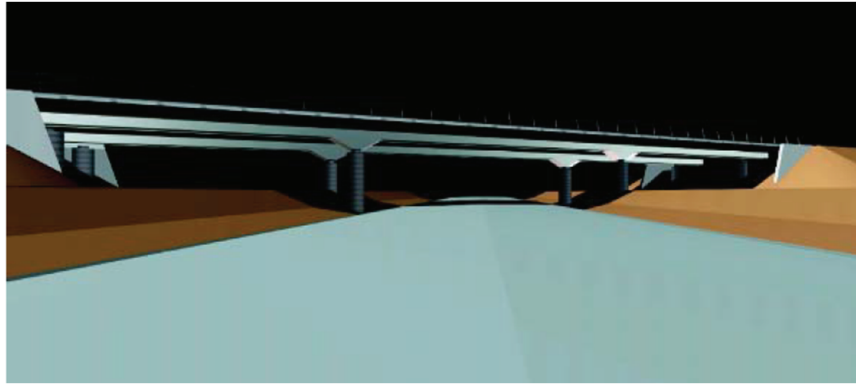
management systems employ LCC as a fundamental tool for determining the best strategy based on the remaining life span [46]. Furthermore, to compute the whole life cycle costs of bridge construction, the expenditures are discounted to their present value [47]. In this context, many other economic evaluation techniques, including the payback method, EAC, and the IRR approach, might be applied to the whole life cycle costs [48].

LCC analysis is a helpful method for determining whether bridges are cost-effective since it considers all expenditures, from acquisition through destruction [5]. The life cycle cost analysis for a bridge should include the initial expenditures, material expenses, and expected maintenance costs during the bridge life cycle [48]. Moreover, the user costs associated with traffic delays, when the average daily traffic volume is high, influence the bridge's total life cycle costs and need to be considered [7, 49].

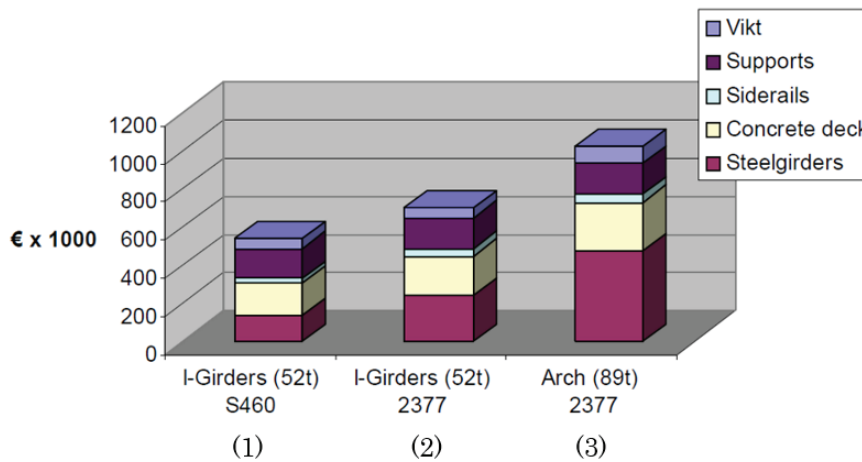
2.5 Stainless steel for bridge construction

Stainless steel is known for its exceptional corrosion resistance and appealing mechanical properties, making it a great choice for bridge construction. Recognizing its potential, several in-depth studies have been conducted with the primary goal of studying the potential and practicality of employing stainless steel in bridge construction.

In 2008, Hechler et al. [17] published the results of designing a highway bridge (designed by Ramböll) carrying the highway E4 over a national road in mid-Sweden for three design alternatives: a haunched three-span I-girder bridge in carbon steel (S460), a haunched three-span I-girder bridge in duplex stainless steel (EN 1.4462), and an arch bridge in duplex stainless steel. Comparing the investment cost for the first two alternatives, which have the same concept and the same material strength, the stainless-steel alternative showed a higher investment cost (700 000 € compared to 550 000 € for the carbon steel alternative); see Figure 5. The stainless-steel cost was assumed to be three times that of carbon steel. The authors stated that stainless steel bridges are unlikely to gain market share before bridge owners begin to consider maintenance expenses in their assessments of the bridge's cost.



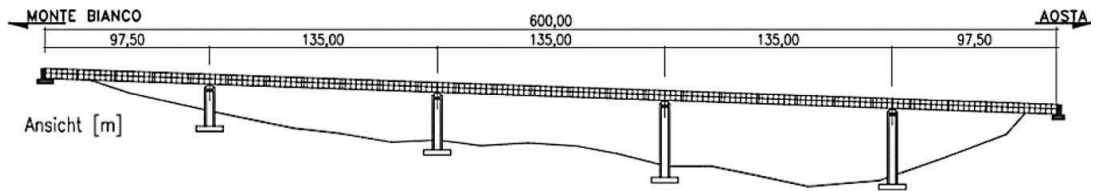
(a)



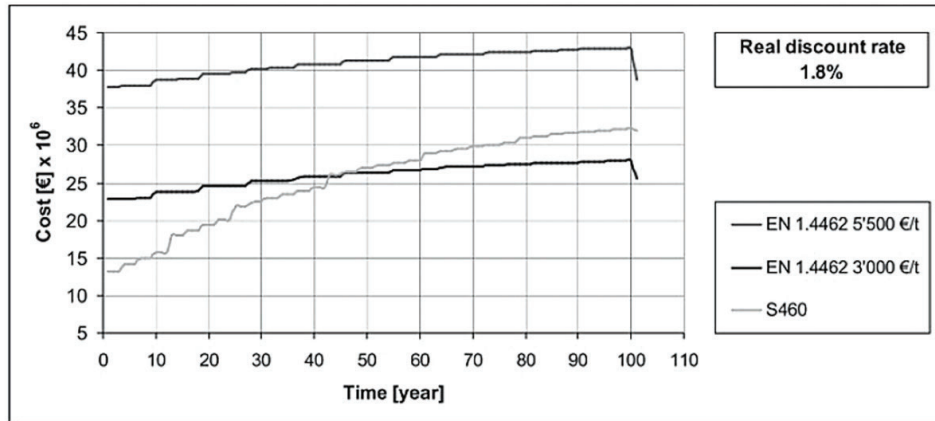
(b)

Figure 5 Results of Hechler et al. [17] study. (a) Bridge configuration. (b) Investment cost comparison for three alternative designs: 1) A haunched three-span I-girder bridge in carbon steel 2) A haunched three-span I-girder bridge in duplex stainless steel 3) An arch bridge in duplex stainless steel.

In 2008, Zilli et al. [13] investigated the application of duplex stainless steel for bridges in aggressive environments (category C5). A case study of a five-span continuous bridge (Verrand Viaduct Bridge in Italy) located in environment class C5 was studied for two alternatives: carbon steel S460 and duplex stainless steel EN 1.4462. The two alternatives were compared with reference to their life cycle costs. Two different discount rates (1.8% and 3.2%) and two different unit costs (5500 €/ton and 3000 €/ton) for stainless steel were studied. The unit cost for carbon steel was 1100 €/ton. The assumed maintenance schedule is illustrated in Figure 7. The results showed that the stainless-steel option wins in terms of LCC for 100 years when the material price is 3000 €/ton; see Figure 6. For a material price of 3000 €/ton and an inflation rate of 1.8%, the initial cost could be recovered around 50 years after construction.



(a) Bridge configuration



(b) LCC comparison

Figure 6 Recovery time of the initial investment. Verrand Viaduct Bridge, Italy [13]

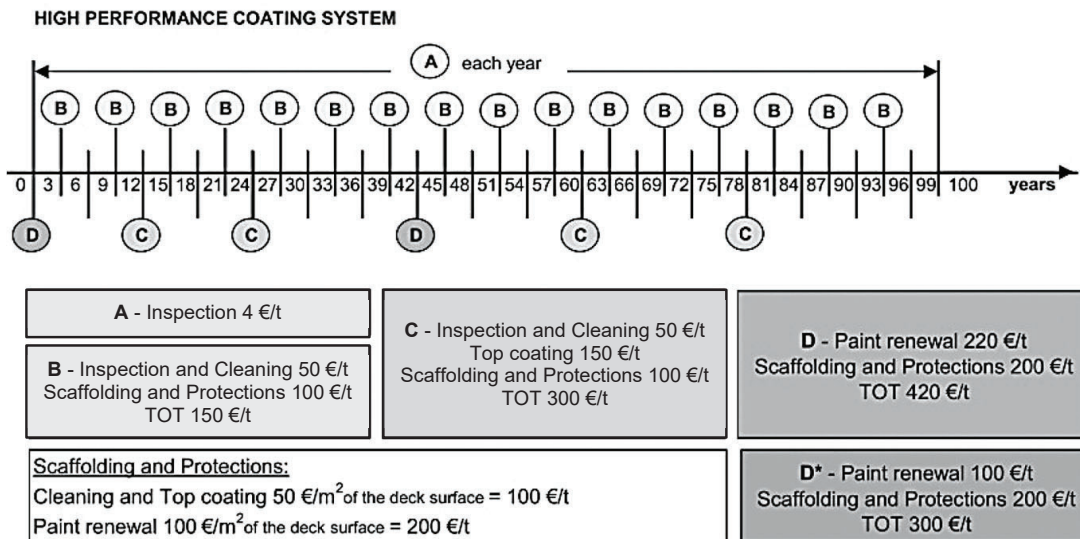


Figure 7 Maintenance schedule of painting systems for S460 at two different performance levels in the environment of category C5 [13]

Another study that investigated the use of stainless steel in bridges was performed by Gedge [14]. The author redesigned a worked

example from SCI (The Steel Construction Institute) [50] for a two-span bridge using weathering steel and duplex stainless steel and compared the lifecycle cost to the original design (S355). The bridge's design life was 60 years. The result of this case study showed that using duplex stainless steel can decrease the weight by 12%, and the ratio increases to 27% if the design is optimized. For weathering steel, on the other hand, the total weight is increased by 6% without optimization and decreased by 21% with optimization. Comparing the life cycle costs, the author stated that the stainless-steel option has the potential to save from 30% to 40% in comparison to the original carbon steel (S355) design; ref. Figure 8.

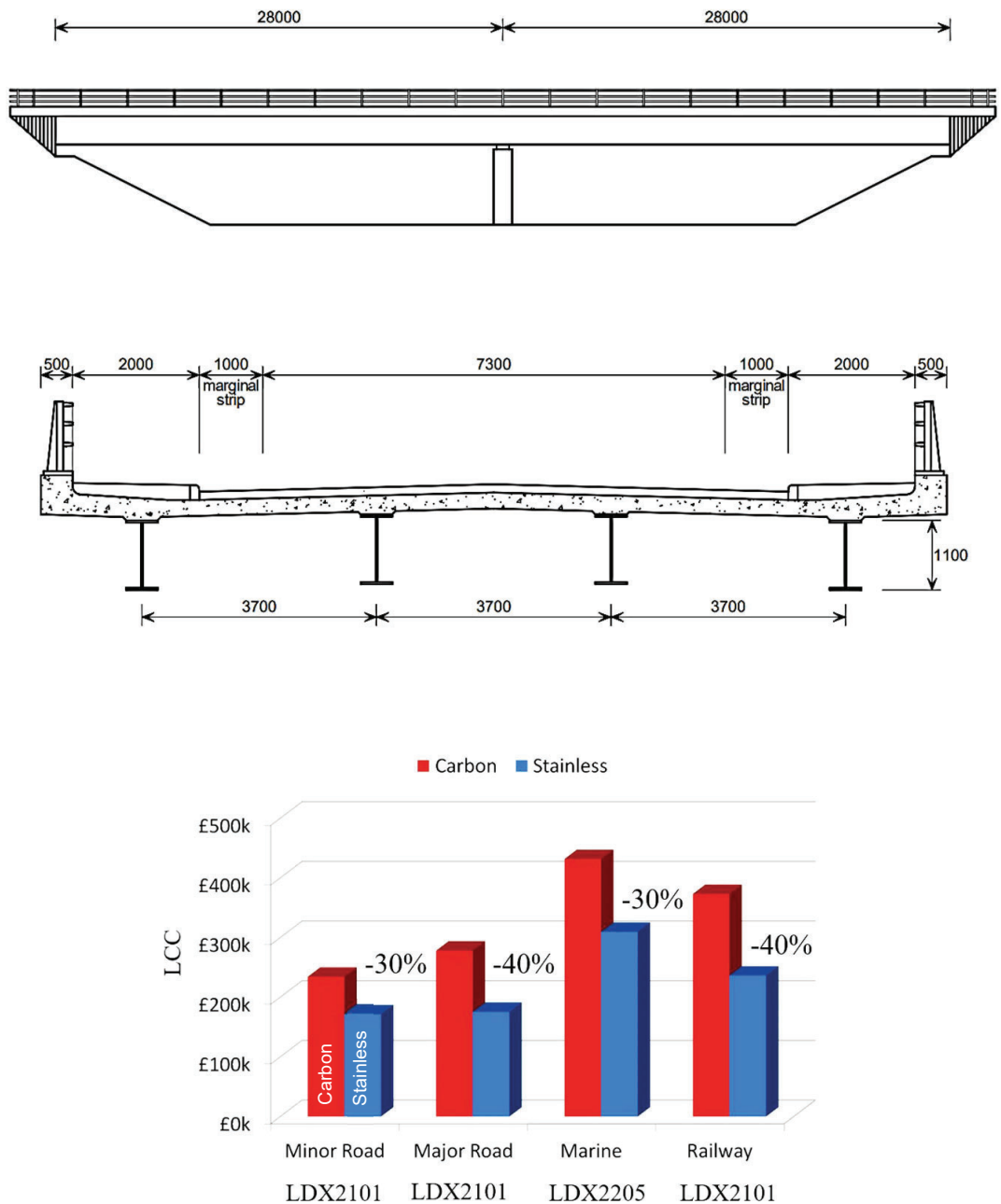
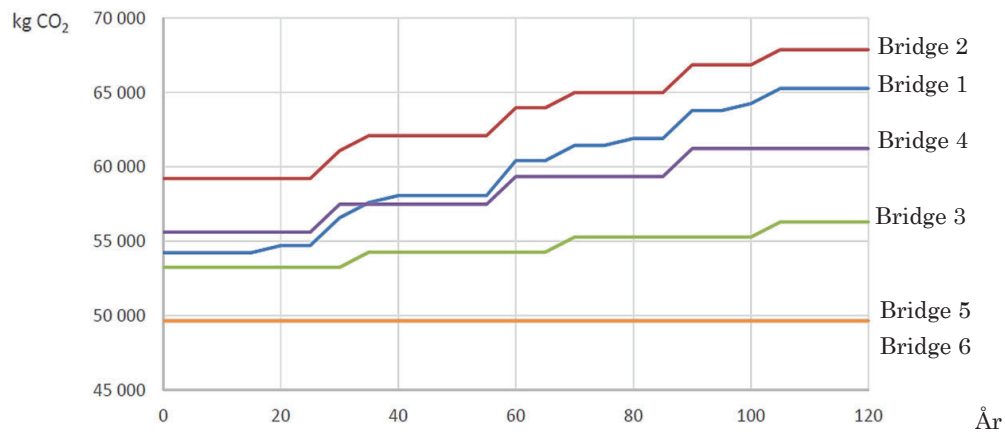


Figure 8 Composite Highway Bridge Design: Worked Example [50]

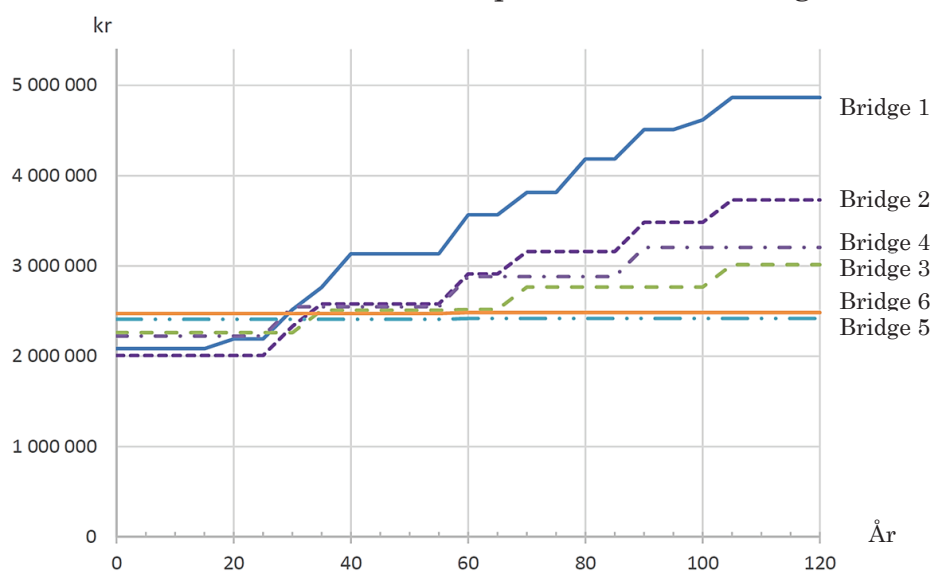
Säll et al. [15] conducted a study on a twin I-girder, a 15-meter long one-span bridge with two traffic lanes and one pedestrian and one cycle lane located in Sweden. Six various bridge concepts were designed to compare the different materials for the steel structure and the concrete reinforcement. The concepts are:

- Bridge 1: painted steel beam, structural concrete with carbon steel reinforcement and waterproofing layer, and asphalt.
- Bridge 2: painted steel beam, structural concrete with carbon steel reinforcement, and concrete surfacing.
- Bridge 3: painted steel beam, structural concrete with stainless steel reinforcement, and concrete surfacing.
- Bridge 4: stainless steel beam, structural concrete with carbon steel reinforcement, and concrete surfacing.
- Bridge 5: stainless steel beam, structural concrete with stainless steel reinforcement, and concrete surfacing.
- Bridge 6: stainless steel beam, grouted concrete with stainless steel reinforcement, and concrete surfacing.

The calculations were performed according to European standards [15]. The average interval before a complete repainting was assumed to be 35 years based on a compilation of maintenance tasks from the Bridge and Tunnel Management system in Sweden (BaTMan) [51]. The result of this investigation showed that a bridge with conventional materials at the end of its life cycle costs twice as much as a bridge with stainless steel when the stainless steel is used in both reinforcement and bridge girders; ref. Figure 9. From an environmental perspective, their results showed that the alternative with stainless steel is better from the beginning due to less materials needed for the same loads; ref. Figure 9.



(a) Environmental impact of the six bridges



(b) Total costs for the six bridges from the investment until the service life is reached

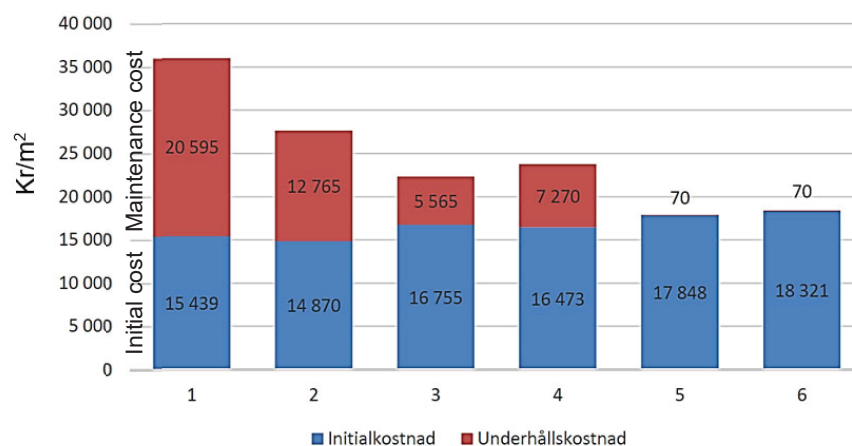
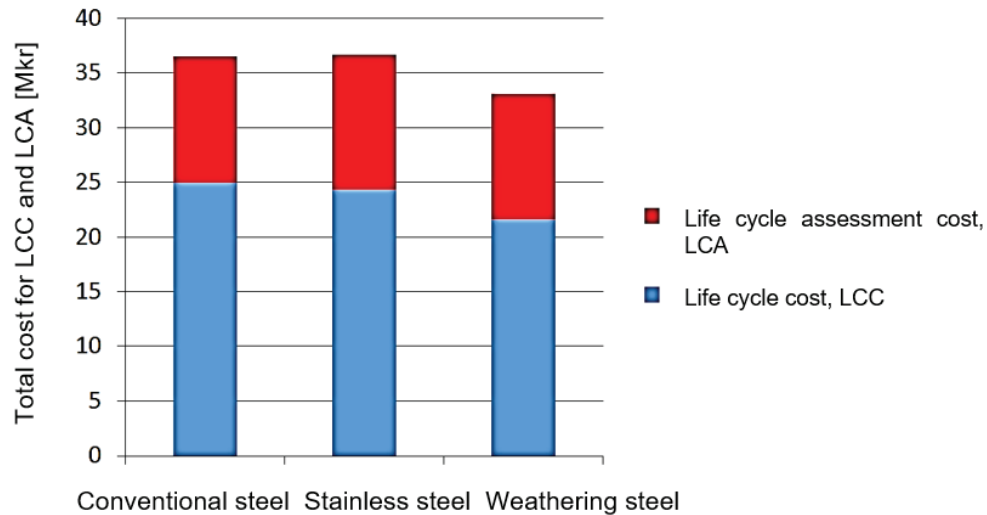
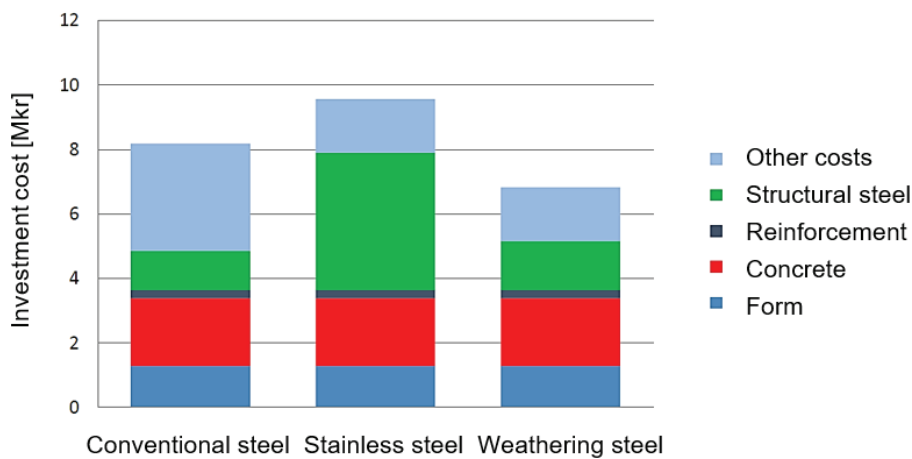
(c) Investment costs (initialkostnad) and maintenance costs (underhållskostnad) per m²

Figure 9 Total costs for the various bridge designs [15]

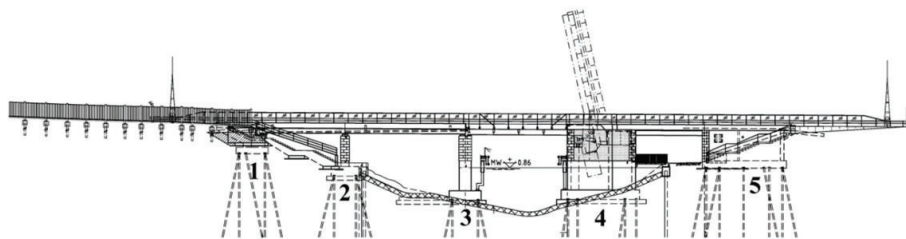
Siklander et al. [16] conducted a study in 2016 to investigate the most cost-effective and environmentally friendly choice of material for a moveable composite bridge, the New Flottsund bridge in Uppsala, Sweden. The bridge is designed as a three-span bridge. The first span (between support 1 and 3 in Figure 10c) is designed as a composite bridge; the second span (between support 3 and 4 in Figure 10c) is designed as an opening bridge; and the last span (between support 4 and 5 in Figure 10c) is designed as a concrete beam bridge. The materials that were compared are steel (420MC), stainless steel (EN 1.4462), and weathering steel (S355J0WP), where the main differences are the larger investment cost for the stainless steel and the lower need for maintenance for the stainless steel and the weathering steel. The life cycle cost is calculated for the three concepts assuming a cost ratio of 4.8 for stainless steel to carbon steel and a ratio of 1.06 between weathering steel and carbon steel. The life cycle environmental impact was also calculated and transferred to a cost in Swedish Kronor with the method Ecovalue12 and merged with the life cycle cost. The results of the study are presented in Figure 10. The result of this study showed that, for this bridge, weathering steel is the most cost-effective and environmentally friendly choice of material, followed by conventional steel and, at last, stainless steel. The authors further examined the sensitivity of the results to the painting time interval. They found that using for stainless steel can lead to a reduced life cycle cost compared to the carbon steel option when repainting the steel structure occurs every 29 years or less (for a real interest rate of 3.5%).



(a) LCC comparison



(b) Investment cost comparison



(c) Flottsund bridge elevation

Figure 10 Results of Siklander et al. [16] study on best design material for Flottsund bridge in Uppsala, Sweden

2.6 Duplex stainless steel

The primary benefit of stainless steel over conventional carbon steel is its capability to resist corrosion [10]. The term "stainless steel" refers to a group of alloys with at least 10.5% chromium that, when exposed to water and oxygen, form a protective layer against corrosion. The most prevalent form of stainless steel is austenitic

stainless steel. Duplex stainless steel is another form of stainless steel that is taken into consideration in this thesis and is made of austenite and ferrite. As mentioned earlier, ferrite improves strength, while austenite is more suitable for structural applications because of its higher corrosion resistance, ductility, and toughness [10].

The stress-strain behaviour of stainless steel and regular carbon steels differs significantly. The linear-elastic range and the start of plasticity at the yield stress f_y are clearly distinguished on a typical stress-strain curve for carbon steels. After then, the curve plateaus and the strain increase until failure. Since there is no distinct yield limit, stainless steel does not behave in the same way. A definition of so-called proof strength is applied to provide a comparable yield strength for stainless steels. The proof strength describes the stress that corresponds to a 0.2% plastic strain upon unloading, as shown in Figure 11.

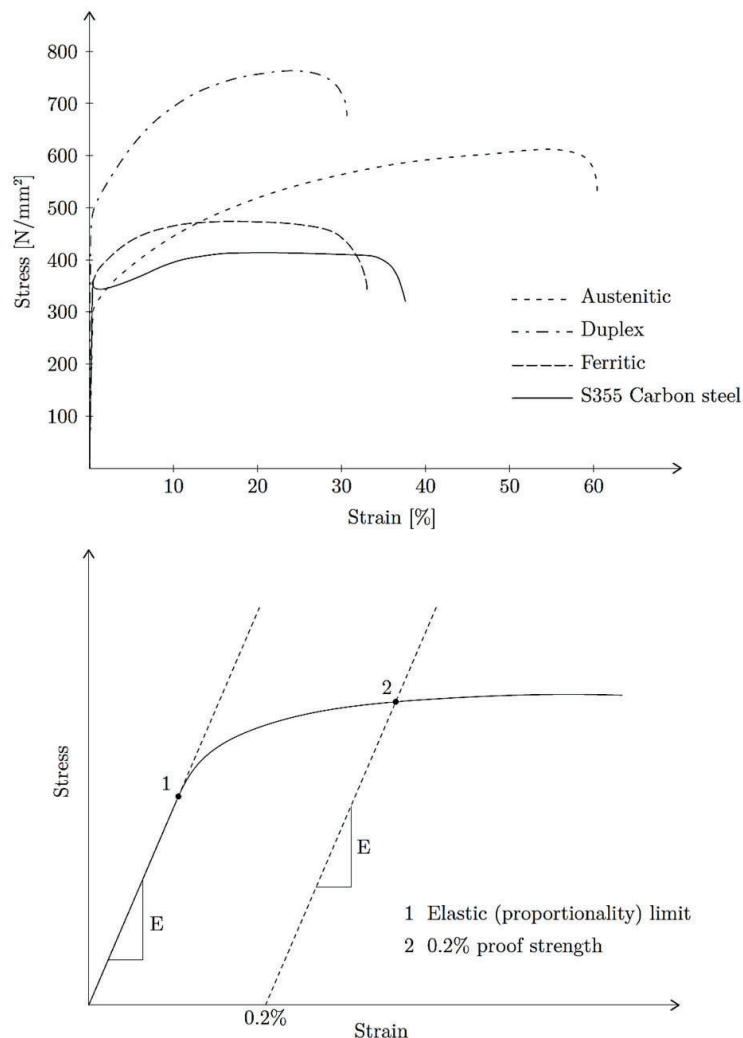


Figure 11 Stress-strain relation for carbon steel and stainless steel of different types and the definition of yield point (the 0.2% limit) of stainless steels. Images adapted from the Design Manual for Structural Stainless Steel [52]

The non-linear behaviour of stainless steel should be taken into account while evaluating the deflection in the Serviceability Limit State (SLS). The secant modulus, which is defined in Equation (2-1), is recommended by EN1993-1-4 [53] as an alternative to the elastic modulus. For the flange under stress, the secant modulus is calculated using Equation (2-2), where $\sigma_{f.SLS}$ is the stress in the flange at serviceability load level and n is the Ramberg-Osgood parameter, taking into account the non-linearity of the materials. EN1993-1-4 specifies that $n = 5$ be used for duplex stainless steel [53].

$$E_s = \frac{E_{sf.t} + E_{sf.c}}{2} \quad (2-1)$$

$$E_{sf} = \frac{E}{1 + 0.002 \left(\frac{E}{\sigma_{f.SLS}} \right) \left(\frac{\sigma_{f.SLS}}{f_y} \right)^n} \quad (2-2)$$

The nominal values of the yield strength, f_y , and the ultimate tensile strength, f_u , for the most common duplex stainless steel used in bridges is presented in Table 2. The value suggested in a new draft for EN1993-1-4 for the thermal coefficient is $\alpha = 13 * 10^{-6}$ 1/K for duplex stainless steels (the value is also available by Outokumpu [54]). The density is 7700 kg/m³ [54].

Table 2 Nominal values of the yield strength f_y and the ultimate tensile strength f_u for structural stainless steels according to EN 10088 without considering the anisotropy and the strain-hardening effect

Austenitic ferritic steel	Grade	Product form							
		Cold rolled strip		Hot rolled strip		Hot rolled plate		Bars, rods and sections	
		Nominal thickness t							
		$t \leq 8$ mm		$t \leq 13,5$ mm		$t \leq 75$ mm		$t \leq 250$ mm	
		f_y	f_u	f_y	f_u	f_y	f_u	f_y	f_u
		MPa	MPa	MPa	MPa	MPa	MPa	MPa	MPa
1.4162	530 ^e	700 ^e	480 ^f	680 ^f	450	650	450 ^b	650 ^b	
1.4462	500	700	460	700	460	640	450 ^b	650 ^b	

b: $t \leq 160$ mm, *e:* $t \leq 6,4$ mm, *f:* $t \leq 10$ mm

2.7 Corrugated web beams

2.7.1 Stress distribution and transverse bending

When designing beams with corrugated webs, it is common to assume that the moment is carried purely by the flanges and the shear force is carried by the web. This assumption is due to the accordion effect in beams with corrugated web, which in turn decreases the moment capacity of such girders [55]. Additionally, prior studies revealed that the corrugated web's shear force flow induces a transverse bending moment in the flanges, adding to the normal stresses initially present [56-58]. The shear stress path in the junction between the web and the flange in corrugated web beams is not as straight as that in flat web beams; it follows, however, the corrugation path as shown in Figure 12. Moment M_1 is produced by the horizontal shear forces that arise at the web-to-flange junction (T_1). Furthermore, shear force (T_2) results in force (F_y), which acts as transverse loads in the flange plane. These effects (M_1, F_y) result in increased normal stresses on the flanges.

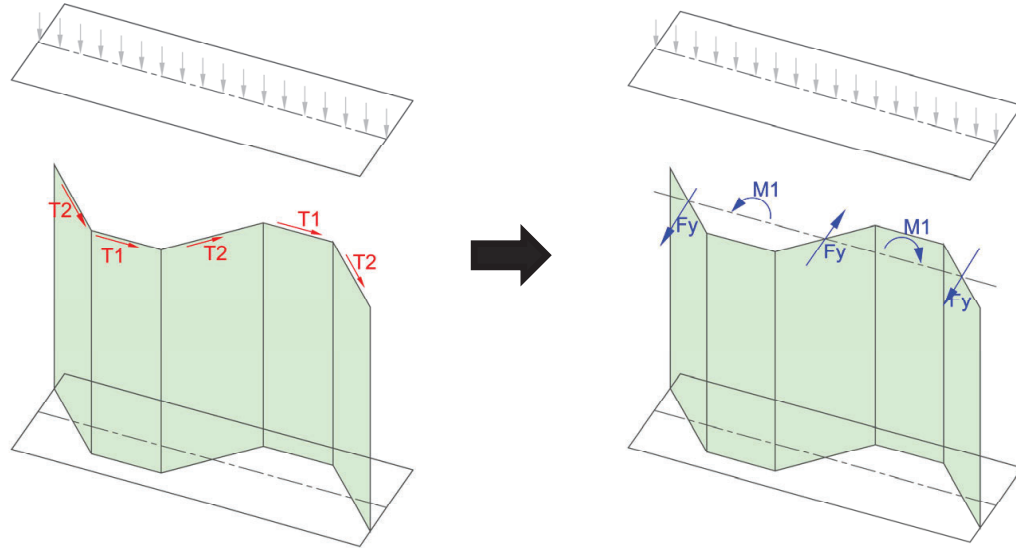


Figure 12 Transverse actions due to shear flow introduction into the flange

However, there are various opinions on the effect of these additional normal stresses on lowering the beam's moment capacity. EN1993-1-5 [24] takes into account the effect of this transverse bending moment by decreasing the yield strength of the flange by a factor, f_T , for both tension and compression flanges. The reduction is dependent on the magnitude of transverse bending stress caused by shear flow in the flanges. Elamary et al. [59] investigated the behaviour of corrugated web beams subjected to bending and shear using experimental, computational, and analytical methods. The four-

point bending test was used, and the failure occurred in the area of combined bending and shear, indicating that the bending and shear interacted. Based on the findings, the authors concluded that the EN1993-1-5 model may be used safely when the load is applied to the inclined fold, and they proposed a new formula for scenarios where the load is applied to the horizontal fold (which gives additional capacity).

Many studies [56, 58, 60] were conducted to quantify transverse bending analytically. Abbas et al. [61] propose two methods, namely, the C-factor method and the fictitious load method, to estimate the transverse bending moment. Baláž, I., and Koleková [60], in 2012, proposed a simple formula to calculate the maximum transverse moment based on two case studies. Following that, the effects of geometric properties, corrugation geometry, lateral and end supports, and different loading conditions were extensively studied by Kövesdi et al. [56] to find the most unfavourable case that gives the maximum additional normal stress to the flange from the shear flow. The maximum transverse moment that was obtained in this study was double what was found in 2012. According to the authors, the highest reduction in bending resistance due to the combined M-V loading scenario was not larger than 4,7%. The observed resistance reduction is not greater than the bending resistance contribution from the web or the shear buckling resistance contribution from the flange. Therefore, the authors stated that, when a plastic design is adopted, there is no interaction between the amount of the transverse bending moment and the reduction in bending resistance.

Moreover, Elgaaly et al. [62-64] investigated the bending and shear resistance of trapezoidal corrugated web girders. The researchers reported that there is no relationship between the bending and shear resistance of trapezoidal corrugated web girders.

Based on the abovementioned results, which showed the reduction in bending capacity due to the accompanying shear forces is negligible [56], [62-64], the bending resistance can be mainly calculated based on the contribution from the flanges, with a focus on the buckling of the compressed flange, which has a considerable effect on the moment resistance.

2.7.2 Flange buckling

EN1993-1-5 design model that accounts for the effect of instability (or buckling) on element resistances, starts by estimating the elastic critical buckling stress (σ_{cr}), i.e., the stress at which the plate is expected to buckle. This buckling stress defines the slenderness of the plate, and it differs based on the plate loading and boundary conditions. The flanges in flat web girders can be assumed to be simply supported plates on three edges. However, due to the existence

of the corrugation, the boundary conditions are different, and thus the buckling stress is expected to be different. The EN1993-1-5 model for flange buckling resistance in flat and corrugated web beams can be summarized as follows:

The flange plate's slenderness is defined as:

$$\bar{\lambda}_p = \sqrt{\frac{f_y}{\sigma_{cr}}} = \frac{\bar{b}}{t} \quad (2-3)$$

where $\varepsilon = \sqrt{\frac{235\text{MPa}}{f_y}}$, $\bar{b} = \frac{b_f}{2}$, t is the plate thickness.

σ_{cr} is the critical elastic buckling stress defined as:

$$\sigma_{cr} = \sigma_E * k_\sigma, \quad \sigma_E = \frac{\pi^2 E t^2}{12(1 - \nu^2) b^2} \quad (2-4)$$

b and t are the width and the thickness of the plate, ν is Poisson's ratio. For flat web $k_\sigma = 0.43$ and for corrugated web $k_\sigma = \min(k_{\sigma 1}, k_{\sigma 2})$

Where $k_{\sigma 1} = 0.43 + \left(\frac{c_f}{a}\right)^2$ and $k_{\sigma 2} = 0.6$

$a = a_1 + 2a_4$ and $c_f = \frac{b_f}{2} + \frac{a_3}{2}$ is the larger flange outstand from the toe of the weld to the flange edge.

The moment capacity is then calculated as:

$$M_{Rd} = \min \left\{ \begin{array}{l} \frac{f_{yf} \cdot b_{cf,eff} \cdot t_{cf}}{\gamma_M} \cdot \left(h_w + \frac{t_{cf} + t_{tf}}{2} \right) \\ \frac{f_{yf} \cdot b_{tf} \cdot t_{tf}}{\gamma_M} \cdot \left(h_w + \frac{t_{cf} + t_{tf}}{2} \right) \end{array} \right. \quad (2-5)$$

Where $b_{cf,eff}$ the effective width of the compressed flange. t_{cf}, t_{tf} top and bottom flanges thicknesses. b_{tf} is the width of the tensioned flange. γ_M is the safety factor.

The effective width of the compressed flange is calculated as follows:

$$b_{cf,eff} = \rho * b_{cf} \quad (2-6)$$

Where ρ is the buckling reduction factor. It is calculated as follows:

$$\rho = 1.0 \text{ for } \bar{\lambda}_p \leq 0.748$$

$$\rho = \frac{\bar{\lambda}_p - 0.188}{\bar{\lambda}_p^2} \leq 1.0 \text{ for } \bar{\lambda}_p > 0.748 \quad (2-7)$$

Johnson and Cafolla [31] investigated which outstands should be employed in the EN1993-1-5 model using finite element modelling and experimental testing. The authors observed the impact of the enclosing effect (R defined as the ratio of areas EFGH and ABCD in Figure 13) on the effective width due to flange buckling. Based on their experimental findings and finite element analysis, the authors established that for $R \leq 0.14$ and a corrugation angle of 30 degrees, the average flange outstand ($b_f/2$) should be used to derive the relative slenderness ratio of corrugated web girders. When R is larger than 0.14, the greater outstand, c_f , should be employed instead.

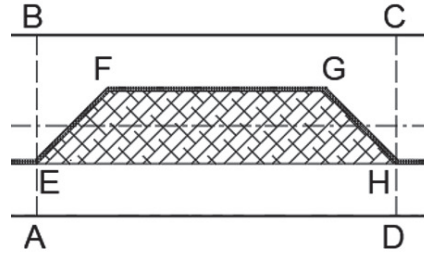


Figure 13 Illustration of enclosing effect in corrugated web beams (R defined as the ratio of areas EFGH and ABCD)

DAST-Richtlinie 015 [32] provide a model for estimating the effective flange width for corrugated web, which is based on the flange thickness and flange yield stress, which is expressed as:

$$b_{f,eff} = 30.7 \cdot t_f \cdot \sqrt{\frac{240}{f_{yf}}} \leq b_f \quad (2-8)$$

Based on the findings of Koichi and Masahiro [7], a design relationship in the form of Equation (2-9) was given for plates that are simply supported at three edges. The buckling coefficient ranged from 0.43 to 1.28.

$$\rho = \frac{c_{f,eff}}{c_f} = \left(\frac{0.7}{\lambda_p} \right)^{0.64} \leq 1.0 \quad (2-9)$$

Where $\lambda_{pf} = \frac{1.052}{\sqrt{k_f}} \frac{b_c}{t_f} \sqrt{\frac{f_{yf}}{E}}$, $b_c = (b_f + a_3)/2$, $k_f = 0.425 + \frac{1}{\alpha^2} \leq 1.28$, $\alpha = (a_1 + a_4)/b_c$.

Furthermore, Jager et al. [30, 65, 66] concluded that EN1993-1-5 predicts unsafe moment resistances for corrugated web beams based on numerical and experimental studies, and they developed a new model for the moment resistance of corrugated web beams with reference to flange buckling. The following is a summary of the model:

The buckling reduction factor is calculated from the following equation:

$$\rho_a = \min \left(1, \left(14 \cdot \varepsilon \cdot \frac{t_f}{c_f} \right)^\beta \right) \quad (2-10)$$

Where the large outstand of the compression flange are:

$$c_f = \frac{b_f + a_3}{2} \quad (2-11)$$

The factor β is defined as:

$$\beta = 5 \cdot \eta \cdot R \cdot \left(\frac{1}{\tan(\alpha)} \right)^\eta \quad \text{where } 0.5 \leq \beta \leq 1 \quad (2-12)$$

The enclosing effect R can be calculated as follows:

$$R = \frac{(a_1 + a_4) \cdot a_3}{(a_1 + 2 \cdot a_4) \cdot b_f} < 0.14 \quad (2-13)$$

The factor η that considers the flange to web thicknesses ratio, and can be estimated as:

$$\eta = 0.45 + 0.06 \cdot \frac{t_f}{t_w} \quad (2-14)$$

Moreover, the authors developed an expression for the buckling factor k_σ based on parametric linear buckling analysis. According to Jager et al. [30], the buckling factor may be estimated as follows:

$$k_\sigma = \min \left(1.3, 0.43 \cdot \left(2.5 \cdot \frac{t_w}{t_f} \right)^{(0.6+R)} + \left(\frac{c_f}{a_1 + 2 \cdot a_4} \right)^2 \right) \quad (2-15)$$

2.7.3 Residual stresses and initial imperfection effects on flange buckling resistance

In buckling problems, residual stresses have been shown to have a significant impact on load-carrying capacity [66]. Pasternak and Kubieniec [67] observed significant nonlinearities in the normal stress distribution during bending in research on the residual stress distribution of sinusoidally corrugated web girders in 2010. In 2014, Lho et al. [68] evaluated residual stresses in the tension flange of corrugated web girders and observed that tensile residual stresses near welds might exceed $0.4fy$. Furthermore, Li et al. [69] employed residual stresses in FE model flanges and noticed that they could reduce the load-carrying capacity of slender flanges by 14%.

Manufacturers have fabrication tolerances for trapezoidal corrugated web girders, and Annex C in EN1993-1-5 suggests a greater magnitude than the fabrication tolerances for equivalent

geometric imperfection. This proposal considers both residual stresses and geometric imperfections, with a suggested value of $\frac{c_f}{50}$ for flange twist. However, this proposal is not limited to corrugated web girders. Therefore, Jager et al. [66] investigated the applicability of the EN1993-1-5 proposal for flange buckling in corrugated web beams using numerical analysis supported by tests. The author concluded that the EN1993-1-5 suggestion might be applied for flange buckling in carbon steel corrugated web beams.

2.7.4 Shear buckling

The research on the shear buckling resistance of corrugated web beams began in 1969. Numerous studies have been conducted. Shear buckling was found to be the most common cause of failure for girders with corrugated webs under shear loading. Three shear buckling modes have been observed from the previous tests: local, global, and interactive buckling [70]; see Figure 14.

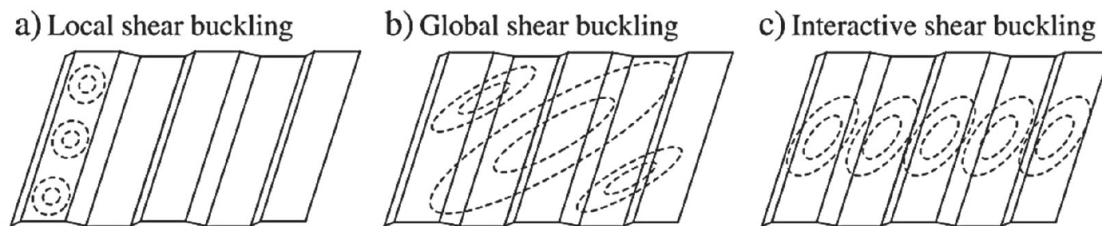


Figure 14 Shear buckling modes of trapezoidal corrugated steel webs [70]

The current Eurocode version includes a design model for estimating the shear capacity of corrugated web beams. The model is presented in EN1993-1-5, Annex D, Section D.2.2. This model considers the local and global buckling modes independently, but not the interaction buckling mode. Other researchers, on the other hand, were focused on defining the relationship between local and global buckling modes to predict the shear resistance of corrugated web beams [71-73].

According to Moon et al. [74], and Sause et al. [73] the ultimate shear capacity of corrugated web girders is determined by buckling load, while Zang et al. [75] believe that flanges can also contribute to shear resistance through frame action. However, shear resistance is likely to be restricted by web buckling in actual bridge girders with considerable distances between stiffeners and flexible flanges.

The shear resistance is defined by Eurocode as the minimal local and global buckling load. Leblouba et al. [71] showed that using the Eurocode design curve yields conservative estimates for local and global buckling [76]. However, based on 125 previous tests, they

provided a new equation for shear strength for the interactive buckling mode (interaction of order $n = 4$) [71].

In the case of stainless steel, the first experimental work was carried out as part of the SUNLIGHT project at Chalmers University of Technology [77]. Four EN1.4162 girders with varying corrugation geometry characteristics were constructed and tested in three-point bending. In comparison to the test findings, the EN 1993-1-5 design model provided rather conservative strengths [22]. Furthermore, two master theses were done at Chalmers University of Technology [26, 27] and limited parametric research was carried out. It was found that employing the present design approach in EN1993-1-5 produces safe results.

2.7.5 Lateral torsional buckling

A beam deflects vertically when a vertical load is applied to it. At the same time, if the beam lacks sufficient lateral stiffness or support, it can deflect laterally in the out-of-loading plane direction even at lower loads than its in-plane capacity. The beam deflects laterally and twists (lateral torsional buckling) only when the applied moment reaches the critical value [78]. However, corrugated web girders withstand lateral torsional buckling more effectively than flat web girders because of their increased transverse bending stiffness, which increases with deeper corrugations [78].

Eurocode provides two methods for LT-buckling, including the exact method, which is defined in Section 6.3.2.2 of EN1993-1-1, and the simplified method of the equivalent compression flange, which is defined in Section 6.3.2.4 of EN1993-1-1. The simplified method in Eurocode is developed only for carbon steel. To use the simplified method, buckling curve d should be used for stainless steel, according to Table 5.3 in the Amendment to 1993-1-4 [79].

The Eurocode standard does not include a formula for calculating the critical buckling moment of corrugated web girders using the exact method. The modified version of Linder, however, provides an adequate estimate of the critical buckling moment [80]. This formulation, proposed by Larsson and Persson [81], considers the influence of corrugation by adding part $\frac{c_w}{G}$ to the torsional constant of flat web beams rather than the additional part $c_w \frac{L^2}{E\pi^2}$ proposed by Linder to be added to the warping constant of flat web beams.

The elastic critical buckling moment is related to its resistance against lateral torsional buckling. Several authors studied the elastic buckling moment and found that it changes based on the bending moment diagram, boundary conditions, load application point, and, of course, the geometric dimensions of the girder. Moon et al. [82] used finite element analysis to investigate the lateral torsional buckling of

I-girders with corrugated webs. They found that the elastic buckling moment of corrugated webs is greater than that of flat webs, especially as corrugation depth increases. However, at angles less than 45 degrees, there is a minimal difference between flat webs and corrugated webs. The two types have the same pure torsional constant, however flat webs have a lower warping constant and a larger shear modulus. Although the study concentrated on curve d, the Eurocode approach is considered applicable and conservative.

Nguyen et al. [83] employed a FEM program to study the moment modification factors of an I-girder with trapezoidal web corrugations when subjected to a concentrated load. Different load positions, such as top flange, shear centre, and bottom flange, as well as different end boundary conditions, such as simply supported, warping fixed, lateral bending fixed, and fixed, have been investigated. The author concluded that the critical buckling moment should be modified by factor C , which is determined by the boundary conditions and the concentrated load position. This effect is planned to be implemented in the new generation of Eurocode [23].

Furthermore, Edvardsson et al. [80] did a nonlinear finite element analysis and compared the results to Eurocode. The EN1993-1-1 design model for lateral torsional buckling was shown to be conservatively applicable to constrained girders with corrugated web as well as flat web.

2.7.6 Patch loading

Few studies have presented approaches to evaluating the patch-loading resistance of corrugated web girders, and the problem is not yet included in the current edition of Eurocode. However, a proposed design model is provided in a draft for the next edition [23].

In 1996, Lou and Edlund [84] used nonlinear finite element analysis to estimate the ultimate load capacity of trapezoidal corrugated web girders under patch loading. An empirical model for determining patch-loading resistance was suggested based on this study. In 1997, Elgaaly et al. [85] did parametric research using FEM to provide a simple design model for patch loading capacity based on failure tests under partial compressive edge loading. Furthermore, new equations for (patch loading & shear) and (patch loading & moment) interactions were proposed.

In 2010, Kövesdi et al. [86] examined 12 large girders that were simply supported in an experimental program. The purpose of the testing was to investigate the patch-loading resistance of corrugated web girders. The ultimate loads were calculated, and the structural behaviour and failure mechanisms (web crippling and local web buckling) were studied and discussed. Based on the test results, Braun and Kuhlmann's previously created design method was

validated and enhanced. The resistance to patch loading in this design model is distributed between the web and the flanges. The design model provided in a draft of the new edition of EN1993-1-5 is based on the model produced by Kövesdi without taking into account the flange's contribution to patch loading resistance [23].

In terms of stainless steel material, a master's thesis was carried out at Chalmers University of Technology to investigate the patch-loading resistance of stainless steel corrugated web girders [28]. A similar finding about the flange contribution to path loading capacity was proven for stainless steel. The EN1993-1-5 model produces such conservative findings because it ignores the flange contribution to patch loading resistance. Based on the results, none of the available models offers a credible estimate of the patch-loading resistance of corrugated web girders. As a result, until a more practicable model is produced, the suggested model in the new draft for EN1993-1-5 is advised to be used [28].

2.7.7 Fatigue resistance

Several fatigue studies have been conducted in the past to compare the fatigue performance of welded stainless-steel details to that of carbon steel details. Several authors, according to Baddoo [52], have examined several types of welded details and earlier tests demonstrated that the fatigue performance of austenitic and duplex stainless steel is comparable to or slightly greater than that of carbon steel. Accordingly, EN 1993 recommends using the same S-N curves for stainless steel as for carbon steel. Furthermore, no design curves for stainless steel are currently accessible in the regulations, and no tests or information are available in the literature for stainless steel corrugated web girder details.

Several previous studies on the fatigue resistance of carbon steel corrugated web beams have been conducted [29]. Previous authors employed a variety of approaches and points of focus, such as loading and welding, for different geometries such as trapezoidal corrugations, sinusoidal corrugations, and discrete corrugations. Two types of stress conditions are considered: four-point bending and three-point bending. The maximum nominal stress ranges at the point of fracture at the top of the bottom flange are specified as the stresses σ_{nom} .

Save et al. [29] compiled and summarized the findings of these investigations in their master thesis, which was performed at Chalmers University of Technology in 2020. Two unexpected findings were observed regarding the fracture zones for four- and three-point bending. Theoretically, fracture is expected in zones of high moment and high shear because of the increased transverse bending moment; however, the study demonstrated that this is not definite.

Approximately half of the girders from the four-point bending examples failed in the constant bending zone, indicating that shear flow-induced transverse bending is not important in these circumstances. Similarly, for three-point bending specimens, the fracture location was anticipated near the highest shear and bending loads, i.e., in the centre of the span. This is often right; however, in a few instances, cracking occurred at a distance from the load [29].

According to the authors [29], when all valid trapezoidal points are picked (excluding outliers), the characteristic fatigue category for corrugated web to flange detail falls into fatigue category 120 MPa; ref. Figure 15.

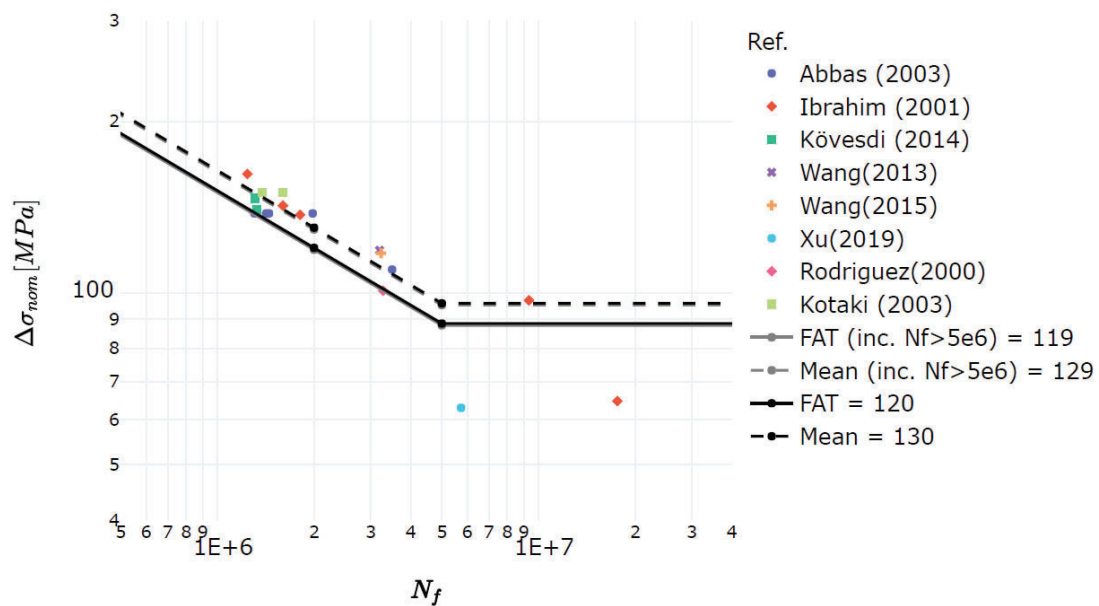


Figure 15 Summary of previous fatigue experiments on trapezoidal CWG, removing outliers. The solid black line represents the fatigue class (95% confidence limit) omitting points greater than 5 million cycles, the solid grey line represents the fatigue class (95% confidence limit) including points greater than 5 million cycles, and the dashed black and grey lines represent the mean fatigue classes [29].

Given that there are no tests or information on the use of stainless steel in corrugated web girders, Save et al. [29] investigated the fatigue performance of CWGs on girders with regular carbon steel and argued that because stainless steel is treated as carbon steel in the codes, the findings in their study are also applicable to austenitic and duplex stainless steel corrugated web girders.

Chapter 3

3 Design optimization of composite road bridges

3.1 Developed optimization routine

3.1.1 Optimization routine scope

The optimization routine in this research, illustrated in Figure 16 is developed to optimize simply supported and continuous road bridges with any number of spans and span lengths. The routine is particularly designed for steel-concrete composite bridges' superstructure, consisting of twin steel I-girders, a concrete deck connected to the steel girders by two rows of shear studs, and cross beams that connect the two main girders in the transverse direction. A typical cross-section for the designed section is presented in Figure 17.

The concrete deck as well as the cross beams are not subjected to optimization. They are designed to fulfil the structural requirements in the ultimate limit state. The concrete deck is designed by keeping the thickness between 250 and 350 mm, which is typical for these types of bridges [87], and the corresponding transverse reinforcement is calculated by assuming the concrete deck as a simply supported beam loaded with load model 1 (LM1). The longitudinal reinforcement is assumed based on the minimum requirements for crack width in EN 1994-2 [88]. The cross beams situated above the supports are designed as frame cross beams to carry the reaction force from only the bridge self-weight, i.e., the traffic loads are assumed to be stopped during the bearing change. The cross beams within the spans are designed as truss cross beams using VKR profiles.

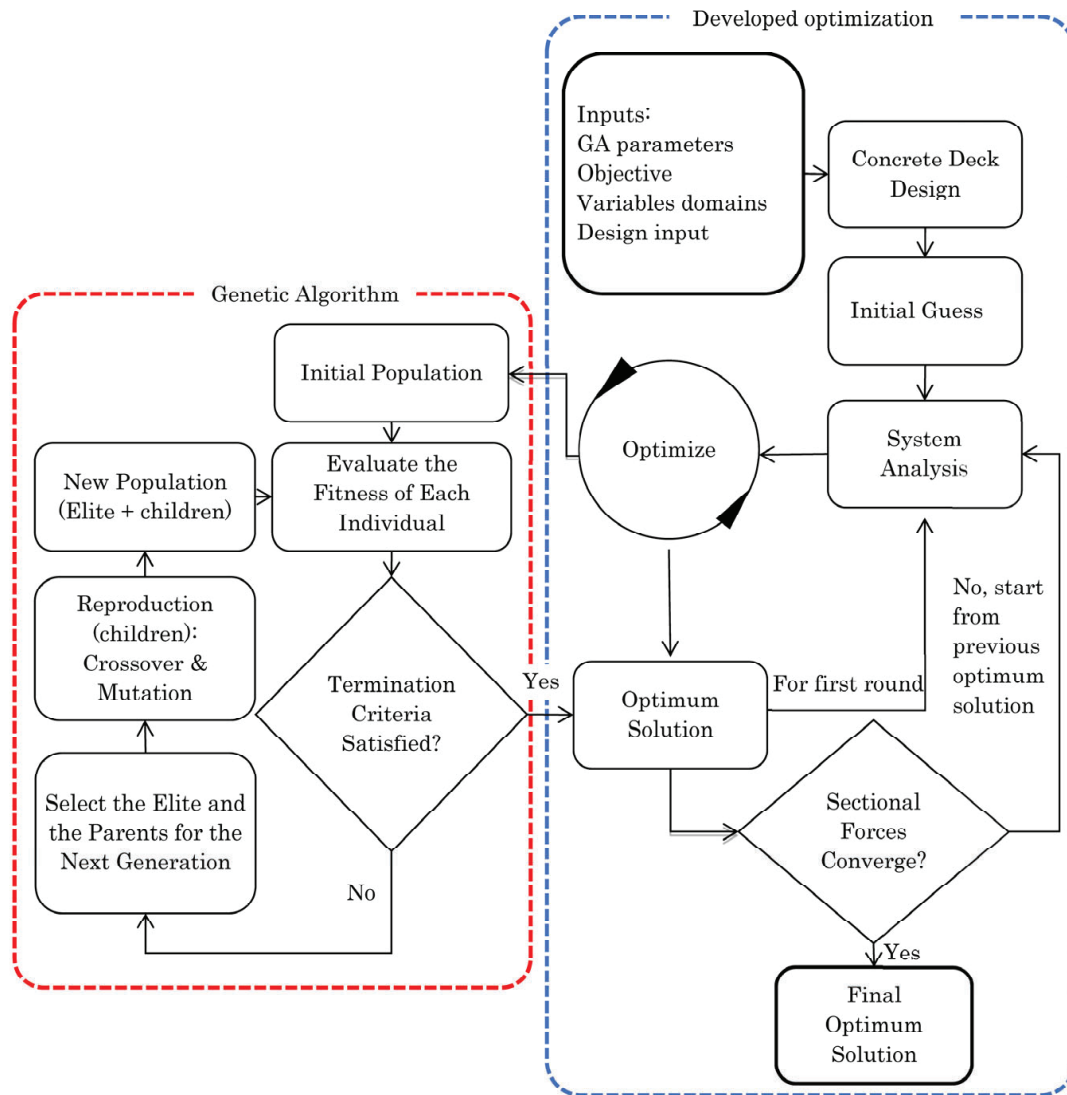


Figure 16 Diagram of the developed optimization routine

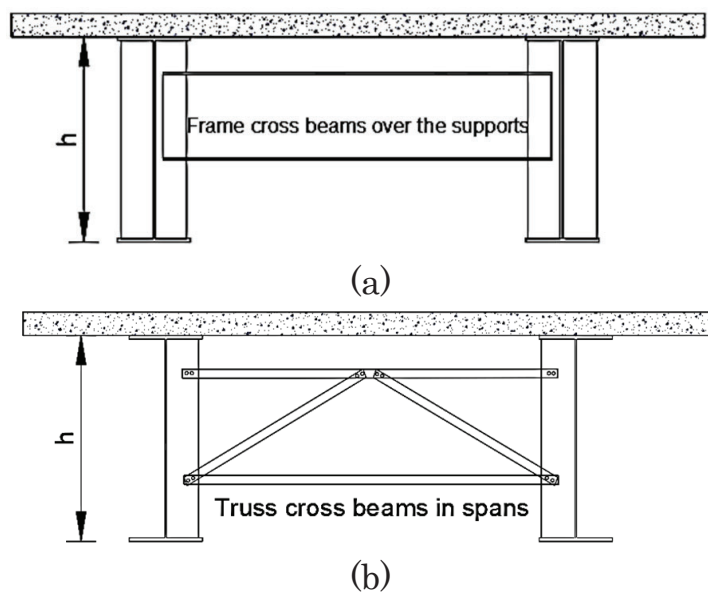


Figure 17 Designed cross-section. (a) above the support (b) in the span

The primary parameters that are focused on in the optimization are the steel girder dimensions ($h_w, t_w, b_{fo}, b_{fu}, t_{fo}, t_{fu}$), the distance between cross beams over the support ($CCB_{support}$), the distance between cross beams in the spans (CCB_{span}), and the corrugation parameters (longitudinal fold length, a_1 , corrugation angle, α , and corrugation depth, a_3). The annotations in Figure 2 provide visual explanations, while Figure 18 summarizes the geometrical parameters that undergo optimization and those that do not.

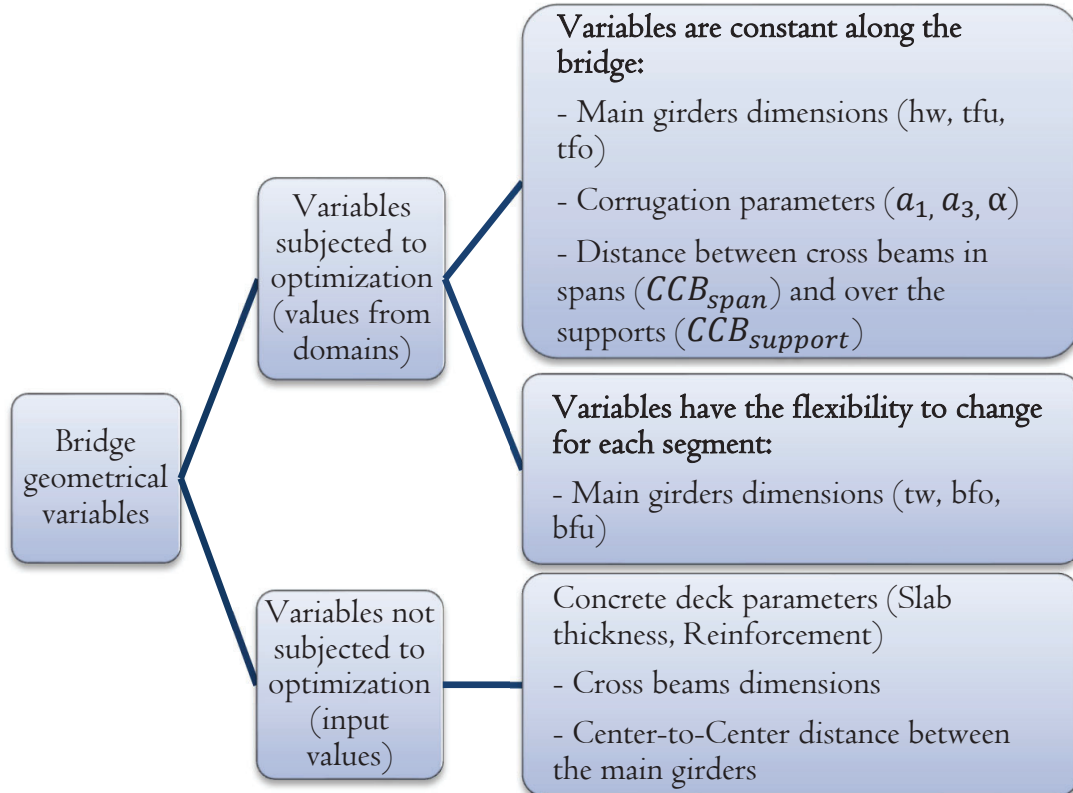


Figure 18 Illustration of the bridge parameters that undergo optimization and those that do not.

Each span is allowed to have a maximum of seven sections; therefore, the length of the optimization vector is determined by the number of spans and can be expressed as follows:

$$X = [h_w, t_{w1}, \dots, t_{wn}, a_1, a_3, \alpha, CCB_{span}, CCB_{support}, b_{fo1}, b_{fu1}, \dots, b_{fon}, b_{fun}, t_{fo}, t_{fu}] \quad (3-1)$$

Where the length of the optimization vector:

$$\text{Len}[X] = 3 * n + 8 \quad (3-2)$$

Where the value of "n" depends on the characteristics of the bridge being designed:

1. If the considered bridge is symmetric:
 - a. When the bridge has an odd number of spans: n denotes the integer number of segments per half bridge+1

- b. When the bridge has an even number of spans: n denotes the integer number of segments per half bridge.
2. If the considered bridge is asymmetric: n denotes the total number of segments along the bridge.

Table 3 showcases examples of how the optimization vector length can be calculated for various scenarios, taking into account the number of spans and their symmetry.

Table 3 Calculations of the optimization vector length

Number of spans	Number of segments per span	Total number of segments	Symmetry	n	$\text{len}[X]$
1	7	$7 * 1 = 7$	Asymmetric	7	$3 * 7 + 8 = 29$
2	7	$7 * 2 = 14$	Asymmetric	14	$3 * 14 + 8 = 50$
1	7	$7 * 1 = 7$	Symmetric, with an odd number of spans	$\text{int}\left(\frac{7}{2}\right) + 1 = 4$	$3 * 4 + 8 = 20$
2	7	$7 * 2 = 14$	Symmetric, with an even number of spans	$\text{int}\left(\frac{14}{2}\right) = 7$	$3 * 7 + 8 = 29$

In this study, the Meta-Heuristic genetic algorithm optimization function has been employed. The algorithm is presented in Figure 16 in relation to the whole optimization routine. The genetic algorithm optimization is a stochastic optimization algorithm and can be summarized in the following steps:

1. Build a population of individuals.
2. Evaluate the fitness of each individual in the population.
3. Check to see if the stopping criteria have been fulfilled. If not, continue to the next step.
4. Select the elite individuals from the current population based on their low fitness values. These elite individuals will be passed on to the next generation.
5. Create new offspring by selecting parents based on their anticipated fitness. The offspring are produced either by mutating a single parent or by combining the genetic components of two parents via crossover. The user defines the

proportion of the old generation that is kept as parents: 'parents_portion'.

6. Create a new generation by keeping the elite of the previous generation and adding the offspring of previous generation parents.
7. Go back to the second step. The algorithm stops when one of the stopping criteria is met.

Herein, the genetic algorithm used was developed by Solgi (2020) and further developed by Demetri Pascal [89] to allow for parallelization. The design vector X , Equation (3-1), which represents each outcome of the genetic algorithm, is referred to as a chromosome, and each of its variables is a gene [41]. For the algorithm to select various values, a design domain must be established for each gene. The algorithm does not handle discrete domains, even though the variables in this study have discrete values in their domains. Therefore, the discrete values of the domains are collected in a vector, and the method is then allowed to select the discrete values from a continuous integer domain between 0 and the length of the vector. Regarding the genetic algorithm parameters, a sensitivity study is conducted to calibrate these parameters for both three-span and single-span bridges.

Table 4 summarizes the employed genetic algorithm parameters.

Table 4 Genetic algorithm parameters used in this study

Parameter	Chosen value for 3 spans	Chosen value for 1 span
Iterations	500	100
Population size	500	100
Mutation probability	0.2	0.2
Elite ratio	0.3	0.3
Parents portion	0.3	0.3
Crossover type	'uniform'	'uniform'
Max iteration without improv	150	50

The algorithm is trained to get closer to the optimal solution by adding constraints and penalizing the solutions that do not meet these constraints. The constraints that are considered in this work are primarily the utilization ratios for main girders, which must all be less than one. Other functional constraints are introduced, such as the top flange being compressed (as this assumption is used when calculating cross-sectional properties). Furthermore, the utilization ratios for the cross beams are constrained. The penalty function is obtained from Bozorg-Haddad et al. [41] and can be expressed as follows:

$$\text{penalty} = \sum g_i(\eta_i(\mathbf{x}))\phi_i + h_j(\xi_j(\mathbf{x}))C \quad (3-3)$$

$$g_i(\eta_i(\mathbf{x})) = \begin{cases} 0 & \text{if } \eta_i \leq 1 \\ 1 & \text{otherwise} \end{cases} \quad i = 1, 2, \dots, J \quad (3-4)$$

$$h_i(\xi_i(\mathbf{x})) = \begin{cases} 0 & \text{if fulfilled} \\ 1 & \text{otherwise} \end{cases} \quad j = 1, 2, \dots, K \quad (3-5)$$

$$\phi_i = \alpha(\eta_i - 1)^\beta + C \quad (3-6)$$

$$F(\mathbf{x}) = f(\mathbf{x}) + \text{penalty} \quad (3-7)$$

Where $F(x)$ is the objective function, $f(x)$ is the fitness function, and $g_i(\eta_i(\mathbf{x}))$ is the penalty function for the constraints of the utilization ratios, and $h_i(\xi_i(\mathbf{x}))$ is the penalty function for the other constraints. J denotes the number of constraints on utilization ratios and K denotes the number of other constraints. The penalty weight factors α, β , and C which aid in the mapping of the genetic algorithm's path, are, as recommended by Bozorg-Haddad et al. [41], calibrated by performing a sensitivity study. The factor β is set to 1 and the other two factors are set to equal values of $\alpha = C = 1 * 10^9$ when the optimization objective is to minimize the total weight. As the penalty function needs to be related to the objective function, α is recalibrated to $1 * 10^{12}$ for the LCC optimization objective and to $1 * 10^{10}$ for the total carbon footprint optimization objective.

3.1.2 LCC calculation model

To compare the different concepts from an economic standpoint, a model that calculates the overall expenses over the bridge's service life is developed in this work based on the classification of life cycle modules of buildings. The model is summarized in Figure 19, and Table 5 provides a complete breakdown of cost estimations for various phases including the investment phase, usage phase, and end-of-life phase. The net present value (NPV) approach, which approximates the present value of all predicted cash inflows and outflows for a project, is used to estimate future costs (user costs, maintenance costs, and reselling costs). The production costs calculation model is developed based on interviews with two bridge Production workshops in Sweden. The manufacturers determined production costs by considering an average manhour cost (550 SEK per hour) and the duration required for various activities such as grinding, plate welding, and shear stud welding. More detailed information on these cost calculations can be found in [90], which will be published as part of the LIGHTSPAN project results ([LIGHTSPAN | LIGHTer](#)). Steel unit pricing was collected from two manufacturers in Sweden for the

fourth quarter of 2022 and they are presented in Section 1 of the appendix.

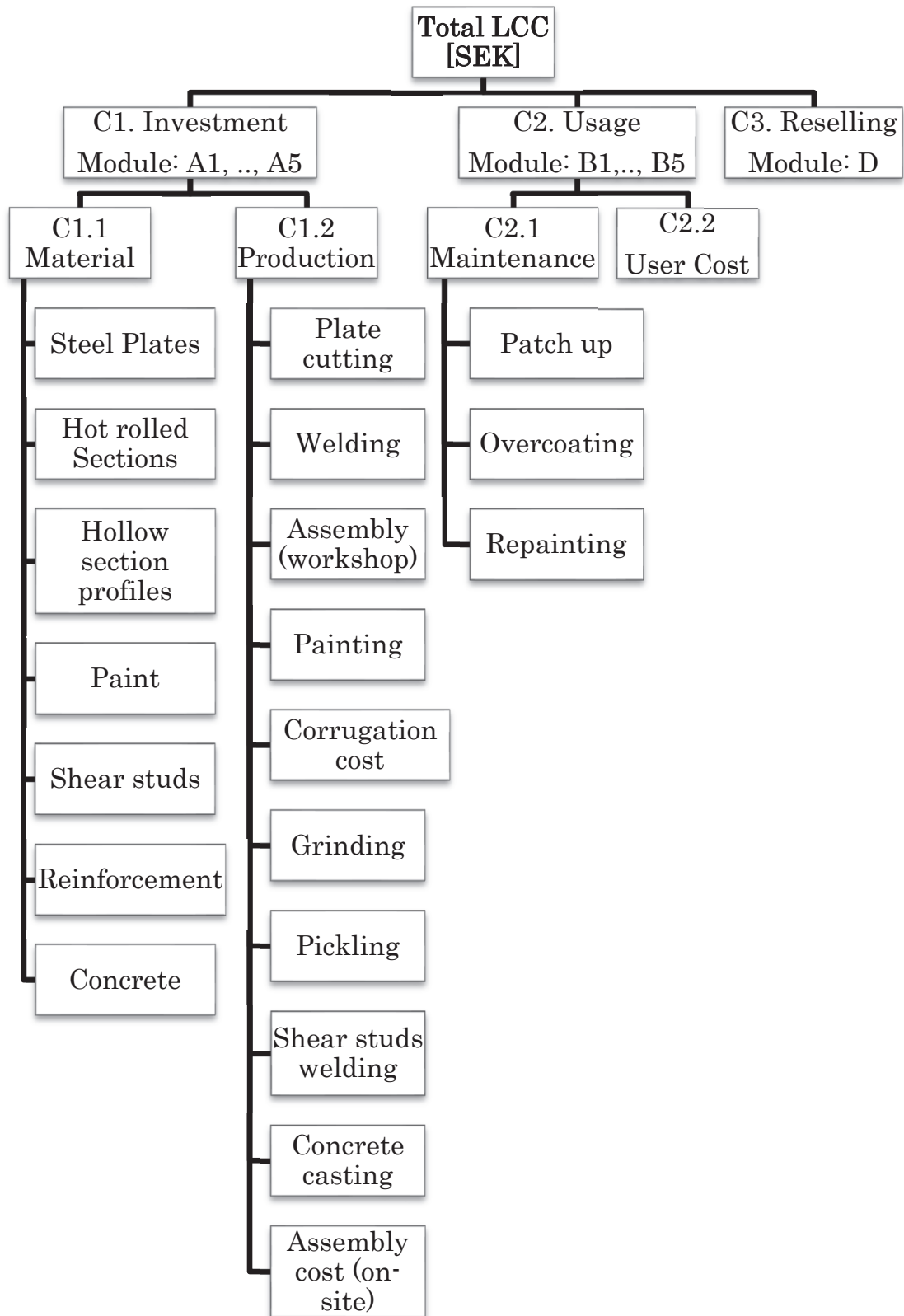
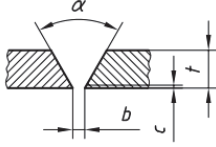


Figure 19 An overview of the LCC system boundaries that are included in the developed model

Table 5 Life cycle cost calculations

#	Item	Description
	Total LCC	Total LCC = Investment cost (C1) + Usage cost(C2) – Revenues from reselling (C3)
C1	Investment cost	Investment cost (C1) = Material cost(C1.1) + Production cost(C1.2)
C1.1	Material cost	Material cost = Main girders + Concrete + Reinforcement + Cross beams + Paint + Shear studs
	Production cost	Production cost = Plate cutting + Welding + Assembly (workshop) + Painting (for carbon steel) + Corrugation cost + Edge grinding to P3 + Pickling cost (for stainless steel) + Shear studs welding + Concrete casting + Assembly cost (on- site)
	Cutting cost	Cutting edges cost = 1650 SEK /ton of steel in the bridge
		Welding cost = $ns * L * c_w / (l)$ ns : number of weld passes required for weld area $ns = \frac{(A_w + 30)}{19}$
C1.2	Welding	 <p>A_w: the welding area for fillet or butt weld [mm^2] c_w: the welding cost per hour SEK/h l: the length that a welder runs per one hour (one pass), or <i>welder productivity</i> L: the welding length [m]. Additional cost for butt weld: Edge preparation = 350 SEK / m of butt weld $t > 20$ mm Edge preparation = 200 SEK / m of butt weld $t \leq 20$ mm</p>
	Assembly cost (workshop)	Assembly cost = 30% * Welding cost
	Painting	Painting cost = Painting area * Painting unit cost Painting unit cost:

	Workshop: $C4 = 800 \text{ SEK} / m^2$ $C5 = 1000 \text{ SEK} / m^2$ On-site $C4 = 2400 \text{ SEK} / m^2$ $C5 = 3000 \text{ SEK} / m^2$
Corrugation cost	Corrugation cost = Corrugation length * Corrugating unit cost Corrugating unit cost = 2000 SEK/m
Grinding cost	Grinding cost = Grinding length * Grinding unit cost Grinding unit cost = 125 SEK/m This applied only to carbon steel
Pickling cost	Pickling cost = Pickling area * Pickling unit cost Pickling unit cost = 300 SEK/m ² This applied only to stainless steel
Shear studs	Shear studs welding = Number of shear studs* Welding cost per piece Welding cost per piece = 45 SEK / piece
Concrete casting	Concrete casting = Concrete volume * Casting unit cost Casting unit cost = 35 SEK/m ³
Assembly cost (on-site)	Assembly cost = Weld main girders to end cross beams + weld main girders splices + bolt intermediate cross beams to the main girders Main girders and end cross beams (welded) = 9000 SEK / splice (= 16 manhours) Intermediate cross beams (bolted) = 2200 SEK /cross beam
C2 Usage cost	Usage cost (C2) = Maintenance activities cost(C2.1) + User cost (C2.2)
C2.1 Maintenance	Maintenance activities cost $= \sum_j \left(\sum_a (A_{a,j} * P * C_{a,j}) \right) * (1 + i/1 + d)^n$ <p>$A_{a,j}$: The process for component j is needed for maintenance activity a. In this study, it refers to the initial painting area [m²] P: The operating percentage for each maintenance activity, i.e., patch-up, overcoating, and repainting [%] $C_{a,j}$: The unit cost of maintenance activity a, for component j [$\frac{\text{SEK}}{m^2}$]</p>

	<p>i: The inflation rate [-] d: The discount rate [-] n: The year number [-]</p>
	<p>User cost =</p> $\sum_j \left(\sum_a \left(\text{Time} * \text{ADT} * T_{a,j} * \left(h_t * p_t + h_p * (1 - p_t) \right) * (1 + i/1 + d)^n \right) \right)$ <p>Where Time = $L_{\text{aff}} * (1/v_r - 1/v_n)$ L_{aff}: Affected road length [km] ADT: Average daily traffic [Vehicle per day] $T_{a,j}$: The time needed for maintenance activity a, for component j [days] h_t: Cost for heavy truck per hour [SEK/hour] p_t: Heavy vehicles percent among the average number of daily traffic [%] h_p: Cost for passenger car per hour [SEK/hour] v_r: Reduced speed [km/hour] v_n: Normal speed [km/hour]</p>
C2.2 User Cost	<p>Revenues from reselling =</p> $\sum_j \left(\sum_m \left(q_{m,j} * r_m * P_{\text{eol}} \right) * (1 + i/1 + d)^Y \right)$ <p>$q_{m,j}$: The quantity of material m in component j [kg] r_m: The recycling rate of material m [%] P_{eol}: The unit price of end-of-life material m: [SEK/kg] Y: The service life of the bridge [years]</p>
C3 Reselling	

The welding details investigated in this study, specifically C1.2 as outlined in Table 5, are illustrated in Figure 20. It is assumed in the cost calculations that, except for crossbeam assembly to the main girders and girder splices done on-site, all welding activities are carried out at the workshop; see Table 6. In addition, the maximum bridge segment length that can be delivered to the side is assumed to be 25 meters.

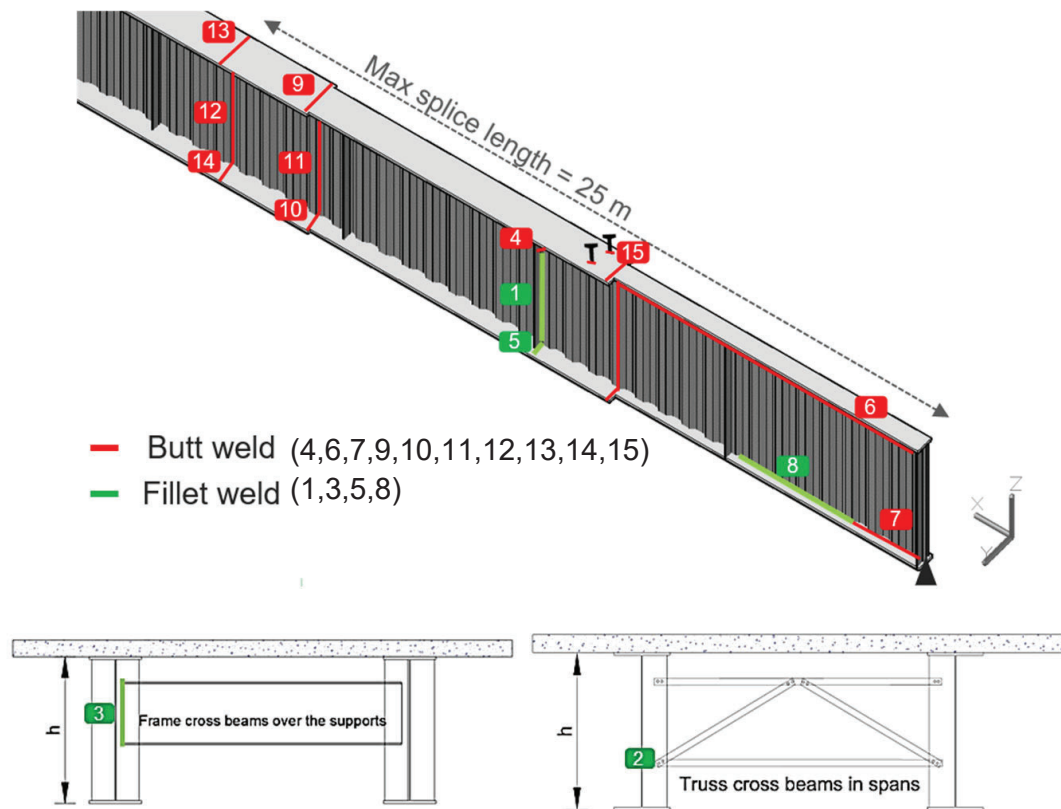


Figure 20 Illustration of the considered welded and bolted details

Table 6 The considered welded and bolted details

Group	#	Description	Connection type	Working place
Stiffeners	1	Web to vertical stiffeners	Fillet weld	Workshop
	2	Span crossbeams to vertical stiffeners	Bolted	On-site
	3	End and support crossbeams to the vertical stiffener.	Fillet weld	On-site
Main girder weld	4	Upper flange to vertical stiffener	Butt weld	Workshop
	5	Lower flange to vertical stiffener	Fillet weld	Workshop
	6	Flanges to the web, top	Butt weld	Workshop
Segment	7	Flanges to the web, bottom, support	Butt weld	Workshop
	8	Flanges to the web, bottom, span	Fillet weld	Workshop
	9	Upper flange	Butt weld	Workshop

change weld	10	Lower flange	Butt weld	Workshop
	11	Web	Butt weld	Workshop
	12	Web splices	Butt weld	On-site
Splices weld	13	Top flange splices	Butt weld	On-site
	14	Bottom flange splices	Butt weld	On-site
Shear studs	15	Number of shear studs	Shear Studs weld	Workshop

3.1.3 LCA calculation model

The environmental impact of a bridge's life cycle is estimated using a parametric model created by SYU [91] and further developed by Nissan et al. [90] and the author of this research. As shown in Figure 21, the model incorporates environmental impacts from various bridge life stages. The total environmental impact is calculated by adding the impacts from all stages, including manufacture, construction, and end-of-life. The CML 2001 method is used to assess the environmental impact, which is based on climate change GWP quantified in kg CO₂-equivalent.

Table 7 provides a complete breakdown of environmental impact estimations for various phases, including the investment phase, usage phase, and end-of-life phase. A more detailed elaboration on these impact calculations can be found in [90]. The LCA data sources are provided in Section 2 of the appendix.

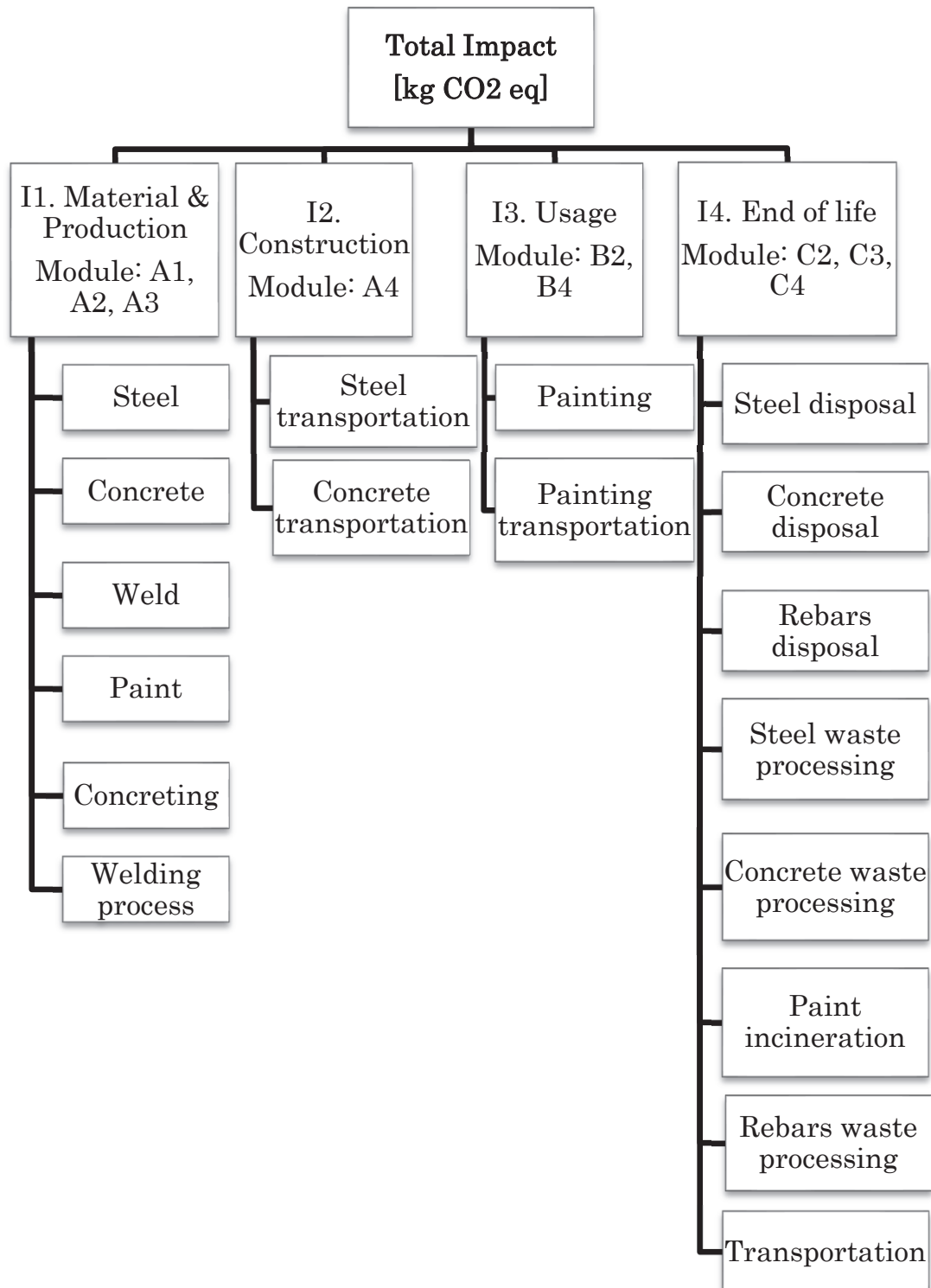


Figure 21 Illustration of the developed LCA calculation model

Table 7 Life cycle environmental impact calculations

#	Item	Description
	Total environmental impact	$Total\ Impact = Production\ phase\ impact\ (I1)$ $+ Construction\ phase\ impact\ (I2)$ $+ Usage\ phase\ impact\ (I3)$ $+ EOL\ impact\ (I4)$
I1	Production phase impact	$Production\ phase\ impact\ [kg\ CO2_{eq}]$ $= Material\ quantity\ [kg]$ $* material\ unit\ impact\ [kg\ \frac{CO2_{eq}}{kg}]$ <i>Material unit impact include material supply and the impact of additional processes needed in the production phase</i>
I2	Construction phase impact	$Construction\ phase\ impact\ [kg\ CO2_{eq}]$ $= Material\ quantity\ [kg]$ $* transport\ distance\ of\ material\ [km]$ $* The\ impact\ assessment\ results\ per\ (ton$ $* km)\ of\ the\ transportation\ [kg\ \frac{CO2_{eq}}{ton * km}]$
I3	Usage phase impact	$Usage\ phase\ impact\ [kg\ CO2_{eq}]$ $= Impact\ of\ paint\ production\ for\ the\ maintenance\ plan\ [kg\ CO2_{eq}]$ $+ Impact\ of\ transportation\ of\ produced\ material\ for\ the\ maintenance\ activities\ [kg\ CO2_{eq}]$
I4	End-of-life (EOL) phase impact	$End - of - life\ phase\ impact\ [kg\ CO2_{eq}] = Impact\ of\ waste\ processing\ [kg\ CO2_{eq}]$ $+ Impact\ of\ disposal\ processes\ [kg\ CO2_{eq}]$ $+ Impact\ of\ transportation\ in\ the\ EOL\ phase\ [kg\ CO2_{eq}]$ $Impact\ of\ waste\ processing\ [kg\ CO2_{eq}]$ $= quantity\ of\ material\ [kg] * recycle\ rate$ $* impact\ assessment\ results\ per\ treatment\ process\ of\ material\ [kg\ \frac{CO2_{eq}}{kg}]$ $Impact\ of\ disposal\ processes\ [kg\ CO2_{eq}]$ $= quantity\ of\ material\ [kg] * (1 - recycle\ rate)$ $* impact\ assessment\ results\ per\ disposal\ material\ [kg\ \frac{CO2_{eq}}{kg}]$ $Impact\ of\ transportation\ in\ the\ EOL\ [kg\ CO2_{eq}]$ $= quantity\ of\ material\ [kg]$ $* transport\ distance\ from\ construction\ site\ to\ landfills\ [kg] * impact\ of\ transportation\ in\ the\ EOL\ phase\ [kg\ \frac{CO2_{eq}}{ton * km}]$

3.2 Case study: Bridge over Dalälven

To investigate the feasibility of employing stainless steel girders with corrugated webs for road bridges. First, the developed design optimization tool is used to optimize a case study of a continuous three-span bridge. The case study is Kyrko Bridge, a bridge in Avesta municipality in Sweden that needs to be replaced. The optimization goal is set to minimize the total weight for three design solutions, including carbon steel flat web girders, stainless steel flat web girders, and stainless-steel corrugated web girders. The optimal solutions are then assessed in terms of their weight, investment cost, life cycle cost (LCC), and environmental impact. The input parameters for this case study are shown in Table 8 and the bridge cross-section is presented in Figure 22.

Table 8 Design inputs for the Kyrko Bridge case study

Case study location	Above Däl River, Avesta municipality, Sweden
Bridge configuration	3 spans of 55m, 80 m, and 55m. a total length of 190 m.
Bridge width	12.8 m, two traffic lanes (3m*2) + one pedestrian lane on one side (2.3m) + one pedestrian and cyclists' lane on the other side (4.1m)
C/C distance between the two main girders	6.8 m
Average daily traffic (ADT)	11 000 Vehicle/day
The indicated number of heavy vehicles per slow lane (N_{obs})	500 000 Vehicle/year
Design lifespan	120 years
Girder height limitation	2.8 m maximum
Painting schedule	Trafikverket paint maintenance schedule [92]
Optimization objective	Weight

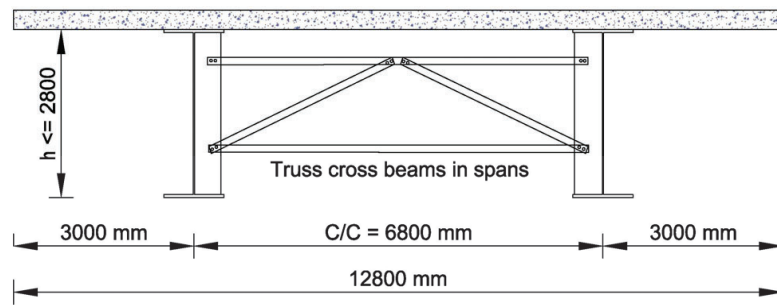
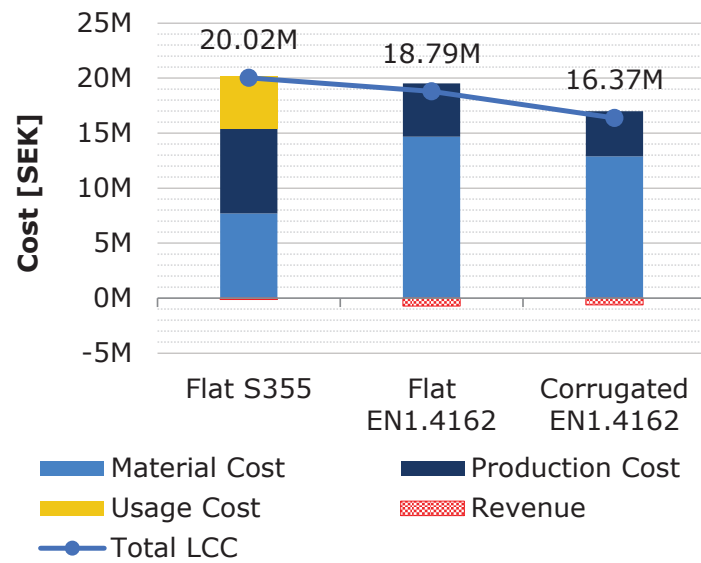


Figure 22 Cross section of Kyrko Bridge case study

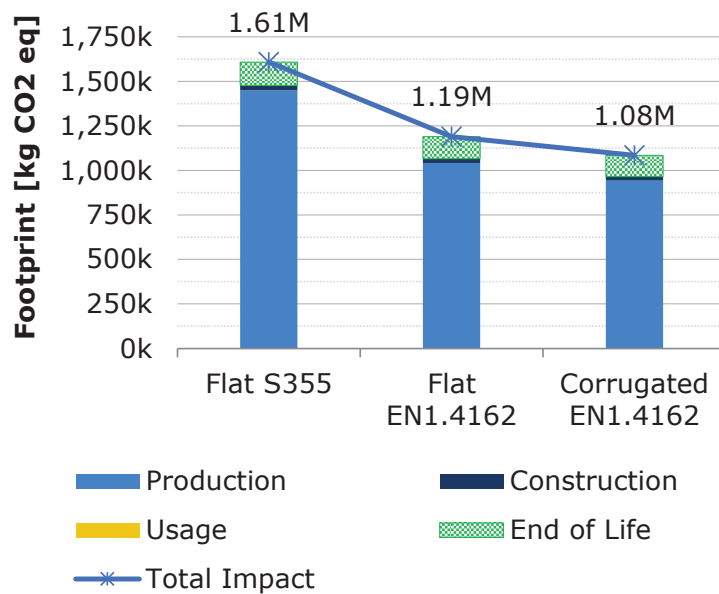
The optimization results of the three design solutions are summarized in Figure 23 and are given in detail in Table 9. When the three optimal options are compared in terms of total weight, it can be seen that the overall weight drops from 386 tons when using the conventional concept of flat web carbon steel girders to 353 tons (approximately 9% less) when the material is changed to stainless steel. Using corrugated web results in an additional 12% reduction in weight (i.e., ca 23% compared to the conventional concept with carbon steel). This weight saving is the result of thinner corrugated webs, ranging from 4 to 10 mm as opposed to 14 to 25 mm for flat webs. The web height is limited to 2.8 m in all design alternatives, although greater saving from flanges is expected when deeper girders are used.

When the three optimal options are compared in terms of LCC (ref. Figure 23 and Table 9), it can be seen that painting during maintenance accounts for a significant portion of the cost for the carbon steel option (about 24%). The Flat EN1.4162 alternative eliminates maintenance costs while raising material costs, resulting in a 6% overall lifecycle cost saving. The corrugated EN1.4162 alternative, on the other hand, eliminates maintenance costs as well, but the 23% weight reduction results in an 18% overall lifecycle cost saving despite the higher material cost. Furthermore, due to the absence of painting and grinding requirements, which are substituted by a less expensive pickling process, flat EN1.4162 has a lower production cost than flat S355. Pickling costs around one-third of the price of the painting. In addition, because there is no painting, no grinding, less cutting, and less welding due to the usage of thinner plates and fewer cross beams are used, the corrugated EN1.4162 option has an even lower production cost than the flat EN1.4162 option.

By evaluating the three optimal options in terms of LCA (Figure 23 and Table 9), it can be observed that the production phase has the greatest CO₂ footprint, while the End-of-life waste processing and disposal phase contributes roughly 10%. When compared to carbon steel, the use of the corrugated web in stainless steel reduces environmental impacts by 32% for the considered bridge.



(a) LCC results



(b) LCA results

Figure 23 optimization results for the three optimized design solution

Table 9 optimization results for the three optimized design solution

	Flat S355	Flat EN1.4162	Corrugated EN1.4162
Total steel weight [ton]	386.4	353.3	296.2
Material cost [SEK]	7 699 414	14 665 096	12 878 076
Production cost [SEK]	7 695 468	4 851 872	4 102 904
Investment cost [SEK]	15 394 882	19 516 967	16 980 980
Usage cost [SEK]	4 753 861	0	0
Revenues from reselling [SEK]	-123 913	-725 580	-608 457
Total LCC [SEK]	20 024 831	18 791 387	16 372 523
Environmental impact during production [$kg CO2_{eq}$]	1 449 133	1 041 043	942 583
Environmental impact during construction [$kg CO2_{eq}$]	25 791	24 701	22 797
Environmental impact during Usage [$kg CO2_{eq}$]	2 807	0	0
Environmental impact at end-of-life [$kg CO2_{eq}$]	130 660	123 601	119 449
Total environmental impact [$kg CO2_{eq}$]	1 608 392	1 189 345	1 084 828

Figure 24 presents a breakdown of the weights for the three optimal solutions. As can be seen, the main saving in weight for the corrugated web concept comes from the web. It is worth mentioning that the height of this bridge was limited to 2.8 m, and fatigue was the governing limit state in a large part of the bridge. The fact that fatigue is governing prevents any additional saving due to the higher strength of stainless steel. If girder height constraints were more generous, deeper girders can be used and the potential saving might be different. Therefore, it would be interesting to see the potential benefits of employing stainless steel corrugated web girders in road bridges when the height limitations are less restrained.

Moreover, the main saving from using the corrugated web in LCC comes from eliminating the painting costs, both during production and maintenance. For this bridge, a painting schedule provided by Trafikverket (Table 11) is used to assess the feasibility of the new concept. However, in relation to the literature (Table 10), this schedule is very “optimistic” as it suggests only a single repainting throughout the entire service life of the bridge (120 years). Therefore,

the benefits of using the new concept will be even higher than what is demonstrated here, if a more extensive maintenance schedule is adopted.

Furthermore, the stainless-steel option is expected to have a higher advantage when the average daily traffic and, thus, the traffic disturbances associated with traffic detouring and reducing vehicle speed limits are high. However, higher ADT means a higher N_{obs} (the indicated number of heavy vehicles per slow lane), which affects the fatigue design. In this case study, ADT and N_{obs} are assumed to be 11 000 vehicle/day and 500 000 Vehicle/year. However, the benefits of the stainless-steel corrugated web solution might also change depending on these two factors.

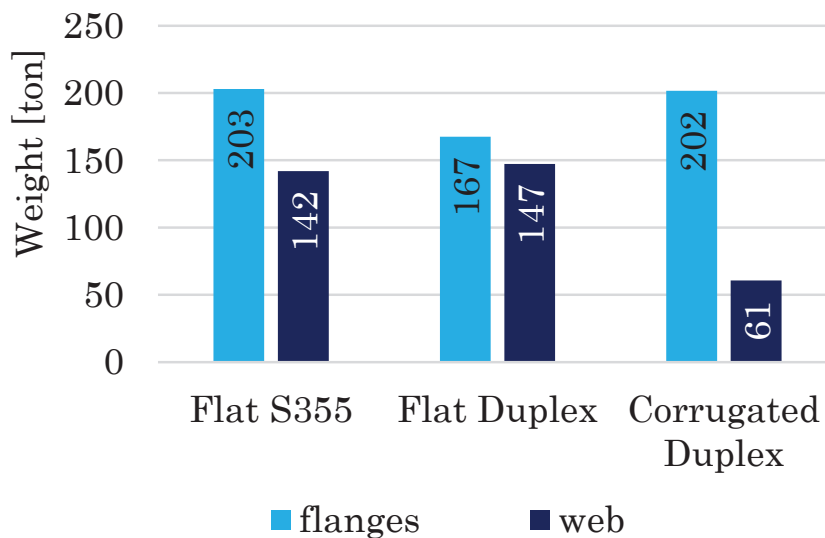


Figure 24 A breakdown of the weight for the three optimal solutions

Regarding the LCC, the results are very sensitive to the assumed inflation (i) and discount (d) rates. Herein, 1.5% and 3.5% are assumed for i and d, respectively. However, the potential LCC benefits of the stainless-steel solution are also dependent on these two factors.

In addition, the optimization objective in this case study is to minimize the weight of the steelwork in the superstructure. However, considering the production costs of the carbon steel option, the painting cost in the production phase (Paint Workshop) was around 3 650 532 SEK, which is around 47% of the total production cost. Based on this, the deep girders with large painting areas and several section changes may decrease the weight but not investment costs or even life cycle costs; therefore, the optimal design solution with regard to weight may not be the same as the optimal design with regard to cost.

Table 10 Painting plan for the structural steelwork of a bridge in the environmental category C4 for 120 years (adopted from Rossi et. al)

Activity	System age	Reference unit	Unit	Relative
Patch up	12.8 years	Initial painted surface	m ²	5%
Overcoating	18.5 years	Initial painted surface	m ²	90%
Remove & replace	31 years	Initial painted surface	m ²	90%

Table 11 Painting plan for the structural steelwork of a bridge in the environmental category C4 for 120 years (provided by Trafikverket)

Activity	System age	Reference unit	Unit	Relative
Patch up	20 years	Initial painted surface	m ²	10%
Overcoating	40 years	Initial painted surface	m ²	20%
Remove & replace	60 years	Initial painted surface	m ²	100%
Patch up	80 years	Initial painted surface	m ²	10%
Overcoating	100 years	Initial painted surface	m ²	30%

3.3 Parametric studies

Based on the understanding gained from the Kyrko Bridge case study (Section 3.2 above), a parametric study that takes into account all of the previously mentioned factors is carried out in a second phase to explore the design space for the new concept. Due to the lengthy time consumed for optimization of the Kyrko Bridge case study, which consists of three spans and 41 optimization variables, the parametric study was conducted on a bridge with a single span to shorten the analysis time and reduce the number of optimization variables, which were brought down to 20 variables.

The parametric study here is focused on the stainless-steel corrugated web design solution and the potential saving from using this concept in comparison with the flat web carbon steel design solution.

A study conducted by Karabulut et al. [12] indicated that if the initial price of steel S460 does not exceed 1.13 times the one of mild steel S355, the total lifecycle cost is comparable (as shown in Figure 25). This is because the cost saving resulting from reduced weight due to

the use of the higher-strength S460 is balanced out by the higher material costs. Additionally, it's worth noting that the advantages of using higher-strength steel decrease when fatigue becomes the governing factor, further reducing the difference in weight between these two types of steel. Likewise, choosing carbon steel corrugated web as a design alternative could assist in lightening the design and cutting down on initial material costs. However, choosing this option would result in a larger painting area, higher painting costs during maintenance, and ongoing costs associated with delays in traffic, of course, this is not an issue when stainless steel is used. Following this reasoning, it was concluded that overall, the results obtained from this parametric study are valid for the case of S460.

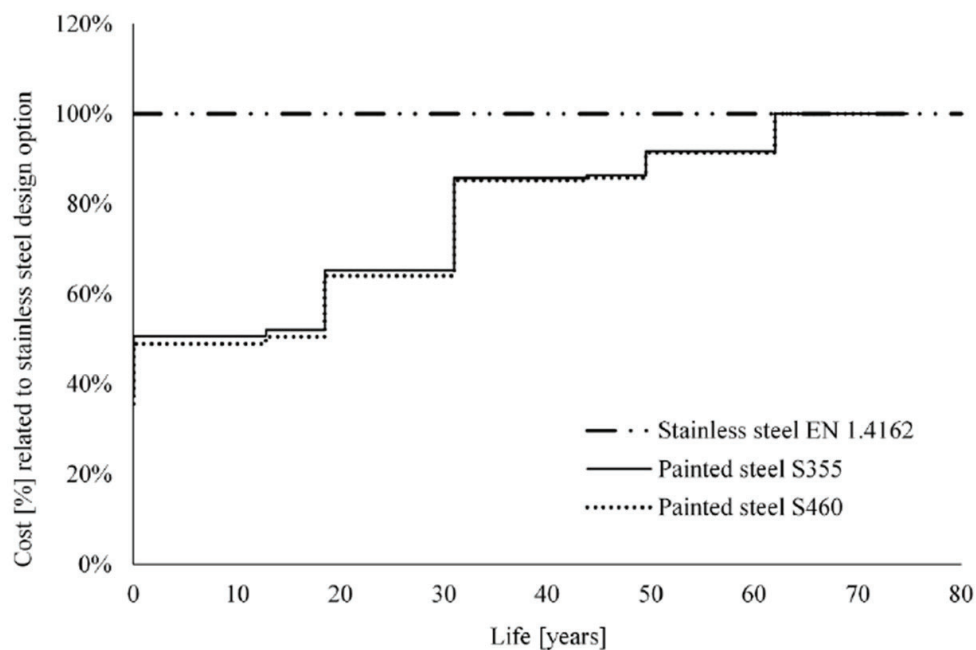


Figure 25 Cost related to stainless steel design option for a case study of a 5-span bridge conducted by Karabulut et al. [12]

A simply supported bridge situated in Böle, Sweden, serves as a reference bridge in this research. The design inputs for this bridge are presented in Table 12.

Table 12 Design inputs for the reference bridge employed in the parametric study

Case study location	Böle, Sweden
Bridge configuration	1 span of 52 m
Bridge width	9.5 m, two traffic lanes (3m*2) + two pedestrian lanes on each side (1.75 m)
C/C distance between the two main girders	5.6 m
Average daily traffic (ADT)	Variable
The indicated number of heavy vehicles per slow lane (N_{obs})	Variable
Design lifespan	120 years
Girder height limitation	Variable
Painting schedule	Variable
Optimization objective	Variable

To initiate the parametric study, the influence of the selected optimization objective is first investigated. Following that, an analysis is performed on the influence of painting schedule, ADT and N_{obs} , as well as that of possible girder height restrictions, and bridge span length. The designations for the full parametric study are presented in Table 13.

Table 13 Parametric models. Painting schedules are adopted from Trafikverket [92] and Rossi et al. [93]

ID	ID1	ID2	ID3	ID4	ID5	ID6	ID7	ID8	ID9
Objective	LCC	Weight	LCA	Investment	LCC	Weight	LCA	Investment	LCC
Material grade	S355	S355	S355	S355	EN1.4162	EN1.4162	EN1.4162	EN1.4162	S355
Span length [m]	52	52	52	52	52	52	52	52	52
N_{obs}	50,000	50,000	50,000	50,000	50,000	50,000	50,000	50,000	50,000
ADT	200	200	200	200	200	200	200	200	200
Allowable height	3 m	3 m	3 m	3 m	3 m	3 m	3 m	3 m	3 m
Painting	Trafikverket	Trafikverket	Trafikverket	Trafikverket	-	-	-	-	Rossi et al.
ID	ID10	ID11	ID12	ID13	ID14	ID15	ID16	ID17	ID18
Objective	LCC	LCC	LCC	LCC	LCC	LCC	LCC	LCC	LCC
Material grade	EN1.4162	S355	S355	S355	S355	S355	EN1.4162	EN1.4162	S355
Span length [m]	52	52	52	52	52	52	52	52	52
N_{obs}	500,000	500,000	500,000	500,000	500,000	500,000	500,000	500,000	125,000
ADT	11,000	11,000	50,000	11,000	11,000	11,000	11,000	11,000	5,000
Allowable height	3 m	3 m	3 m	3 m	1.5 m	1.8 m	1.5 m	1.8 m	3 m
Painting	-	Rossi et al.	Rossi et al.	Trafikverket	Trafikverket	Trafikverket	-	-	Trafikverket
ID	ID19	ID20	ID21	ID22	ID23	ID24	ID25		
Objective	LCC	LCC	LCC	LCC	LCC	LCC	LCC		
Material grade	EN1.4162	S355	S355	S355	EN1.4162	EN1.4162	EN1.4162		
Span length [m]	52	30	30	30	30	30	30		
N_{obs}	125,000	50,000	125,000	500,000	50,000	125,000	500,000		
ADT	5,000	200	5,000	11,000	200	5,000	11,000		
Allowable height	3 m	2 m	2 m	2 m	2 m	2 m	2 m		
Painting	-	Trafikverket	Trafikverket	Trafikverket	-	-	-		

To investigate the sensitivity of the best solution to the optimization objective, the reference bridge is optimized with respect to weight, investment cost, life cycle cost, and life cycle impact. This is done for two concepts: carbon steel (S355) flat web girders and stainless steel (EN1.4162) corrugated web girders. Table 14 shows the results of optimization for the different optimization targets for the S355 flat web option, labelled ID1, ID2, ID3, and ID4. As can be observed, when the optimization target is weight, or LCA, ID2, ID3, the algorithm proposes deep girders with lighter weights. When the optimization target is investment cost, ID4, the algorithm selects girders with smaller depths and thicker flanges, resulting in a lower painting area. Due to the expense of painting during maintenance activities, the painting area is reduced even further when the optimization target is LCC, ID1.

Table 14 Comparison of the optimal solution for different optimization targets for flat web carbon steel (S355) concept

ID	Objective	<i>bfo</i> [mm]	<i>bfu</i> [mm]	<i>tfo</i> [mm]	<i>tfu</i> [mm]	<i>hw</i> [m]	<i>tw</i> [mm]
ID1	LCC	500 to 900	400 to 1000	35	50	2.2	14 to 16
ID2	Weight	500 to 800	400 to 1100	30	30	2.9	14 to 15
ID3	LCA	500 to 1000	400 to 1100	28	30	2.9	14 to 15
ID4	Investment cost	500 to 900	400 to 1000	30	40	2.6	15
ID	<i>Painting area</i> [m ²]	<i>Weight</i> [ton]		<i>LCC</i> [MSEK]			
ID1	830	84		4.324			
ID2	1000	75.4		4.538			
ID3	973	76		4.539			
ID4	916	80		4.427			

Table 15 shows the results of optimization for several optimization targets for the corrugated web stainless steel option, labelled as ID5, ID6, ID7, and ID8 for LCC, weight, LCA, and investment cost objectives, respectively. As can be seen, the optimal solution, in this case, is not affected by the optimization objective. The solutions obtained for various optimization targets provide solutions with close values for pickling area, web height, and overall weight. This is due to the lack of painting expenses during both maintenance and production.

Table 15 Comparison of the optimal solution for different optimization targets for corrugated web stainless steel (EN1.4162) concept

ID	Objective	<i>bfo</i> [mm]	<i>bfu</i> [mm]	<i>tfo</i> [mm]	<i>tfu</i> [mm]	<i>hw</i> [m]	<i>tw</i> [mm]
ID5	LCC	600 to 700	500 to 800	28	45	2.9	4 to 6
ID6	Weight	500 to 800	500 to 900	28	40	2.9	4 to 6
ID7	LCA	500 to 600	500 to 900	35	40	2.8	4 to 7
ID8	Investment cost	500 to 700	600 to 1100	30	35	2.8	4 to 7
ID	<i>Pickling area</i> [m ²]	<i>Weight</i> [ton]		<i>LCC</i> [MSEK]			
ID5	970	57		3.296			
ID6	999	56		3.279			
ID7	945	59		3.463			
ID8	969	57		3.331			

Figure 26 compares the number of cross-sectional changes in optimal solutions for LCC and weight optimization targets. In contrast to LCC optimization objectives (ID1 and ID5), weight optimization objectives (ID2 and ID6) exhibit higher cross-sectional variations. It is important to highlight that when optimizing for life cycle cost (LCC), the carbon steel concept exhibits a higher weight compared to the duplex corrugated web concept. However, when considering different objectives, the variations in sections differ for the duplex corrugated web concept, but the overall weights remain similar, i.e., the algorithm finds different solutions that lead to minimal weight.

Based on this understanding of how changing the optimization objective affects the design outcome, and because the work aims to study the potential cost benefits of using the new concept, the optimization objective is set to LCC in the remaining parametric studies in the current research work.

Considering the findings presented in Table 14 and Table 15, various observations can be drawn about the potential saving offered by the new concept. The potential saving in LCC, weight, and LCA, from using the new concept are summarized in Figure 26. The top flange width along the bridge obtained from the optimization

Table 16. The analysis of life cycle costs indicates a decrease ranging from 24% to 28%, while the life cycle impact exhibits a reduction of 32% to 37%. In terms of weight, there is a decrease ranging from 23% to 32%. Although the material cost shows a significant cost difference,

implementing stainless steel results in just a 2%–5% increase in investment costs.

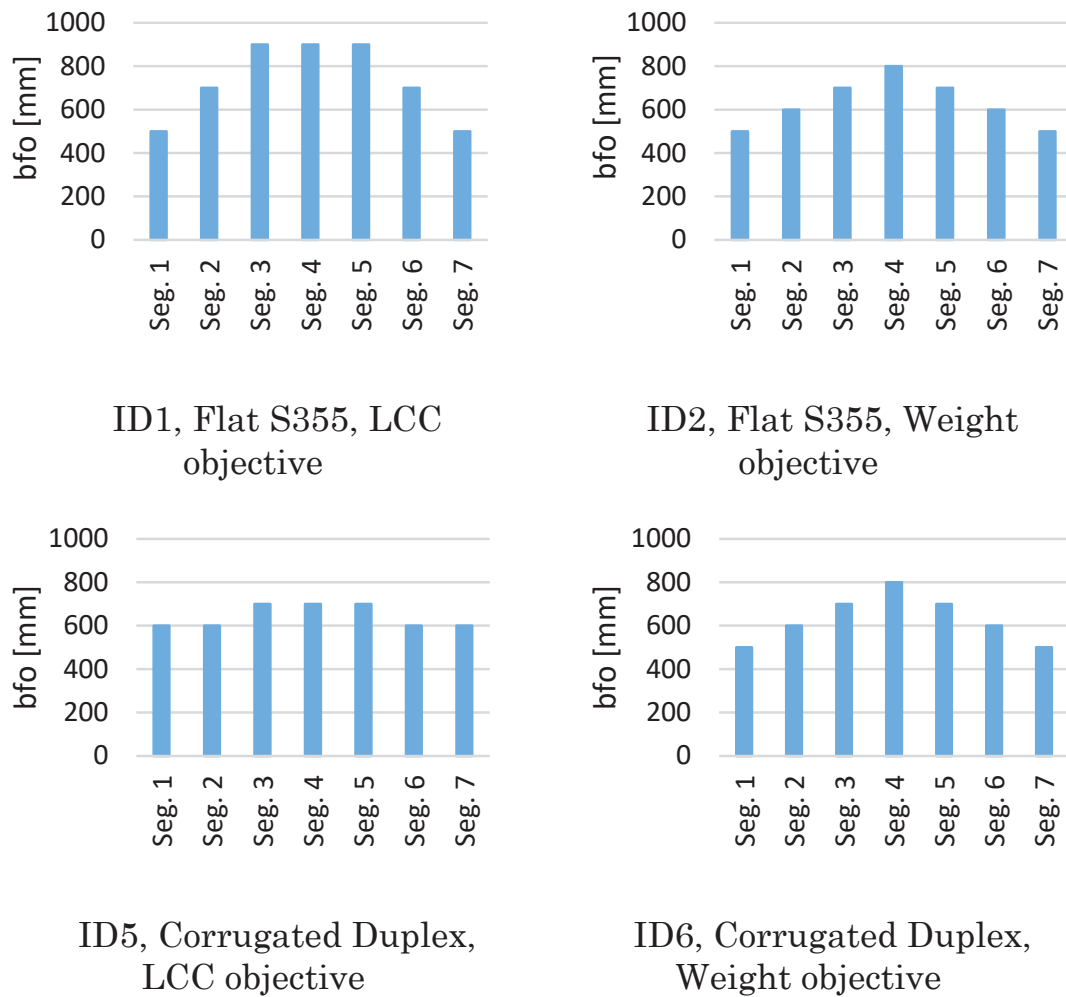


Figure 26 The top flange width along the bridge obtained from the optimization

Table 16 LCC, LCA, weight, and investment cost comparison for ID1 to ID8

	Objective	LCC difference	Investment cost difference	LCA difference	Weight difference
ID1 vs ID5	LCC	-24%	+4%	-37%	-32%
ID2 vs ID6	Weight	-28%	+2%	-34%	-26%
ID3 vs ID7	LCA	-26%	+4%	-32%	-23%
ID4 vs ID8	Investment cost	-25%	+5%	-35%	-28%

Comparing ID1 to ID5, Table 17 shows the elements that make the potential saving in weight, LCC, and environmental impact

associated with the new concept. To begin with, the new concept significantly reduces LCC costs by avoiding the necessity for painting during maintenance. Second, the lower production and material consumption costs balance the higher material cost. Through the elimination of grinding and painting, as well as lower cutting and welding costs, production costs are decreased by 46%. Thirdly, by using a deeper girder and a corrugated web with a better shear capacity, the corrugation concept decreases steel weight by around 32%, with saving in flange material (25%) and web material (49%) as a result.

Table 17 Costs and footprint comparison for ID1 and ID5

	ID1, Flat S355	ID5, Corrugated EN1.4162	Saving
Total weight [ton]	84	57	-32%
Flanges weight [kg]	52 308	39 125	-25%
Web weight [kg]	26 171	13 321	-49%
Production cost [SEK]	1 731 959	936 996	-46%
Investment cost [SEK]	3 290 301	3 413 809	+4%
Maintenance Cost [SEK]	1 060 821	0	-100%
LCC [SEK]	4 324 213	3 296 227	-24%
LCA [kg CO2 eq]	338 502	211 991	-37%

Regarding LCA, material production is the main source of environmental impact, with stainless steel having a significantly lower unit impact than S355 (1.7kg CO2 eq/kg compared to 2.63kg CO2 eq/kg). This disparity explains the noteworthy reduction in environmental impact achieved by the new concept, 37% in Table 17. Moreover, even if the unit impact of both materials were the same, the new design would still have a lower environmental impact due to its reduced material usage.

3.3.1 Effect of painting schedule

As discussed in Section 3.2, one of the primary differences between carbon steel and stainless steel is their surface treatment, particularly when it comes to painting. For carbon steel bridge girders, the initial application of paint during manufacture is critical to preventing corrosion, and frequent repainting is required throughout their service life. Stainless steel girders, on the other hand, are pickled during manufacture and do not require any further surface treatment. Therefore, the major saving from using stainless steel is that it eliminates painting costs.

Maintenance activities may be divided into three categories: patching up, overcoating, and repainting. The viability of employing corrugated web stainless steel girders is strongly dependent on the

scheduling of these activities and the accompanying painting costs, which are represented in the net present value (NPV) of the life cycle costs (LCC).

In this study, two distinct paint maintenance schedules, Table 10 and Table 11, are assessed. Case ID1 in Table 14 was optimized using Trafikverket's paint maintenance schedule [92] (Table 11). The same bridge is re-optimized here based on the paint maintenance schedule proposed by Rossi et al. [93] (Table 10), and the design optimization results are denoted by ID9. In Table 18, the weight, life cycle cost, life cycle impact, and investment cost of the optimized designs for flat web carbon steel design solutions with different painting schedules (ID1, ID9) are compared to those for the stainless-steel corrugated web design solution (ID5). The results show that changing the painting schedule from the Trafikverket schedule to the one proposed by Rossi et al.[93] increases the saving in life cycle costs significantly (from 24% to 43%), indicating that the new design solution is beneficial for both studied paint maintenance schedules and more competitive for cases that require more extensive maintenance activities.

Table 18 Comparison of three optimized solutions of girders ID1, ID9, and ID5

	Weight [ton]	Investment cost [MSEK]	LCC [MSEK]	Footprint [Kg CO2 eq]
ID1 (Flat S355, TRV schedule)	84	3.29	4.3	339k
ID9 (Flat S355, Rossi et al. schedule)	93	3.39	5.8	368k
ID5 (Corrugated Duplex)	57	3.41	3.3	212k
Saving using ID5 instead of ID1	-32%	+3.8%	-24%	-37%
Saving using ID5 instead of ID9	-39%	+1%	-43%	-42%

3.3.2 Effect of inflation and discount rates

The assumed discount and inflation rates are two parameters that might have a considerable impact on LCC results. In economics, the inflation rate indicates the different growth of certain product and/or service costs over time. It is used to indicate price fluctuations (of building materials, energy costs, or labour) that deviate from the overall inflation rate [94]. The discount rate is defined as 'the component indicating the time value of money that is used to transform cash flows happening at different times to a common time'. Discounting implies that future costs and saving are less important

than current costs and saving. Future expenses are just as important as present costs when $d = 0\%$. The higher the discount rate, the greater the significance placed on the near-present and the less importance given to what happens in the future [94]. In theory, employing a high discount rate will favour alternatives with low investment costs, a short lifespan, and high usage costs, and vice versa. Sensitivity analysis of the influence of changing the discount rate on the final choice is critical in both bridge management and investment because it allows decision-makers to assess their confidence in selecting the best option [95].

The results reported in Section 3.2 and Section 3.3.1 are based on predictions of a 1.5% inflation rate and a 3.5% discount rate. The values are adopted from Safi [95], based on notations from Trafikverket 2013. To investigate the impact of changes in discount and inflation rates on the conclusions, a sensitivity analysis is performed. In addition to the basic discount rate of 3.5%, two additional discount rates, 2% and 5%, are investigated. Likewise, in addition to the original inflation rate of 1.5%, two additional inflation rates of 0% and 3% are tested, and the findings are shown in Figure 27. As can be seen, the saving from life cycle costs (LCC) decline from 43% at a 3.5% discount rate to 28% at a 5% discount rate. In contrast, increasing the inflation rate from 1.5% to 3% increases LCC saving from 43% to 68%. These statistics demonstrate that expected inflation and discount rate values have a major influence on LCC outcomes, however, there is considerable LCC saving (28% to 68%) generated by the new concept, irrespective of what values these rates take.

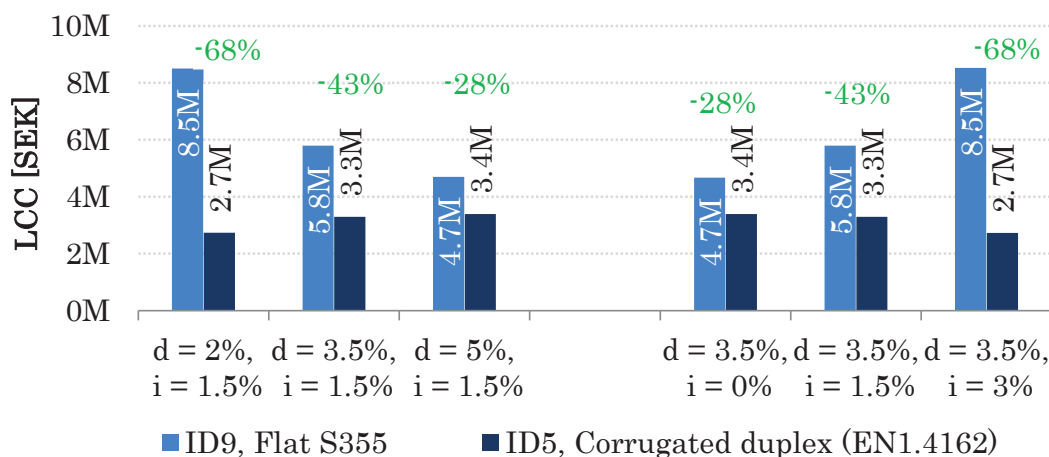


Figure 27 Sensitivity of LCC calculations to discount and inflation rates

3.3.3 Effect of average daily traffic (ADT) and the indicated number of heavy vehicles per slow lane (N_{obs})

A bridge's average daily traffic (ADT) is determined by its location and whether it is in an urban or rural region with varied traffic flow rates. The volume of ADT is proportional to the number of heavy vehicles indicated in each slow lane, designated as N_{obs} [96], which has a substantial influence on the fatigue design of the bridge structure [97]. As N_{obs} increases, if the fatigue limit state governs the design, the permitted stress on the flanges decreases, necessitating bigger flanges to fulfill the design criteria. Furthermore, in the context of LCC, increasing ADT raises user costs during maintenance activities.

To study this effect, three scenarios are considered, including flat web carbon steel girders designated by ID9, ID11, and ID12 for ADT & N_{obs} of 200 & 50 000, 11 000 & 500 000, and 50 000 & 500 000, and corrugated web stainless steel girders designated by ID5 and ID10 for ADT & N_{obs} of 200 & 50 000 and 11 000 & 500 000. The third case is not optimized because it only impacts the user cost, which does not exist in stainless steel.

Figure 28 compares the life cycle costs of optimal designs with various ADT & N_{obs} . Figure 28 demonstrates a possible reduction of 43% in the overall LCC from employing the corrugated web stainless-steel design option with a low ADT & N_{obs} of 200 & 50 000. By analysing this scenario, it turned out that, in addition to reducing costs of maintenance (100%), the stainless-steel option (ID5) saves costs on production (46%). This reduction is attributable to three factors: first, the removal of the requirement for grinding and painting; second, a decrease in the cost of cutting (owing to a 38% reduction in weight); and finally, a reduction in the cost of welding due to the use of thinner flanges and webs. Furthermore, in the case of ID5 (corrugated web stainless steel girders), the weight reduction is due in part to the use of smaller flanges for the stainless-steel solution because the optimization tool chooses a deeper web for a corrugated web girder, resulting in a lower flange area, and in part to thinner webs due to the higher shear capacity of the corrugated webs.

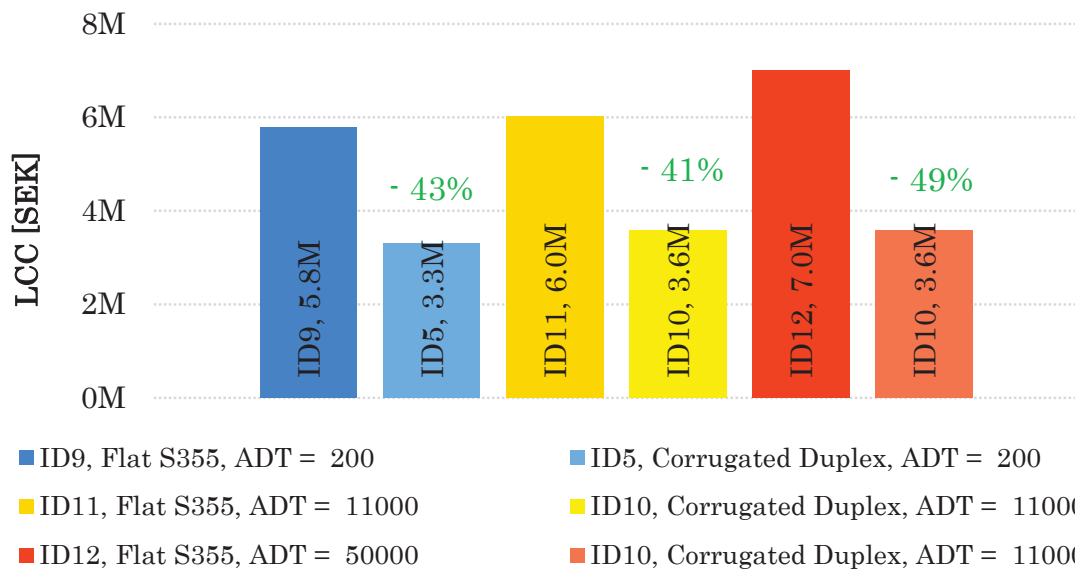


Figure 28 Sensitivity of the Life Cycle Saving to average daily traffic ADT and number of slow vehicles in the slow lane N_{obs}

The LCC saving reduce somewhat to 41% in the second scenario, which considers bridges with larger ADT and N_{obs} , respectively 11 000 and 500 000, as shown in Figure 28. This is explained by the fact that when the N_{obs} increases, the fatigue becomes more prominent, and the design tool selects heavier girders to fulfil the fatigue requirements. Yet, the saving is considerable.

The saving increases again to 49% (Figure 28) for the third scenario due to the higher ADT, i.e., higher user cost. In this study, the effect of ADT is not highly apparent since the user cost assumes a time delay of 2 days, 5 days, and 5 days, respectively, for patch-up, overcoating, and repainting operations. It should be mentioned that these time delays vary by case and can range from a few weeks to a few months, in which case the benefits of utilizing duplex stainless steel become clearer. Maintenance tasks, on the other hand, can be conducted without any traffic delays, a situation with minimal user cost which is close to what has been considered in this study.

In summary, irrespective of ADT and N_{obs} design values, the investigated concept consistently reduces costs in LCC compared to the conventional concept. The saving is especially obvious for bridges with high ADT, which reflects the greater user cost. Importantly, the user cost assumptions are very conservative.

3.3.4 Effect of height limitations

The available free height underneath the bridge often limits the allowable web height in bridge design. Furthermore, one of the key limitations of adopting deep girders for flat web designs is the possibility of the web buckling as the web height grows. This needs the inclusion of longitudinal and transversal stiffeners or a thicker web, both of which result in greater material consumption. However,

because of the high shear buckling strength of corrugated web plates, they do not provide as much of an obstruction, making deeper girders a more practical alternative.

Table 19 The allowable and optimal web (TRV schedule is used for Flat S355)

ID	ID14	ID16	ID15	ID17	ID13	ID10
Concept	Flat S355	Corrugated EN1.4162	Flat S355	Corrugated EN1.4162	Flat S355	Corrugated EN1.4162
Allowable web height	1.5 m	1.5 m	1.8 m	1.8 m	3 m	3 m
Optimal web height	1.4 m	1.5 m	1.7 m	1.8 m	2.3 m	2.9 m
Weight of optimal solution	119 ton	95 ton	104 ton	79 ton	82 ton	63 ton

Three scenarios are considered to study the effect of height restrictions. Table 19 shows the designation, permissible heights, and heights chosen by the optimization process. Table 19 indicates that the optimization tool selects equivalent depths for stainless steel and carbon steel girders at two height limits of 1.5 m and 1.8 m. However, with a height constraint of 3 m, the tool seeks to lower the LCC for the S355 option by reducing the painting area. As a result, the algorithm chooses a web height of 2.3 m with a flat web, resulting in a smaller painting surface with a heavier solution (82 tons). Note here that when the optimization for ID13 is repeated but the aim is altered to reduce weight, the algorithm chooses a height of 2.9 m for the S355 option, resulting in the lowest weight (74 tons).

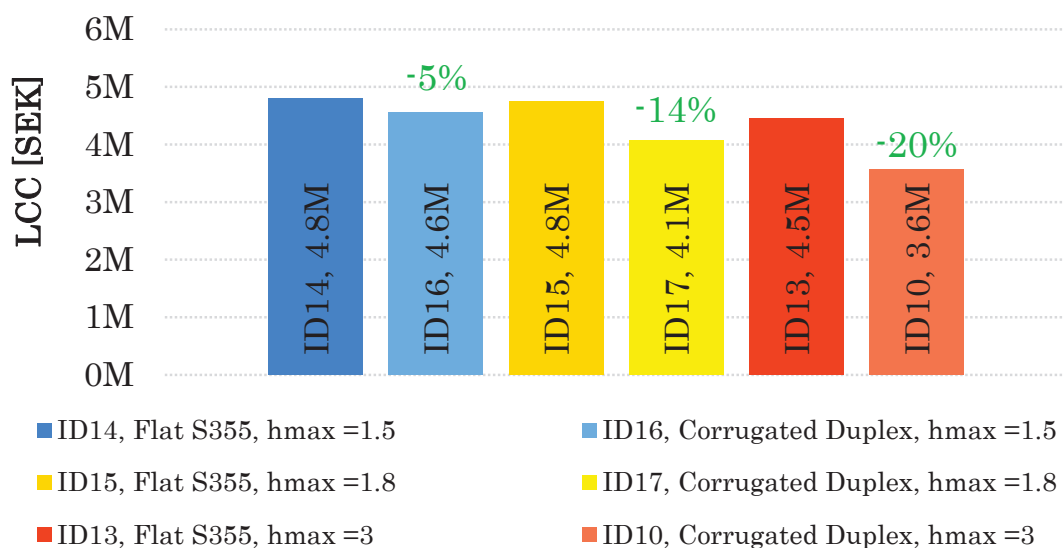


Figure 29 LCC saving for different allowable web heights

Figure 29 displays the LCC results. As can be seen, the LCC saving grows as the permitted web depth increases; for height constraints of 1.5m, 1.8m, and 3m, the LCC saving increase from 5% to 14% to 20%, respectively. As previously stated, raising the web height to minimize weight increases the painting area in carbon steel but not in stainless steel. As a result, it is more advantageous to employ deeper girders for stainless steel, as raising the web height does not influence the painting area.

3.3.5 Effect of span length

As a last phase in the parametric investigation, the purpose is to determine if the conclusions achieved are relevant for varied span lengths. The optimization is conducted for each span length across three distinct levels of Average Daily Traffic (ADT): low, medium, and high, corresponding to N_{obs} of 50 000, 125 000, and 500 000. Table 20 shows the designations and ADT& N_{obs} assumptions.

Table 20 the bridges considered to study the span length effect

Span = 52 m						
ADT* N_{obs}	200*50 000		5 000*125 000		11 000* 500 000	
ID	ID1	ID5	ID18	ID19	ID13	ID10
Concept	Flat S355	Corrugated EN1.4162	Flat S355	Corrugated EN1.4162	Flat S355	Corrugated EN1.4162
Span = 30 m						
ID	ID20	ID23	ID21	ID24	ID22	ID25
Concept	Flat S355	Corrugated EN1.4162	Flat S355	Corrugated EN1.4162	Flat S355	Corrugated EN1.4162

Figure 30 compares the life cycle cost of optimal designs with varying ADT. The results from the shorter-span scenario (30 m) are found to be relatively consistent with those from the longer-span example (52 m). Life cycle cost (LCC) saving range from 20% to 26% for long-span bridges and from 18% to 22% for short-span bridges. These findings show that the saving is comparable in all cases regardless of span, ADT, or N_{obs} , indicating that the saving is not sensitive to span length.

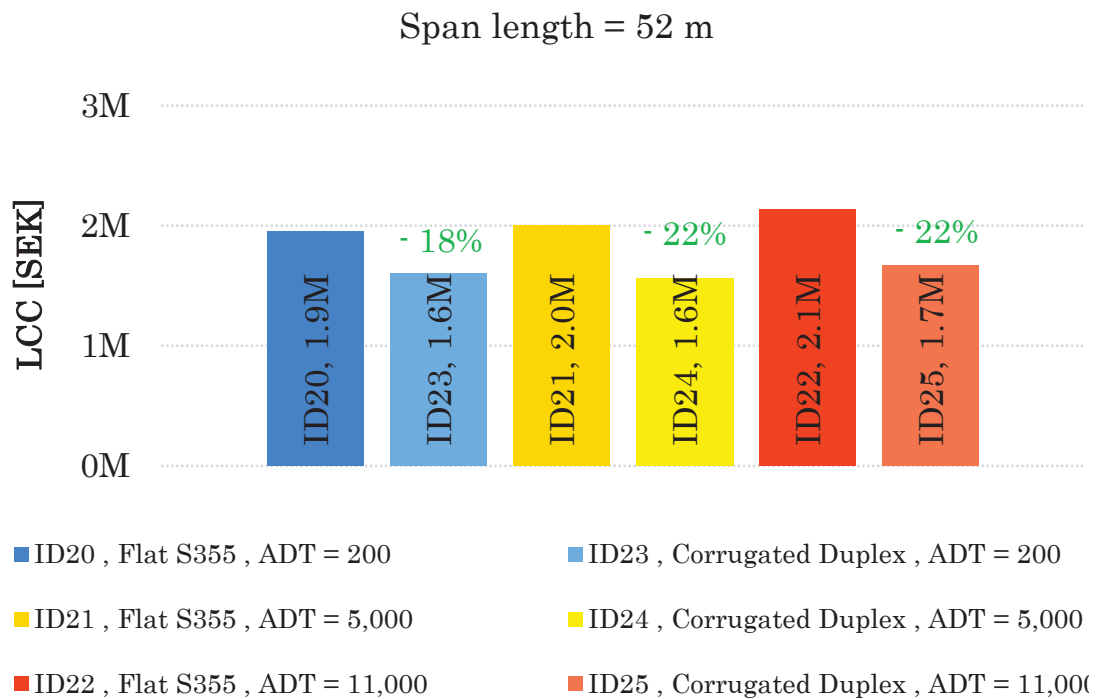
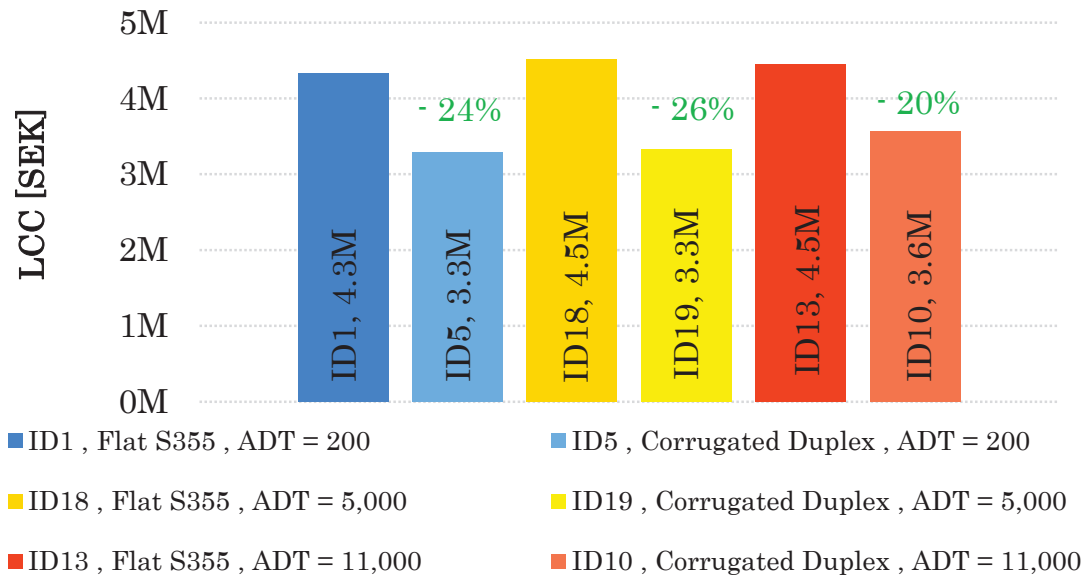


Figure 30 Evaluation of weight and LCC potential saving for different bridge span lengths

3.4 Optimal corrugation parameters

Even though a recommendation on the optimal corrugation parameters cannot be reached based on the limited parametric study conducted here, several observations are made from the optimization findings reported in Table 21. The corrugation parameters obtained from the optimization tool are summarized in Table 22. It can be observed that the corrugation angle ranges from 30 to 40 degrees in

all investigated designs. The optimal corrugations lie on the intermediate slenderness, where the local buckling governs the design. This might be explained by the fact that having a local buckling mode indicates a lower decrease in shear resistance, implying a more material-efficient design. In other words, having global buckling with a very thin and shallow web means a significant drop in shear buckling resistance, which is materially wasteful because more material is required to provide the required shear capacity.

Table 21 Corrugation dimensions for the optimal designs

	Span [m]	a1 [mm]	a2 [mm]	a3 [mm]	Alpha [degree]	a1/a2	Buckling Mode
ID5	52	225.00	150.00	75.00	30.00	1.50	global
ID6	52	225.00	116.68	75.00	40.00	1.93	local
ID7	52	325.00	200.00	100.00	30.00	1.63	local
ID8	52	350.00	150.00	75.00	30.00	2.33	local
ID10	52	300.00	250.00	125.00	30.00	1.20	local
ID16	52	150.00	100.00	50.00	30.00	1.50	local
ID17	52	175.00	100.00	50.00	30.00	1.75	local
ID19	52	275.00	174.34	100.00	35.00	1.58	local
ID23	30	125.00	150.00	75.00	30.00	0.83	local
ID24	30	200.00	100.00	50.00	30.00	2.00	local
ID25	30	175.00	150.00	75.00	30.00	1.17	local

Table 22 Optimal corrugation parameters obtained from the optimization tool

Shear buckling mode	Local (mostly)
Corrugation angle	30 to 40 degrees
a1	125 to 350
a2	100 to 250
a3	50 to 125
Flat to inclined fold ratio $a1/a2$	0.83 to 2.3

Chapter 4

4 Flange buckling resistance

4.1 Flange buckling problem description and approach

When a beam is subjected to a bending moment, the top flange will be subjected to compression, and if the flange is slender, i.e., in CSC4, the flange plate will buckle locally, resulting in a significant decrease in the beam moment capacity. To understand the effect of this instability on the resistance, the critical buckling stress of the compressed plate, i.e., the stress at which the plate buckles, needs to be defined. This buckling stress defines how slender the plate is, and based on this slenderness, the yielding moment needs to be reduced by a factor of ρ . The critical buckling stress for a plate can be calculated by the following equation:

$$\sigma_{cr} = k_{\sigma} * \sigma_E \quad \text{Where} \quad \sigma_E = \frac{\pi^2 E}{12(1-\nu^2)} \left(\frac{t}{b}\right)^2 \quad (4-1)$$

Where b and t are the width and the thickness of the plate, ν is Poisson's ratio, and k_{σ} is the buckling coefficient.

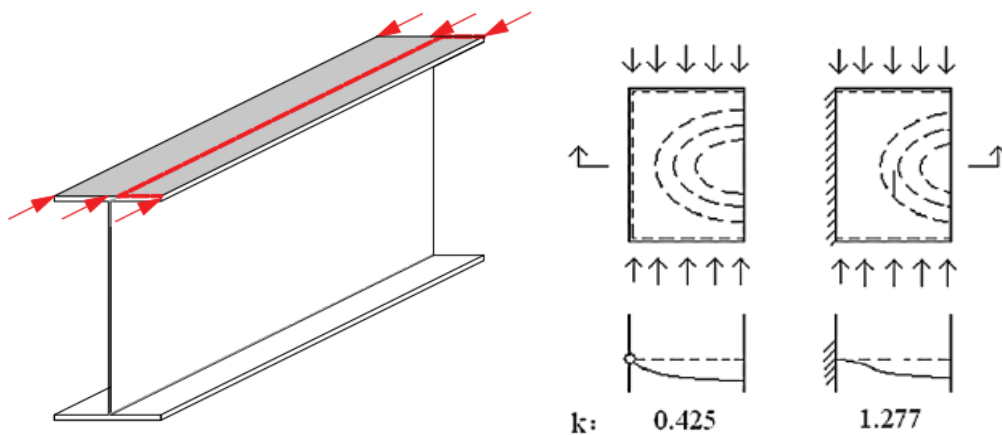


Figure 31 The buckling factor k_{σ} for flanges in flat web girders

The buckling coefficient k_σ differs based on the plate loading and the boundary conditions. The flange in a flat web girder can be considered a long plate simply supported on three edges and subjected to uniform compression; see Figure 31. In this case, the buckling factor k_σ is 0.425 [98]. The behavior of the flange under normal stress in corrugated web beams is different from that for the flat web. Due to the corrugation, the boundary conditions of the flange are different. Many parameters affect the buckling mode for corrugated web girder flanges, e.g., the flange slenderness, $\frac{b_f}{t_f}$, the corrugation parameters, a_1, a_3, α , and the flange-to-web thickness ratio, $\frac{t_f}{t_w}$.

To provide a similar design procedure that is adopted in EN1993-1-5 for flat web to corrugated web, the procedure illustrated in Figure 32 is adopted in this work. A parametric finite element model is created to investigate the performance of stainless steel (EN1.4162 [99]) girders under compressive normal stresses. The model is illustrated in Figure 33. The shell edges of the web and flanges on both ends are attached to their corresponding section master middle nodes, which are positioned at the cross-section gravity centre (Nodes 1 and 2 in Figure 33), to make sure that the outside sections hold to the condition of "a plane section remaining plane". Pinned and roller supports are assumed at Nodes 1 and 2, respectively. At these master points, equal and opposite end moments are applied to load the model with pure bending.

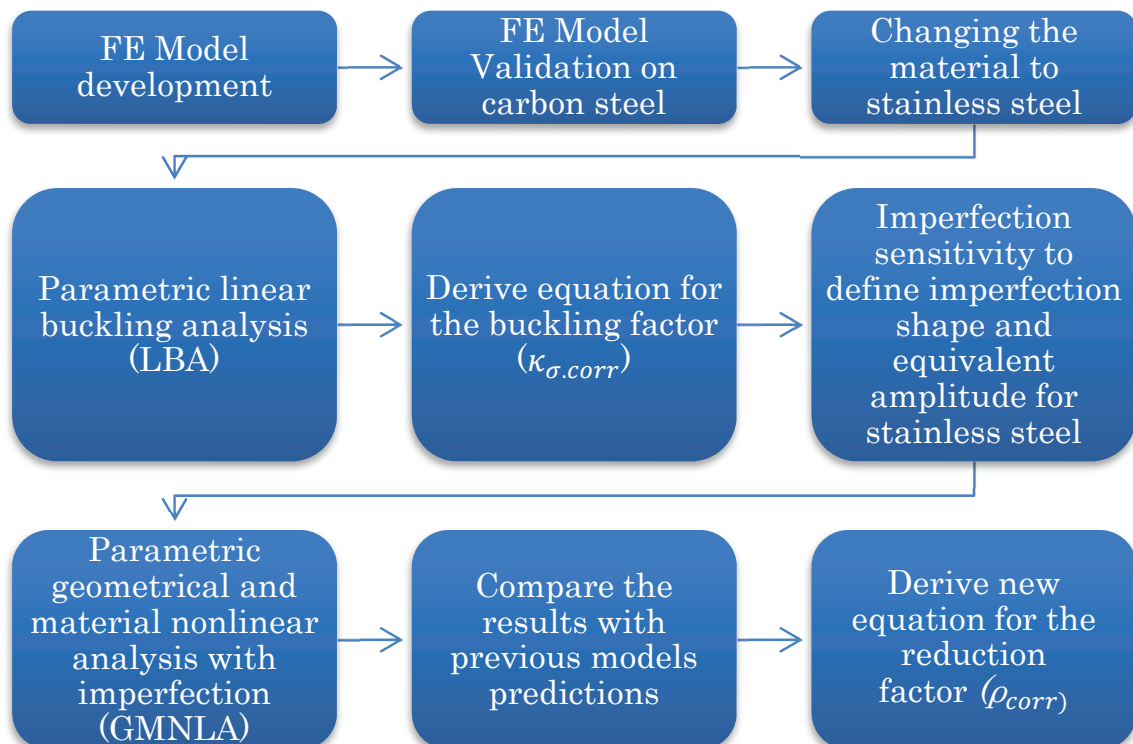


Figure 32 An illustration of the procedure that is used to address the flange buckling problem

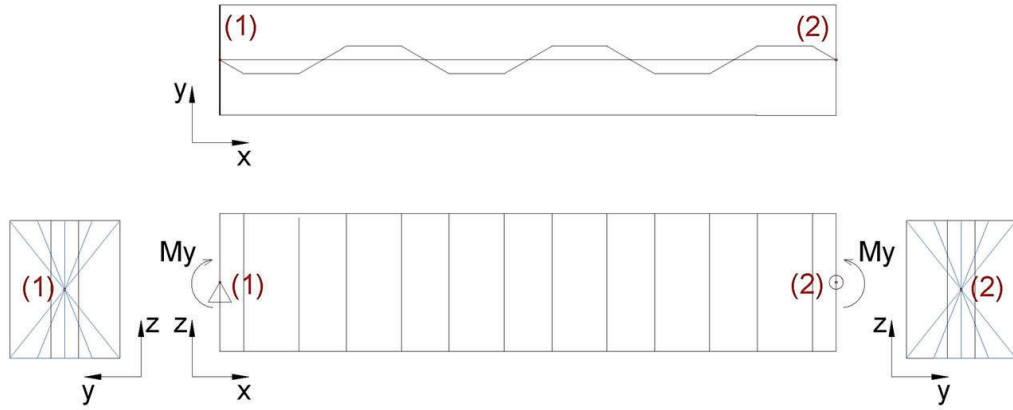


Figure 33 Parametric finite element model

Since there are no experiments available for stainless steel material, the developed finite element model is validated using tests performed on carbon steel by Jager et al. [30, 65, 66] and Elamary et al. [55]. Five beams from the Jager et al. [30] experimental program and one girder from Elamary et al. [55] experimental program are modelled as a first step in the validation. The properties of these girders are summarized in Table 23.

Table 23 Properties of girders considered in numerical model validation

Specimen	a_1 [mm]	a_3 [mm]	α [°]	t_f [mm]	b_f [mm]	t_w [mm]	h_w [mm]	f_{yf} [MPa]	f_{uf} [MPa]	f_{yw} [MPa]	f_{uw} [MPa]
2TP1-1	97	69	45	7.9	250	5.97	500	452	548	406	530
7TP1	97	69	45	12.2	250	3.84	500	364	496	474	584
9TP3	88	44	30	12.16	247	4.04	500	365	500	457	584
3TP1-1	97	69	45	14.59	250	3.01	500	387	516	363	514
4TP10	134	67	30	12.2	250	3.89	500	361	488	457	560
CWNC101	100	50	45	4	100	2.1	400	320	390	310	390

The analysis starts with linear buckling analysis (LBA), which is subsequently followed by nonlinear analysis employing the first eigen buckling mode as the initial imperfection shape with an equivalent geometrical imperfection of $\frac{cf}{50}$. The outcome of the study is referred to as *Mult.num.geo.eq*. Then, this moment capacity is compared with an analogous numerical value provided by Jager et al. [30], referred to as *Mult.num.Jager.geo.eq*, where the authors used an equivalent geometric imperfection in their validated numerical model. Table 24 illustrates the results.

The same analysis is repeated using the measured initial imperfection reported by Jager et al. [30]. The results are designated as *Mult.num.geo.m*, which are compared to their corresponding

numerical values from the Jager et al. [30] numerical model's outcomes (*Mult. num. Jager. geo. m*). Table 24's results reveal a high degree of agreement between the outcomes of the constructed parametric model and the validated numerical model developed by Jager et al. [30], for both cases, with a difference of less than 3%. Moreover, the ultimate moment capacity obtained for the girder *CWNCF101* (Elamary et al. [55]) shows good agreement with test results.

Table 24 Numerical model validation

Specimen	2TP1-1	7TP1	9TP3
Measured imperfection [mm]	1.1	1.22	1.42
Equivalent imperfection Cf/50 [mm]	3.19	3.19	2.91
Mexp [kNm]	369	588	585
Mult. num. geo. m	408	553	558
Mult. num. geo. eq	359	517.6	535
Mult. num. Jager. geo. m	413.3	571.5	576.2
Mult. num. Jager. geo. eq	360.4	521.2	541.9
Mult. num. geo. m/Mexp	1.11	0.94	0.95
Mult. num. geo. m /Mult. num. Jager. geo. m	0.99	0.97	0.97
Mult. num. geo. eq /Mult. num. Jager. geo. eq	1.00	0.99	0.99
Specimen	3TP1-1	4TP1 0	CWNCF101
Measured imperfection [mm]	1.22	1.2	Not reported
Equivalent imperfection Cf/50 [mm]	3.19	3.17	1.5
Mexp [kNm]	743	572	43
Mult. num. geo. m	713	544.4	-
Mult. num. geo. eq	672.5	503	43.3
Mult. num. Jager. geo. m	Not reported	569.9	-
Mult. num. Jager. geo. eq	681.5	515.2	-
Mult. num. geo. m/Mexp	0.96	0.95	-
Mult. num. geo. m/ Mult. num. Jager. geo. m	-	0.96	-
Mult. num. geo. eq/ Mult. num. Jager. geo. eq	0.99	0.98	-

Regarding the employed mesh type and size, a mesh sensitivity study is conducted for two mesh types, namely an eight-node second-order structural element (S8R) and a four-node first-order structural element (S4R), for linear elastic buckling analysis (LBA). Figure 34 displays the mesh sensitivity investigation for the first eigenvalue for three girders: 9TP3, 7TP1, and 2TP1-1. According to the results, the

S8R mesh type converges with a coarser mesh size, which shortens the computing time. Therefore, the S8R mesh type is used in the second mesh sensitivity investigation, which was conducted on the ultimate moment capacity derived from the nonlinear analysis. An example of the results obtained from this mesh sensitivity is illustrated in Figure 35. In both buckling and nonlinear studies, the S8R mesh type with a mesh size equal to fold length/4 yielded good results, as shown in Figure 34 and Figure 35. As a result, this mesh size is chosen to proceed with.

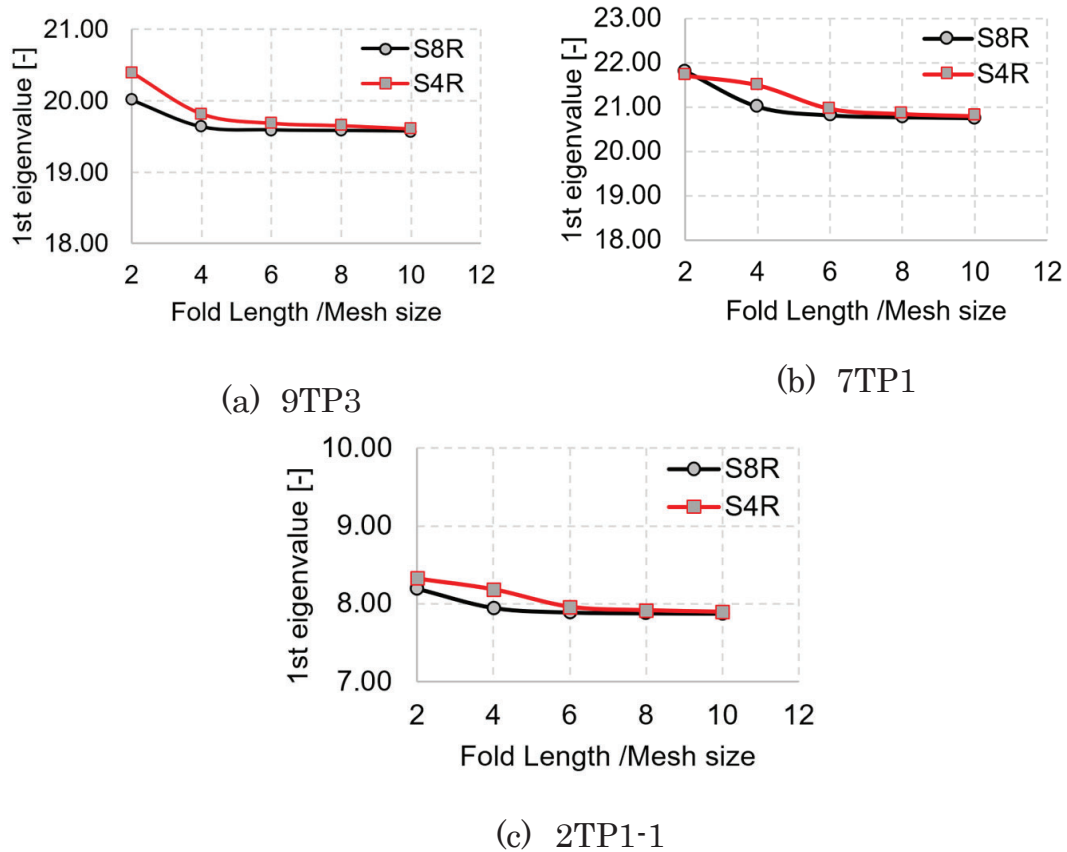


Figure 34 Mesh sensitivity study for 1st eigenvalue for girders 9TP3, 7TP1, and 2TP1-1

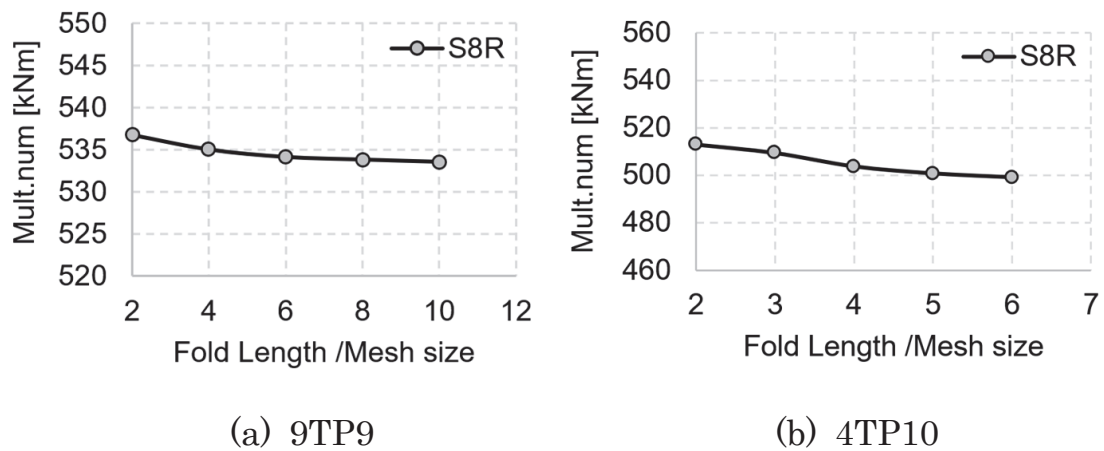


Figure 35 Mesh sensitivity study for ultimate moment capacity for girders 9TP3 and 4TP10

In addition to the ultimate moment capacities shown in Table 24, the validation procedure includes a load-displacement curve for girder 9TP3. Figure 36 illustrates the comparison. The load-relative flange displacement curves from the experiment [66] and the finite element model have shown good agreement.

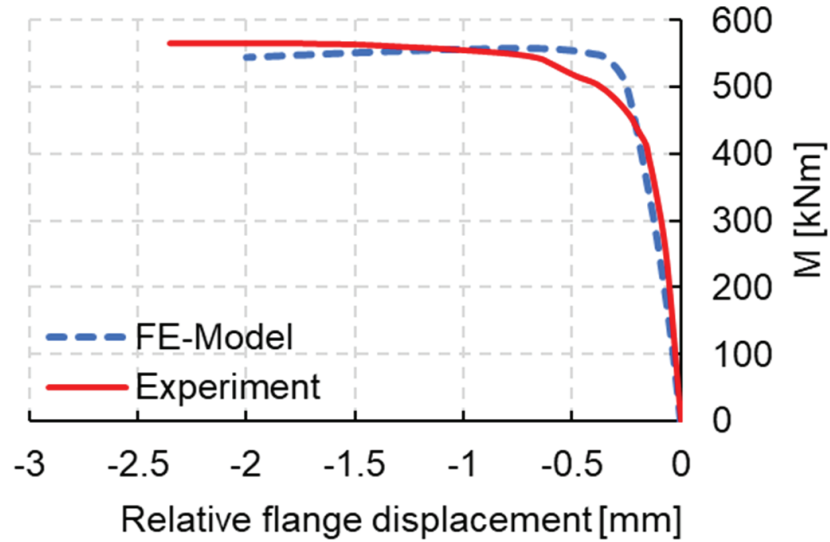


Figure 36 Validation of load-relative flange displacement curve for girder 9TP3

4.2 Parametric study and design model development

The developed and validated parametric model is used to analyze 410 girders with dimensions typical for bridge girders to ensure the practicality of the findings. The chosen parameters are tabulated in Table 25.

Table 25 Investigated parameters range

Parameter	Investigated range
α [deg]	30 – 45 – 60
b_f/a_3	2 – 2.4 – 2.7 – 3 – 3.2 – 3.3 – 4 – 5 – 6 – 6.7 – 8
a_1/a_3	2 – 3 – 4
t_f/t_w	2.5 – 3.5 – 4.17 – 5 – 5.83 – 6.25 – 8.33 – 8.75 – 12.5
b_f [mm]	400 – 600 – 800 – 1000

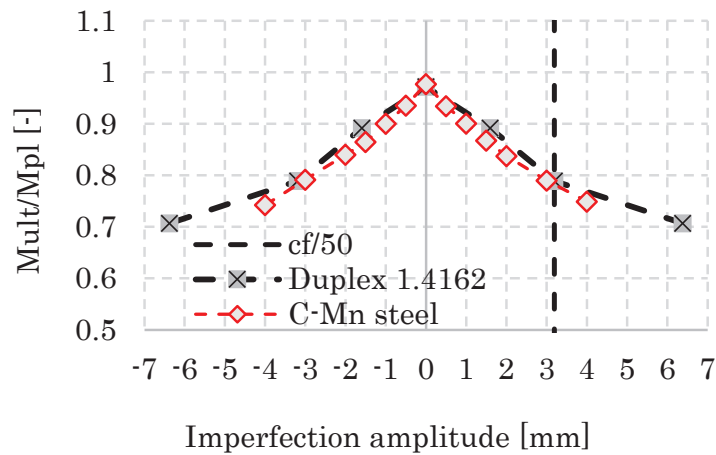
Linear buckling analysis (LBA) is performed on the 410 girders to estimate the buckling factor k_σ . The elastic buckling stress is calculated according to Equation (4-2). The numerical buckling factor is then calculated using Equation (4-3). Based on the parameters that are thought to influence the buckling factor, which is the corrugation depth to flange width ratio $\frac{a_3}{b_f}$, the web-to-flange thickness ratio $\frac{t_w}{t_f}$, the flange width to flange thickness ratio $\frac{b_f}{t_f}$, and finally, the folded to unfolded lengths of one-half wave ratio $\frac{w}{s}$, linear regression analysis and a genetic algorithm are employed to develop an equation for the buckling factor κ_σ . Equation (4-4) reflects the resulting equation for the buckling factor κ_σ . The first and fourth parameters describe the influence of corrugation depth and shape on buckling length. The web-to-flange thickness ratio reflects the rotational support supplied by the web against flange torsion. Finally, the ratio $\frac{b_f}{t_f}$ defines the flange's slenderness.

$$\sigma_{cr.num} = \frac{N_{cr.num}}{b_f \cdot t_f} \text{ where } N_{cr.num} = \frac{M_{cr.num}}{h_w + t_f} \quad (4-2)$$

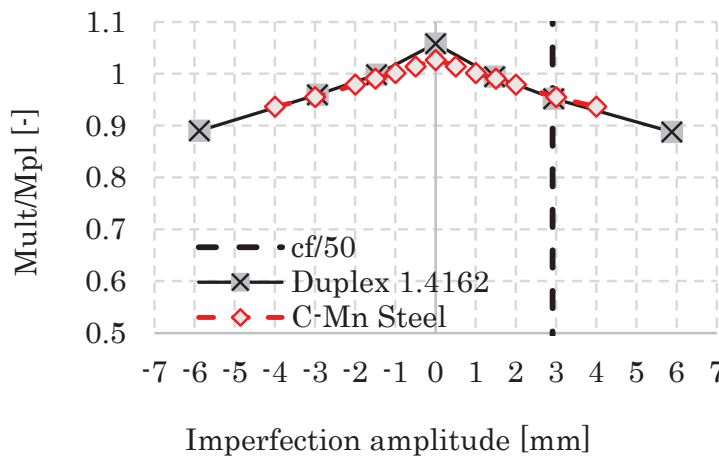
$$\kappa_{\sigma.num} = \frac{\sigma_{cr.num} \cdot 12 \cdot (1 - \nu^2) \cdot \left(\frac{c_f}{t_f}\right)^2}{\pi^2 \cdot E} \quad (4-3)$$

$$\kappa_{\sigma,corr} = 1,7 - \sqrt{\frac{a_3}{b_f}} + 0,76 \cdot \frac{t_w}{t_f} + 0,94 \left(\frac{b_f}{t_f}\right)^{0,17} - 2,56 \left(\frac{w}{s}\right)^2 \quad (4-4)$$

Before the nonlinear parametric study, an imperfection sensitivity analysis is performed to establish a suitable amplitude for the initial imperfection in duplex stainless steel (1.4162) beams. Based on an imperfection sensitivity study, previous research showed that the 1st eigenmode shape for flange buckling of trapezoidal corrugated web girders is suitable with a magnitude of $\frac{c_f}{50}$ according to EN1993-1-5, Annex C for flange twisting [30]. The same imperfection sensitivity study is conducted for duplex stainless steel (1.4162), and the resulting curves are compared to the imperfection sensitivity curves reported by Jager et al. [30]. The comparison is shown in Figure 37, which shows that the imperfection sensitivity curves are similar for Carbon steel and EN1.4162 stainless steel. Accordingly, using an equivalent imperfection amplitude of $\frac{c_f}{50}$ for duplex stainless steel is justified.



(a) 2TP1-1



(b) 9TP3

Figure 37 Imperfection sensitivity curves for specimen 9TP3 and 2TP1-1 for Carbon steel and EN1.4162

Following that, a material and geometric nonlinear analysis (GMNIA) is conducted on the 410 girders, considering the first eigenshape as a geometric initial imperfection shape with an equivalent amplitude of $c_f/50$. The moment resistance ($M_{ult. num}$) is extracted from the load-displacement curve, and the reduction factor (ρ_{num}) is then calculated using Equation (4-5).

$$\rho_{num} = \frac{M_{ult. num}}{b_f \cdot t_f \cdot (h_w + t_f) \cdot f_{yf}} \quad (4-5)$$

To establish the limit for cross-section class 4 (CSC4), the reduction factor obtained from the numerical analysis is plotted against $c_f/t_f/\varepsilon/\sqrt{k_\sigma}$, as illustrated in Figure 38. It is observed that there is no reduction in the moment capacity when $c_f/t_f/\varepsilon/\sqrt{k_\sigma} < 11.36$. By substituting this value ($11.36\varepsilon\sqrt{k_\sigma}$) for c_f/t_f in $\bar{\lambda}_p = \sqrt{\frac{f_y}{\sigma_{cr}}} = \frac{c_f/t_f}{28.4\varepsilon\sqrt{k_\sigma}}$, the limit for CSC4 is found to be $\bar{\lambda}_p = 0.4$.

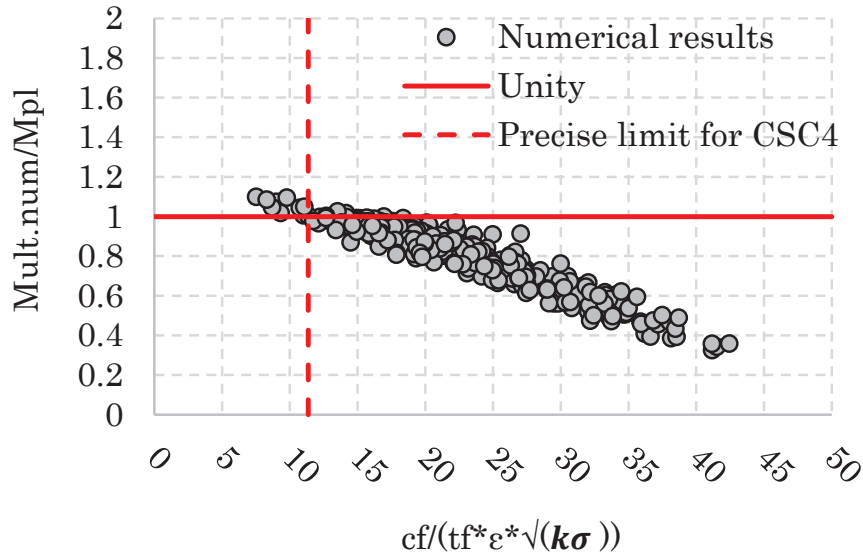


Figure 38 $M_{ult. num}/M_{pl}$ versus flange slenderness defined as $c_f/t_f/\varepsilon/\sqrt{k_\sigma}$

Based on the results, a buckling curve, presented in Figure 39 and Equation (4-6), is proposed for stainless steel corrugated web girders.

$$\rho_{corr} = \begin{cases} 1,0 & \text{for } \bar{\lambda}_p \leq 0,4 \\ \frac{0,69}{\bar{\lambda}_p} - \frac{0,1}{\bar{\lambda}_p^2} - 0,1 \leq 1,0 & \text{for } \bar{\lambda}_p > 0,4 \end{cases} \quad (4-6)$$

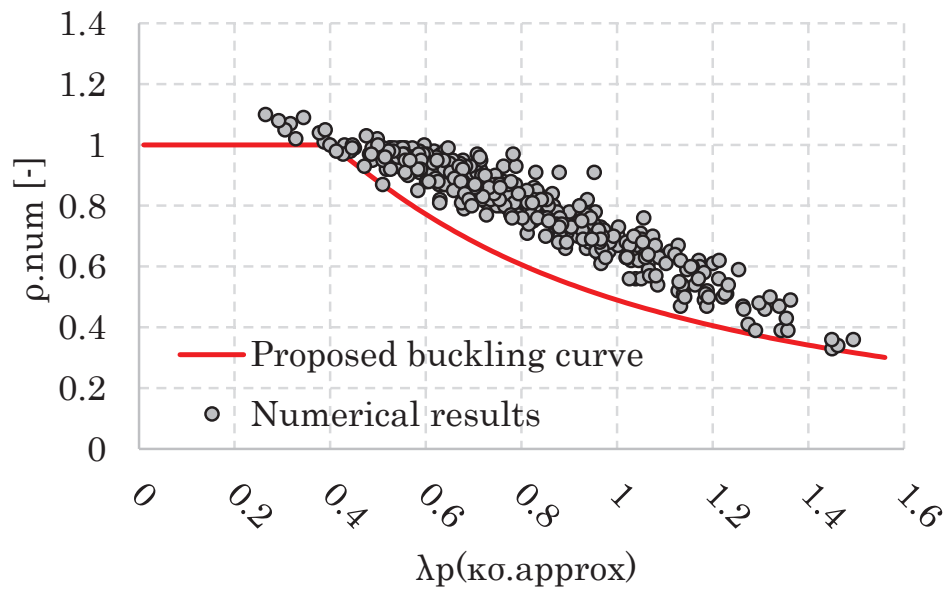


Figure 39 Developed buckling curve for flanges in duplex girders with corrugated webs

4.3 Evaluation of the developed design model and previous design models

Figure 40 (a) and (b) show the buckling factor obtained from the numerical analysis compared to the buckling factors calculated according to EN1993-1-5 [24], the expression suggested by Jager et al. [30], and the expression derived in this work (Equation (4-4) in Section 4.2). As can be seen, there is a large scatter in the results for both EN1993-1-5 [24] and Jager et al. [30] expressions, which indicates that both models don't show applicability on duplex stainless steel. On the other side, the buckling factor obtained from the numerical analysis fits very well with the results obtained using the derived equation for k_{σ} (Equation (4-4)) in this work, as shown in Figure 40c.

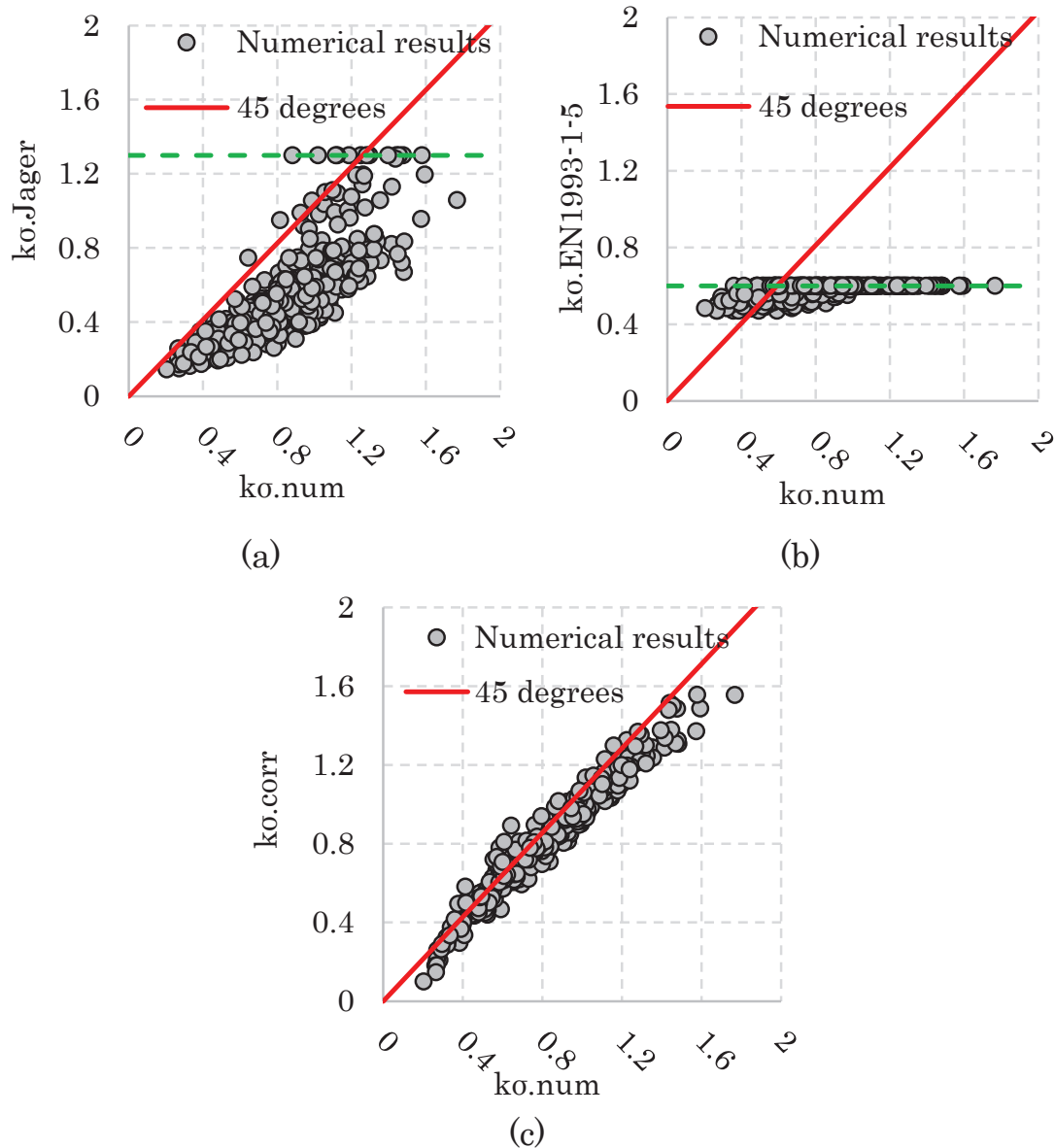


Figure 40 Comparison of previous expressions and the proposed expression for the buckling factor k_σ based on numerical results

The same comparison is repeated for the numerical outcomes of the nonlinear analysis. Figure 41 displays the numerical outcomes using the developed design model in this study as well as the pre-existing models, namely, EN1993-1-5 [24], DAST Richline 015 [32], and Jager et al. [30]. The numerical results are shown on the vertical axis, while the capacity as determined by the relevant model is shown on the horizontal axis. As can be observed in Figure 41, several results of the EN1993-1-5 model end on the unsafe side with significant dispersion. The same holds for the model Jager et al. provided, however, the dispersion is lower in this case. The DAST Richline 015 model has shown the largest scatter since this model disregards the corrugation parameters. The proposed model, on the other hand, provides safe

results within the examined parameter ranges. The proposed model, however, underestimates some resistance values.

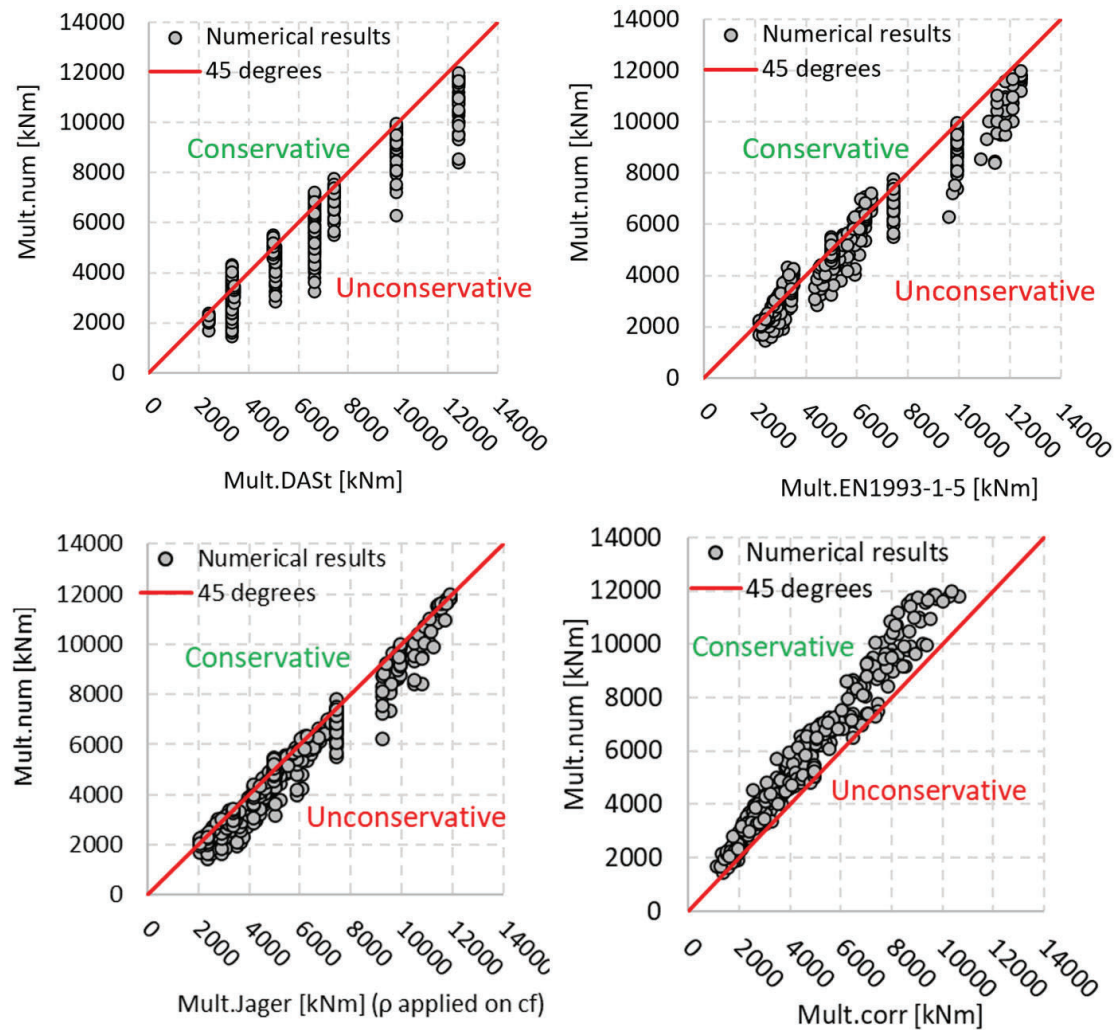


Figure 41 Comparison of previous design models and the proposed design model for flange buckling resistance based on numerical results

Chapter 5

5 Conclusions and future work

5.1 Conclusions on the benefits of using stainless steel corrugated web girders in road bridges (Paper I and II)

The following conclusions are the outcome of the investigations on the advantages of employing stainless steel corrugated web girders in composite road bridges:

- The new concept (stainless-steel corrugated web girders) outperformed the conventional flat web carbon steel concept in terms of weight, life cycle cost (LCC), and environmental impact for both simply supported and continuous bridges considered in this work.
- The new concept demonstrated significant environmental impact reduction, surpassing 30%, in both simply supported and continuous bridge cases. This is because the unit environmental impact for stainless steel obtained from EPD was substantially lower than that for carbon steel. Note that if the unit impact of both materials were the same, the new design would have a lower environmental impact because the environmental impact is related directly to the amount of material used and the new concept use less amount of material.
- With reference to investment costs, the new concept can be achievable with a slightly higher investment cost for both simply supported and continuous bridges (4% to 10% higher investment cost compared to the traditional concept made of flat web carbon steel girders and 13% lower investment cost compared to the stainless-steel flat web solution). The new concept effectively reduces material consumption, resulting in considerable cost saving. This material consumption reduction is mostly due to the use of thinner webs in the corrugated web

design. Additional savings in girder flanges can be gained when the highest permissible girder height limit in the optimization is set generously. Furthermore, because painting and grinding are no longer required, production expenses are lowered. Furthermore, the reduction in material weight results in lower cutting costs. Welding expenses are also reduced by using fewer cross beams, stiffeners, and thinner steel plates.

- With reference to LCC, besides the above-mentioned points, the new concept reduces maintenance costs by reducing the requirement for steel works' corrosion protection maintenance activities. Also, by eliminating these repair activities, the accompanying traffic disruption expenses are eliminated.
- The resulting optimal designs after optimization may differ depending on the optimization target. For stainless steel (flat and corrugated webs), the cost and life cycle impact are both primarily affected by the amount of material used. Therefore, regardless of the optimization target used, the optimization algorithm seeks to reduce material usage. For bridges of carbon steel, however, the optimization process acts differently. For instance, painting expenses contributed to 23% of the investment cost in the Kyrko Bridge case study. Therefore, painting area minimization is a major objective of the optimization process when the cost (investment or LCC) is chosen as the objective function. However, if LCA, or weight, is the desired objective function, weight reduction is the algorithm's main goal.
- When bridge height constraints are generous, the new concept proves to be more beneficial in terms of material saving. In other words, deeper girders allow for larger material saving. This reduction in material costs associated with using deeper girders leads to higher painting costs for carbon steel, whereas it has no similar impact on bridges built of stainless steel. Therefore, increasing the permissible girder height results in greater LCC potential saving.
- In LCC analysis, the assumed paint maintenance schedule affects the results. However, even when using the more conservative of the two maintenance schedules examined in this study, the new concept demonstrated a significant enhancement in life cycle cost, with reductions ranging from 5% to 27% compared to the conventional carbon steel concept for simply supported bridges and 18% saving in case of the studied continuous bridge. The LCC saving increased from 24% to 43% when a more intensive paint maintenance schedule was adopted.

- In LCC analysis, inflation and discount rates impose uncertainty and can affect predicted life cycle costs, hence influencing the findings reached from comparative LCC studies. Despite the uncertainty induced by these rates, all evaluated scenarios consistently revealed significant benefits associated with the implementation of the new concept.
- The possible influence of ADT and N_{obs} on the optimal design outcome is different. On the one hand, by moving the governing criterion from the ultimate limit state (ULS) to the fatigue limit state (FAT), raising N_{obs} restricts the benefits of employing the higher-strength material and minimizes the potential saving. On the other hand, user costs increase along with the related average daily traffic (ADT). These expenses depend on the anticipated closing time for each repair job, which can be anything from zero (no traffic diversions) to several weeks or months. Although the investigated scenarios are believed to be very conservative, the new concept has shown a significant amount of potential LCC saving.

5.2 Conclusions on flange buckling resistance (Paper III)

The research into the flange buckling resistance of stainless-steel corrugated web girders has led to the following conclusions:

- The three considered models for flange buckling resistance of carbon steel corrugated web girders: EN1993-1-5, DAST-Richtlinie 015 [32], and the model provided by Jager et al. [30] are nonconservative for duplex 1.4162 trapezoidal corrugated web girders. Both the elastic buckling coefficient and the buckling reduction factor " ρ " obtained by these models fit poorly with the results of the numerical analysis. The model given in EN1993-1-5 does not consider the stiffness of the web-to-flange junction, which has been found to be an essential influencing parameter. The DAST-Richtlinie 015 model does not take corrugation geometry into account. The model developed by Jager et al. produces better results since it considers both the web-to-flange junction stiffness and the corrugation geometry; nonetheless, the model produces capacities that are on the unsafe side for many girders.
- According to the results of the imperfection sensitivity analysis, the 1st eigen buckling mode with an imperfection amplitude of $c_f/50$, as suggested by EN1993-1-5 for flange twisting, is suitable for flange buckling in corrugated web beams made of duplex 1.4162.

- The suggested buckling curve, which is based on the proposed elastic buckling coefficient formulation, is found to yield satisfactory results for all observed failure modes. However, due to the problem's complexity and several affecting elements, some underestimating of flange buckling resistance is accepted.
- The proposed buckling curve yields a relative slenderness limit of $\bar{\lambda}_p \leq 0.4$ for duplex trapezoidal corrugated web beams. Consequently, a cross-sectional class 4 limit of $c_f/t_f > 11.36\varepsilon\sqrt{k_\sigma}$.

5.3 Future work

The work in this thesis was focused on verifying the benefits of the new concept of bridge girders with a corrugated web in stainless steel in terms of life cycle cost and life cycle impact. One design aspect (flange buckling resistance) was considered, and a design model has been proposed to consider this design aspect. However, the other design issues must be thoroughly investigated to establish a safe design guideline for stainless steel girders with corrugated webs. The following topics are suggested for future research:

- Verify the fatigue resistance of stainless-steel corrugated web girders by performing fatigue experiments to evaluate the detail category of web-to-flange weld: While some fatigue tests have already been conducted on carbon steel, demonstrating a good detail category (120 MPa), the fatigue resistance of stainless steel has not been examined through experimental studies.
- Employing parametric finite element analysis to investigate the correlation between hot spot stress and nominal normal stress and corrugation parameters: The existence of corrugation is predicted to create a relationship between corrugation parameters and hot spot stress in critical locations on beam flange. Performing physical investigations to validate this relationship might be difficult in terms of practicality, time, and cost. In this aspect, finite element analysis (FEA), validated by experiments, can provide a suitable investigation method for this issue. The idea is to provide a parametric relation between the geometrical parameters and the hot spot stress such that an accurate fatigue design of bridge girders of this type can be performed. Today, the connection between the corrugated web and beam flange is not covered by EN 1993-1-9 or by other design standards.

- A combination of experimental and numerical investigations can be conducted to generate a safe prediction model for the patch-loading resistance of corrugated web beams made of both carbon steel and stainless steel. Steel girders are frequently subjected to patch loading in a variety of circumstances, such as during transportation and construction. Particularly when the bridge is erected by launching. There have been few studies on the patch loading capacity of trapezoidal corrugated web girders, and there is currently no design model in EN1993-1-5 for the patch loading resistance of beams with corrugated web.
- A combination of experimental and numerical research may be conducted to develop a credible prediction model for the lateral torsional buckling resistance of corrugated web beams made of both stainless steel and carbon steel. Lateral torsional buckling is an important aspect to consider, particularly during the construction phase when the steel girders are functioning alone with no lateral support from the concrete deck. The designers typically employ the simplified approach to verify the lateral stability of girders; nevertheless, this method is much on the safe side. Consequently, a design model that provides improved prediction for lateral torsional buckling of corrugated web girders will increase material utilization. Particularly since lateral torsional buckling governs the design of steel girders during the construction phase and sometimes the section above the supports during the service phase, where a considerable gain from using the corrugated web is expected.
- A numerical study may be conducted to develop a reliable prediction model for the shear buckling resistance of corrugated web beams made of stainless steel. The model in EN1993-1-5 is derived for carbon steel but not updated for stainless steel. In the SUNLIGHT project, experimental work on stainless steel was conducted; however, more research is required to first propose an appropriate imperfection amplitude and then run a numerical analysis to propose a new buckling curve that might make better use of the stainless-steel material.

References

- [1] United-Nations. (2015) Transforming our World: The 2030 Agenda for Sustainable Development; <https://sustainabledevelopment.un.org/>
- [2] European-Commission. (2016) Communication from the Commission on Next steps for a sustainable European future European action for sustainability; <https://eur-lex.europa.eu/legal-content/EN/TXT/?uri=COM%3A2016%3A739%3AFIN>
- [3] European-Commission. (2011) The Roadmap to a Resource Efficient Europe; https://ec.europa.eu/environment/resource_efficiency/about/roadmap/index_en.htm
- [4] European-Commission. Buildings and Construction; https://single-market-economy.ec.europa.eu/industry/sustainability/buildings-and-construction_en
- [5] Mara, V., Haghani, R. , Sagemo,A. ,Storck , L., Nilsson, D. . (2013) Comparative study of different bridge concepts based on life-cycle cost analyses and life-cycle assessment; https://publications.lib.chalmers.se/records/fulltext/193796/local_193796.pdf
- [6] Collin, P., Johansson, B., Sundquist, H. (2008) Steel concrete composite bridges. Stockholm: Royal Institute of Technology; Luleå Technical University; <https://www.diva-portal.org/smash/record.jsf?pid=diva2%3A1008648&dswid=-1161>
- [7] Wahlsten, J., Heshmati, Mohsen , Al-Emrani, Mohammad (2018) Sustainable Infrastructure through increased use of Stainless Steel;
- [8] Baddoo, N.R., Kosmač, A. (2010) Sustainable Duplex Stainless Steel Bridges; <https://www.shortspansteelbridges.org/wp->

- [content/uploads/2022/03/Sustainable Duplex Stainless Steel Bridges.pdf](#)
- [9] Rossi, B. (2014) Discussion on the use of stainless steel in constructions in view of sustainability; <http://dx.doi.org/10.1016/j.tws.2014.01.021>,
- [10] ISSF. (2019) The stainless-steel family: International Stainless Steel Forum; <https://www.worldstainless.org/Files/issf/non-image-files/PDF/TheStainlessSteelFamily.pdf>
- [11] outokumpu. <https://www.outokumpu.com/sv-se/expertise/2016/embodying-essence-of-life>
- [12] Karabulut, B., Ferraz, G., Rossi, B. (2021) Lifecycle cost assessment of high strength carbon and stainless steel girder bridges; in Journal of Environmental Management; <https://doi.org/10.1016/j.jenvman.2020.111460>,
- [13] Zilli, G., Fattorini, F., Maiorana, E. (2008) Application of duplex stainless steel for welded bridge construction in aggressive environment; <https://www.researchgate.net/publication/265668326>
- [14] Gedge, G. Stainless Steel In Bridge Design; Arup Materials Consulting, Solihull, UK; <http://www.steel-stainless.org/media/1128/1-stainless-steel-in-structures.pdf>
- [15] Säll, J., Tiderman, Anna. (2013) Maintenance-free material in bridge superstructures: Benefits in a cost- and environment prospective in use of stainless steel and directly molded durable concrete; Kungliga Tekniska Högskolan;
- [16] SIKLANDER, O., ÅQVIST, ANNA. (2016) Livscykelanalyser för en öppningsbar vägbro: Studie av Nya Flottsundsbron byggd med konventionellt, rostfritt eller rosttrögt stål; Kungliga Tekniska Högskolan (KTH);
- [17] Hechler, O., Collin, P. (2008) On the use of duplex stainless steels in bridge construction;
- [18] Leblouba, M., Karzad, Abdul Saboor, Tabsh, Sami W., Barakat, Samer. (2022) Plated versus Corrugated Web Steel Girders in Shear: Behavior, Parametric Analysis, and

- Reliability-Based Design Optimization;
<https://doi.org/10.3390/buildings12122046>,
- [19] Boutillon, L., Combault, Jacques, Ikeda, Shoji, Imberty, Florent, Mori, Takuya, Nagamoto, Naoki, Novak, Balthasar, Saito, Kimio. (2015) Corrugated-steel-web bridges;
<https://www.fib-international.org/publications/fib-bulletins/corrugated-steel-web-bridges-detail.html>
- [20] <https://structurae.net/fr/ouvrages/pont-de-la-corniche>
- [21] D. Wilson, A. ADVANCES IN HIGH PERFORMANCE STEELS FOR HIGHWAY BRIDGES;
<https://www.aisc.org/globalassets/nsba/technical-documents/advances-in-high-performance-steels-for-highway-bridges.pdf>
- [22] Amani, M., Al-Emrani, Mohammad, Flansbjer, Mathias. (2023) Shear Behavior of Stainless Steel Girders with Corrugated Webs;
<https://doi.org/10.1016/j.jcsr.2023.108086>,
- [23] Hlal, F., Al-Emrani, Mohammad, Amani, Mozhdeh. (2022) Preliminary Study on Plate Girders with Corrugated Webs; Chalmers University of Technology; Report ACE 2022:3,
- [24] EN1993-1-5. (2006);
- [25] EN1993-1-5. (2019) Final draft of EN1993-1-5 (2019-11-12);
- [26] Hlal, F., Mohra, Naheel. (2021) Stainless Steel Bridge Girders with Corrugated Webs - A parametric study to investigate the sensitivity of Stainless steel girder's shear behaviour to initial imperfection; Chalmers University of Technology;
- [27] Karlsson, E. (2018) Stainless Steel Bridge Girders with Corrugated Webs; Chalmers University of Technology;
- [28] SÆMUNDSSON, D., INGÓLFSDÓTTIR, SIGNÝ. (2021) Nonlinear finite element analysis of stainless steel corrugated web girders subjected to patch loading; Chalmers University of Technology;

- [29] SAVE, E., ÅKERMO, KARL. (2020) Fatigue Performance of Welded Steel Girders with Corrugated Webs; Chalmers University of Technology;
- [30] Jäger, B., Dunai, L., Kövesdi, B. (2017) Flange buckling behavior of girders with corrugated web Part II: Numerical study and design method development; in *Thin-Walled Structures*. p. 238-252;
<https://doi.org/10.1016/j.tws.2017.05.020>,
- [31] JOHNSON, R.P., CAFOLLA, J. (1997) Local flange buckling in plate girders with corrugated webs;
<https://doi.org/10.1680/istbu.1997.29304>,
- [32] Pasternak, H., Hannebauer, Dina. (2004) Träger mit profilierten Stegen;
<https://www.researchgate.net/publication/342644235>
- [33] KOICHI, W., MASAHIRO, KUBO. (2006) In-plane bending capacity of steel girders with corrugated web plates;
doi:10.2208/jsceja.62.323,
- [34] Hlal, F., Al-Emrani, M. (2023) Flange buckling in stainless-steel corrugated webs I-girders under pure bending: Numerical study; *Journal of Constructional Steel Research*;
<https://doi.org/10.1016/j.jcsr.2023.108031>,
- [35] Chisari, C., Amadio, Claudio. (2018) TOSCA: a Tool for Optimisation in Structural and Civil engineering Analyses; *International Journal of Advanced Structural Engineering* 10:401–419; <https://doi.org/10.1007/s40091-018-0205-1>,
- [36] CHALOUHI, E.K. (2022) Optimal design solutions of road bridges considering embedded environmental impact and cost; KTH Royal Institute of Technology;
- [37] Hassan, M.M. (2013) Optimization of stay cables in cable-stayed bridges using finite element, genetic algorithm, and B-spline combined technique; *Engineering Structures*;
<http://dx.doi.org/10.1016/j.engstruct.2012.11.036>,
- [38] Park, J., Chun, Yun-Hee, Lee, Jungwhee. (2016) Optimal Design of an Arch Bridge with High Performance Steel for Bridges using Genetic Algorithm; *International Journal of Steel Structures*;
<https://link.springer.com/article/10.1007/s13296-016-6024-y>

- [39] Skoglund, O., Leander, John, Karoumi, Raid. (2020) Optimizing the steel girders in a high strength steel composite bridge; in Engineering Structures; <https://doi.org/10.1016/j.engstruct.2020.110981>,
- [40] Yang, X.-S. (2010) Engineering Optimization An Introduction with Metaheuristic Application; Chalmers Library E-book Collection
- [41] Bozorg-Haddad, O., Solgi, Mohammad, A. Loaiciga, Hugo. (2017) Meta-Heuristic and Evolutionary Algorithms for Engineering Optimization; <https://ebookcentral.proquest.com/lib/chalmers/reader.action?docID=5015534>
- [42] Solgi, R.M. (2020); <https://pypi.org/project/geneticalgorithm/>
- [43] SS-EN-ISO-14040:2006. Environmental management – Life cycle assessment – Principles and framework;
- [44] SS-EN-15978:2011. (2011);
- [45] SS-EN-15804:2012+A2:2019. (2019);
- [46] Martínez-Muñoz, D., Martí, J. V., Yepes, V. (2020) Steel-Concrete Composite Bridges: Design, Life Cycle Assessment, Maintenance, and Decision-Making; <https://doi.org/10.1155/2020/8823370>,
- [47] Gervásio, H., da Silva, Luís Sim[otilde]es. (2008) Comparative life-cycle analysis of steel-concrete composite bridges; <https://doi.org/10.1080/15732470600627325>,
- [48] EUROPEAN-COMMISSION. (2013) Sustainable steel-composite bridges in built environment (SBRI); <https://doi.org/10.2777/50286>,
- [49] Cope, A., Bai, Q., Samdariya, A., Labi, S. (2011) Assessing the efficacy of stainless steel for bridge deck reinforcement under uncertainty using Monte Carlo simulation; <http://dx.doi.org/10.1080/15732479.2011.602418>,
- [50] SCI. (2010) Composite Highway Bridge Design: Worked Examples; SCI (The Steel Construction Institute);

- [51] BaTMan. <https://batman.trafikverket.se/>
- [52] Baddoo, N. (2018) Design Manual for Structural Stainless Steel; SCI, Silwood Park, Ascot;
- [53] EN1993-1-4. (2006);
- [54] Outokumpu. Duplex stainless steels-Outokumpu Forta range datasheet; <https://www.outokumpu.com/sv-se/products/product-ranges/forta>
- [55] Elamary, A.S., Saddek, Amr B., Alwetaishi, Mamdooh. (2017) Effect of corrugated web on flexural capacity of steel beams: International Journal of Applied Engineering Research https://www.ripublication.com/ijaer17/ijaerv12n4_09.pdf
- [56] Kövesdi, B., Jáger, B., Dunai, L. (2016) Bending and shear interaction behavior of girders with trapezoidally corrugated webs; in Journal of Constructional Steel Research. p. 383-397; <http://dx.doi.org/10.1016/j.jcsr.2016.03.002>,
- [57] Kövesdi, B., Jáger, B., Dunai, L. (2012) Stress distribution in the flanges of girders with corrugated webs; <https://doi.org/10.1016/j.jcsr.2012.07.023>,
- [58] Abbas, H.H., Sause, Richard, Driver, Robert G. (2007) Analysis of flange transverse bending of corrugated web I-girders under in-plane loads; in Journal of structural engineering. p. 347–355; [https://doi.org/10.1061/\(ASCE\)0733-9445\(2007\)133:3\(347\)](https://doi.org/10.1061/(ASCE)0733-9445(2007)133:3(347)),
- [59] Elamary, A.S., Alharthi, Yasir.M., Hassanein, Mostafa F., Sharaky, Ibrahim.A. (2022) Trapezoidally corrugated web steel beams loaded over horizontal and inclined folds; <https://doi.org/10.1016/j.jcsr.2022.107202>,
- [60] Baláž, I., Koleková, Y. (2012) Influence of Transverse Bending Moment in the Flange of Corrugated I-Girders; in Procedia Engineering. p. 26-31; <https://www.researchgate.net/publication/257725189>
- [61] Abbas, H.H., Sause, Richard, Driver, Robert G. (2007) Simplified analysis of flange transverse bending of corrugated web I-girders under in-plane moment and shear; in Engineering Structures; <https://doi.org/10.1016/j.engstruct.2007.01.006>,

- [62] Elgaaly, M., Seshadri, Anand (1998) Depicting the behavior of girders with corrugated webs up to failure using non-linear finite element analysis; [https://doi.org/10.1016/S0965-9978\(98\)00020-9](https://doi.org/10.1016/S0965-9978(98)00020-9),
- [63] Elgaaly, M. (1997) Bending strength of steel beams with corrugated webs: Journal of structural engineering; [https://doi.org/10.1061/\(ASCE\)0733-9445\(1997\)123:6\(772\)](https://doi.org/10.1061/(ASCE)0733-9445(1997)123:6(772)),
- [64] Elgaaly, M., Hamilton Robert W., Seshadri Anand. (1996) Shear strength of beams with corrugated webs; in Journal of Structural Engineering; [https://doi.org/10.1061/\(ASCE\)0733-9445\(1996\)122:4\(390\)](https://doi.org/10.1061/(ASCE)0733-9445(1996)122:4(390)),
- [65] Jáger, B., Kövesdi, Balázs, Dunai, László. (2017) Flange buckling resistance of trapezoidal web girders: Experimental and numerical study: EUROSTEEL 2017. p. 4088-4097; <https://doi.org/10.1002/cepa.465>,
- [66] Jáger, B., Dunai, L., Kövesdi, B. (2017) Flange buckling behavior of girders with corrugated web Part I: Experimental study; in Thin-Walled Structures. p. 181-195; <https://doi.org/10.1016/j.tws.2017.05.021>,
- [67] Pasternak, H., Kubieniec, Gabriel. (2010) Plate girders with corrugated webs; in Journal of Civil Engineering and Management. p. 166-171; <https://doi.org/10.3846/jcem.2010.17>,
- [68] Lho, S.-H., Lee, Chang-Hwan, Oh, Jin-Tak, K. Ju, Young, Kim, Sang-Dae. (2014) Flexural capacity of plate girders with very slender corrugated webs;
- [69] Li, G.-Q., Jiang, Jian, Zhu, Qi. (2014) Local buckling of compression flanges of H-beams with corrugated webs; <http://dx.doi.org/10.1016/j.jcsr.2015.04.014>,
- [70] Nie, J.-G., Zhu, Li, Tao, Mu-Xuan, Tang, Liang. (2013) Shear strength of trapezoidal corrugated steel webs; in Journal of Constructional Steel Research. p. 105-115; <http://dx.doi.org/10.1016/j.jcsr.2013.02.012>,
- [71] Leblouba, M., Barakat, Samer, Altoubat, Salah, Junaid, Talha M., Maalej, Mohamed. (2017) Normalized shear strength of trapezoidal corrugated steel webs; in Journal of

- Constructional Steel Research;
<http://dx.doi.org/10.1016/j.jcsr.2017.05.007>,
- [72] Driver, R.G., Abbas, Hassan H., Sause, Richard. (2006) Shear behavior of corrugated web bridge girders; in Journal of Structural Engineering;
[https://doi.org/10.1061/\(ASCE\)0733-9445\(2006\)132:2\(195\)](https://doi.org/10.1061/(ASCE)0733-9445(2006)132:2(195)),
- [73] Sause, R., Braxtan, Thomas N. . (2011) Shear strength of trapezoidal corrugated steel webs; in Journal of Constructional Steel Research;
<https://doi.org/10.1016/j.jcsr.2010.08.004>,
- [74] Moon, J., Yi, Jongwon, Choi, Byung H., Lee, Hak-Eun (2009) Shear strength and design of trapezoidally corrugated steel webs; in Journal of Constructional Steel Research;
<https://doi.org/10.1016/j.jcsr.2008.07.018>,
- [75] Zhang, B., Yu, Jiangjiang, Chen, Weizhen, Wang, Hui, Xu, Jun. (2020) Stress states and shear failure mechanisms of girders with corrugated steel webs; in Thin-Walled Structures;
<https://doi.org/10.1016/j.tws.2020.106858>,
- [76] Leblouba, M., Junaid, M. Talha, Barakat, Samer, Altoubat, Salah, Maalej, Mohamed. (2017) Shear buckling and stress distribution in trapezoidal web corrugated steel beams; in Thin-Walled Structures;
<http://dx.doi.org/10.1016/j.tws.2017.01.002>,
- [77] Al-Emrani, M., Amani, M., Björnstedt, P., Borg, P., Forsgren, E., Hedegård, J., Hällmark, R., Hlal, F., Janiak, P., Lundstjälk, A, Nilsson, P., Persson, L., Trydell, K., Zachrisson, J., Zamiri, F.,. (2022) SUNLIGHT – Sustainable, maintenance-free and lighter beams for stronger Swedish infrastructure;
- [78] Denan, F., Osman, Mohd, Saad, Sariffuddin. (2010) The study of lateral torsional buckling behaviour of beam with trapezoid web steel section by experimental and finite element analysis; in International Journal of Research and Reviews in Applied Sciences (IJRRAS). p. 233–240;
- [79] EN1993-1-4. (2021) Amendment to Stainless steel design rules in Eurocode SS-EN 1993-1-4;

- [80] EDVARDSSON, G.E., LUNDQUIST, BENGT. (2014) Influence of Purlins on Lateral-Torsional Buckling of Steel Girders with Corrugated W; Chalmers University of Technology;
- [81] LARSSON, M., PERSSON, JOHN. (2013) Lateral-torsional buckling of steel girders with trapezoidally corrugated webs; Chalmers University of Technology;
- [82] Moon, J., Yi, Jong-Won, Choi, Byung H., Lee, Hak-Eun. (2009) Lateral-torsional buckling of I-girder with corrugated webs under uniform bending; in *Thin-Walled Structures*; <https://doi.org/10.1016/j.tws.2008.04.005>,
- [83] Nguyen, N.D., Han, Seung-Ryong, Lee, Gyu-Sei, Kang, Young-Jong. (2011) Moment modification factor of I-girder with trapezoidal-web-corrugations considering concentrated load height effects; in *Journal of Constructional Steel Research*; <https://doi.org/10.1016/j.jcsr.2011.05.002>,
- [84] Luo, R., Edlund, B. (1996) Ultimate strength of girders with trapezoidally corrugated webs under patch loading; in *Thin-Walled Structures*; [https://doi.org/10.1016/0263-8231\(95\)00029-1](https://doi.org/10.1016/0263-8231(95)00029-1),
- [85] Elgaaly, M. (1997) Beams with corrugated webs under partial compression; in *Journal of structural engineering*;
- [86] Kövesdi, B., Braun, B., Kuhlmann, U., Dunai, L. (2010) Patch loading resistance of girders with corrugated webs; in *Journal of Constructional Steel Research*; <https://doi.org/10.1016/j.jcsr.2010.05.011>,
- [87] Jean-Paul, L., Manfred, A. Hirt. (2013) *Steel Bridges Conceptual and Structural Design of Steel and Steel-Concrete Composite Bridges*; <https://doi.org/10.1201/b15429>,
- [88] EN1994-2. (2005) Eurocode 4 - Design of composite steel and concrete structures - Part 2: General rules and rules for bridges;
- [89] Pascal, D. (2023) pypi.org; <https://pypi.org/project/geneticalgorithm2>
- [90] NISSAN, A., WOLDEYOHANNES, YOHANNES. (2022) Life Cycle Assessment and Life Cycle Cost for Composite Bridges;

- Stainless Steel Corrugated Web Girders vs. Carbon Steel Flat Web Girders; Chalmers University of Technology;
- [91] FU-SIANG, S. (2021) Comparative life cycle analysis for bridges made of conventional steel and stainless steel in the early design phases; Chalmers University of Technology;
- [92] (2022) Personal communication;
- [93] Rossi, B., Marquart, S., Rossi, G. (2017) Comparative life cycle cost assessment of painted and hot-dip galvanized bridges; in *Journal of Environmental Management*. p. 41-49;
<https://doi.org/10.1016/j.jenvman.2017.03.022>
- [94] Wallbaum, H. (2021) Life Cycle Cost Assessment (LCCA); Chalmers University of Technology;
- [95] Safi, M. (2013) Life-Cycle Costing; <https://www.diva-portal.org/smash/get/diva2:660312/FULLTEXT03.pdf>
- [96] Collin, P., Nilsson, Martin, Häggström, Jens (2011) International Workshop on Eurocode 4-2, Composite Bridges;
- [97] EN1991-2. (2002) Eurocode 1: Actions on structures - Part 2: Traffic loads on bridges;
- [98] Al-Emrani, M., ÅKESSON, BJÖRN (2020) Steel Structures Report ACE2030:13; in Department of Architecture and Civil Engineering, Chalmers University of Technology;
<http://bit.ly/3H3T3tv>
- [99] SS-EN1993-1-4:2006/A1:2015. (2015) Design of steel structures – Part 1-4: General rules – Supplementary rules for stainless steels;
- [100] SSAB. (2022) Environmental Product Declaration (EPD) In accordance with ISO 14025 and EN 15804+A1;
[https://www.ssab.com/en/download-center#sort=%40customorder%20descending&f:document=\[3f0a0e364ca54f74a30faff866bd87ff\]](https://www.ssab.com/en/download-center#sort=%40customorder%20descending&f:document=[3f0a0e364ca54f74a30faff866bd87ff])
- [101] SSAB. (2019) Environmental Product Declaration (EPD) In accordance with ISO 14025 and EN 15804+A1;
<https://www.ssab.com/en/news/2016/06/ssabs-environmental-product-declaration>

- [102] SSAB. (2022) Environmental Product Declaration (EPD) In accordance with ISO 14025 and EN 15804:2012+A2:2019; [https://www.ssab.com/en/download-center?dcFilter=environmentalpr&dcSearch#sort=%40custo%20morder%20descending&f:document=\[3f0a0e364ca54f74a30faf866bd87ff\]](https://www.ssab.com/en/download-center?dcFilter=environmentalpr&dcSearch#sort=%40custo%20morder%20descending&f:document=[3f0a0e364ca54f74a30faf866bd87ff])

Appendix

1 LCC data

Table 26 Assumed material prices

Material	Unit	Unit Cost	Reference
Steel plates	kg	EN1.4162: 30SEK/kg	Carbon steel: Producer in Sweden [92]
		S355: 10 SEK/kg	Stainless steel: Producer in Sweden [92]
Hot rolled sections	kg	EN1.4162: 30 SEK/kg	Carbon steel: Producer in Sweden [92]
		S355: 10 SEK/kg	Stainless steel: Producer in Sweden [92]
Hollow sections profiles	kg	EN1.4162: 48 SEK/kg	Carbon steel: Producer in Sweden [92]
		S355: 16 SEK/kg	Stainless steel: Producer in Sweden [92]
Reinforcement	kg	9.6 SEK/kg	Trafikverket Ecoinvent, CML 2001 (superseded) concrete,
Concrete	m ³	2400 SEK/m ³	40MPa//[RoW] concrete production, 40MPa, ready-mix, with Portland cement

Table 27 Assumed values for reselling costs

Material	Recycle rate	Reselling cost	Reference
S355	0.95	3,5 SEK/kg	Producer in Sweden [92]
EN1.4162	0.95	22,5 SEK/kg	Producer in Sweden [92]

2 LCA data

Table 28 Module A1, A2, A3

Type	Unit	Unit Impact	Reference
Steel plates production	kg	Stainless steel: 1.7 kg CO ₂ eq/ kg Carbon steel: 2.63 kg CO ₂ eq/ kg	Producer in Sweden [11] Producer in Sweden [100]
Hot rolled sections production	kg	Stainless steel: 1.7 kg CO ₂ eq/ kg Carbon steel: 2.16 kg CO ₂ eq/ kg	Producer in Sweden [11] Producer in Sweden [101]
Hollow sections production	kg	Stainless steel: 1.7 kg CO ₂ eq/ kg Carbon steel: 2.35 kg CO ₂ eq/ kg	Producer in Sweden [11] Producer in Sweden [102]
Weld	kg	Stainless steel: 5.02 kg CO ₂ eq/ kg Carbon steel: 2.066 kg CO ₂ eq/ kg	Ecoinvent, CML 2001 (superseded) LCIA: climate change: GWP 100a Stainless steel: steel, chromium steel 18/8, hot rolled//[RER] steel production, chromium steel 18/8, hot rolled Carbon steel: steel, low-alloyed//[RER] steel production, converter, low-alloyed
Paint	kg	3.52 kg CO ₂ eq/ kg	epd-norge.no
Concrete	kg	0.166 kg CO ₂ eq/ kg	Source (Trafikverket online tool)
Reinforcement	kg	0.7 kg CO ₂ eq/ kg	Source (Trafikverket online tool)
Welding process	m	0.18 kg CO ₂ eq/ m	Ecoinvent, CML 2001 (superseded) LCIA: climate change: GWP 100a welding, gas, steel//[RER] welding, gas, steel

Table 29 Module A4. Data retrieved from OpenLCA 25-01-2023 LCIA method: CML2001, Ecoinvent v3.8 database

Type	Unit	Unit Impact	Reference
Plate Transport Railway	ton*km	0.04517 [kg CO ₂ eq/ton.km]	Distances: https://klimatkalkyl-pub.ea.trafikverket.se/Klimatkalkyl/Moddell Unit Impact: Ecoinvent, CML 2001 (superseded) LCIA: climate change: GWP 100a transport, freight train//[Europe without Switzerland] market for transport, freight train

Plate Transport Truck National	ton*km	0,0863 [kg CO2 eq/ton.km]	Ecoinvent, CML 2001 (superseded) LCIA: climate change: GWP 100a transport, freight, lorry >32 metric ton, EURO6//[RER] market for transport, freight, lorry >32 metric ton, EURO6
Plate Transport Truck Regional	ton*km	0,09075 [kg CO2 eq/ton.km]	Ecoinvent, CML 2001 (superseded) LCIA: climate change: GWP 100a transport, freight, lorry >32 metric ton, EURO3//[RER] market for transport, freight, lorry >32 metric ton, EURO3
Plate Transport Truck Local	ton*km	0,165 [kg CO2 eq/ton.km]	Ecoinvent, CML 2001 (superseded) LCIA: climate change: GWP 100a transport, freight, lorry >32 metric ton, EURO3//[RER] market for transport, freight, lorry >32 metric ton, EURO5
Hotrolled Transport Railway	ton*km	0,04517[kg CO2 eq/ton.km]	Ecoinvent, CML 2001 (superseded) LCIA: climate change: GWP 100a transport, freight train//[Europe without Switzerland] market for transport, freight train
Hotrolled Transport Truck national	ton*km	0,0863 [kg CO2 eq/ton.km]	Ecoinvent, CML 2001 (superseded) LCIA: climate change: GWP 100a transport, freight, lorry >32 metric ton, EURO6//[RER] market for transport, freight, lorry >32 metric ton, EURO6
Hotrolled Transport Truck regional	ton*km	0,09075 [kg CO2 eq/ton.km]	Ecoinvent, CML 2001 (superseded) LCIA: climate change: GWP 100a transport, freight, lorry >32 metric ton, EURO3//[RER] market for transport, freight, lorry >32 metric ton, EURO3
Hotrolled Transport Truck local	ton*km	0,165 [kg CO2 eq/ton.km]	Ecoinvent, CML 2001 (superseded) LCIA: climate change: GWP 100a transport, freight, lorry 16-32 metric ton, EURO5//[RER] market for transport, freight, lorry 16-32 metric ton, EURO5
Concrete transport impact	ton*km	0,165 [kg CO2 eq/ton.km]	Ecoinvent, CML 2001 (superseded) LCIA: climate change: GWP 100a transport, freight, lorry 16-32 metric ton, EURO5//[RER] market for transport, freight, lorry 16-32 metric ton, EURO5

*Table 30 Module B2, B4. Data retrieved from OpenLCA 25-01-2023
LCIA method: CML2001, Ecoinvent v3.8 database*

Type	Unit	Unit Impact	Reference
Paint impact	kg	3,52 [kg CO2 eq/ kg]	epd-norge.no
Paint transport impact national	kg	0,0863 [kg CO2 eq/tkm]	Ecoinvent, CML 2001 (superseded) LCIA: climate change: GWP 100a transport, freight, lorry >32 metric ton, EURO6//[RER] market for transport, freight, lorry >32 metric ton, EURO6
Paint transport impact local	kg	0,165 [kg CO2 eq/tkm]	Ecoinvent, CML 2001 (superseded) LCIA: climate change: GWP 100a transport, freight, lorry 16-32 metric ton, EURO5//[RER] market for transport, freight, lorry 16-32 metric ton, EURO5

Table 31 Module C2, C3, C4. Data retrieved from OpenLCA 25-01-2023 LCIA method: CML2001, Ecoinvent v3.8 database

Type	Unit	Unit Impact	Reference
Disposal plates (C4)	kg	0,0052 [kg CO2 eq/ kg]	Ecoinvent, CML 2001 (superseded) LCIA: climate change: GWP 100a scrap steel//[RoW] treatment of scrap steel, inert material landfill
Disposal hot rolled (C4)	kg	0,0052 [kg CO2 eq/ kg]	Ecoinvent, CML 2001 (superseded) LCIA: climate change: GWP 100a scrap steel//[RoW] treatment of scrap steel, inert material landfill
Disposal hollow section (C4)	kg	0,0052 [kg CO2 eq/ kg]	Ecoinvent, CML 2001 (superseded) LCIA: climate change: GWP 100a scrap steel//[RoW] treatment of scrap steel, inert material landfill
Disposal weld (C4)	kg	0,0052 [kg CO2 eq/ kg]	Ecoinvent, CML 2001 (superseded) LCIA: climate change: GWP 100a scrap steel//[RoW] treatment of scrap steel, inert material landfill
Disposal concrete (C4)	kg	0,0139 [kg CO2 eq/ kg]	Ecoinvent, CML 2001 (superseded) LCIA: climate change: GWP 100a waste reinforced concrete//[Europe without Switzerland] treatment of waste reinforced concrete, collection for final disposal
Disposal rebars (C4)	kg	0,065 [kg CO2 eq/ kg]	Ecoinvent, CML 2001 (superseded) LCIA: climate change: GWP 100a waste reinforcement steel//[RoW] treatment of waste reinforcement steel, collection for final disposal
Plates waste processing	kg	0,045 [kg CO2 eq/ kg]	Ecoinvent, CML 2001 (superseded) LCIA: climate change: GWP 100a

(C3)			iron scrap, sorted, pressed//[Europe without Switzerland] treatment of metal scrap, mixed, for recycling, unsorted, sorting
Hot rolled waste processing (C3)	kg	0,045 [kg CO2 eq/ kg]	Ecoinvent, CML 2001 (superseded) LCIA: climate change: GWP 100a iron scrap, sorted, pressed//[Europe without Switzerland] treatment of metal scrap, mixed, for recycling, unsorted, sorting
Hollow section waste processing (C3)	kg	0,045 [kg CO2 eq/ kg]	Ecoinvent, CML 2001 (superseded) LCIA: climate change: GWP 100a iron scrap, sorted, pressed//[Europe without Switzerland] treatment of metal scrap, mixed, for recycling, unsorted, sorting
Weld waste processing (C3)	kg	0,045 [kg CO2 eq/ kg]	Ecoinvent, CML 2001 (superseded) LCIA: climate change: GWP 100a iron scrap, sorted, pressed//[Europe without Switzerland] treatment of metal scrap, mixed, for recycling, unsorted, sorting
Concrete waste processing (C3)	kg	0,016 [kg CO2 eq/ kg]	Ecoinvent, CML 2001 (superseded) LCIA: climate change: GWP 100a waste reinforced concrete//[Europe without Switzerland] treatment of waste reinforced concrete, recycling + waste reinforced concrete//[Europe without Switzerland] treatment of waste reinforced concrete, sorting plant
Rebars waste processing (C3)	kg	0,057 [kg CO2 eq/ kg]	Ecoinvent, CML 2001 (superseded) LCIA: climate change: GWP 100a waste reinforcement steel//[CH] treatment of waste reinforcement steel, recycling
Paint incineration (C3)	kg	3,51 [kg CO2 eq/ kg]	Ecoinvent, CML 2001 (superseded) LCIA: climate change: GWP 100a waste paint//[Europe without Switzerland] treatment of waste paint, hazardous waste incineration, with energy recovery + waste paint on metal//[RoW] treatment of waste paint on metal, sorting plant
Transportation on EOL (C2)	ton. km	0,165 [kg CO2 eq/tkm]	Ecoinvent, CML 2001 (superseded) LCIA: climate change: GWP 100a transport, freight, transport, freight, lorry 16-32 metric ton, EURO5//[RER] market for transport, freight, lorry 16-32 metric ton, EURO5